Integrating renewables into the Japanese power grid by 2030

A frequency stability and load flow analysis of the Japanese system in response to high renewables penetration levels

STUDY

自然エネルギー財団
RENEWABLE ENERGY INSTITUTE

Agora Energiewende

egi elia grid international
www.eliagrid-int.com

GRIDLAB

Integrating renewables into the Japanese power grid by 2030

IMPRINT

STUDY
Integrating renewables
into the Japanese power grid by 2030

A frequency stability and load flow analysis
of the Japanese system in response
to high renewables penetration levels

STUDY BY
Peter Merk, Elia Grid International
MSc. Rena Kuwahata, Elia Grid International
Dr. Steffen Rabe, GridLab
Assoc. prof. Tatsuya Wakeyama,
Renewable Energy Institute and Kyushu University
Shota Ichimura, Renewable Energy Institute
Dimitri Pescia, Agora Energiewende

COMMISSIONED BY
Renewable Energy Institute
8F, DLX Building, 1-13-1 Nishi-Shimbashi
Minato-ku | Tokyo 105-0003 | Japan

Agora Energiewende
Anna-Louisa-Karsch-Straße 2
10178 Berlin | Germany

Proofreading: WordSolid, Berlin
Layout: RadiCon | Berlin · Kerstin Conradi,
UKEX GRAPHI, Urs Karcher, Cover: Meriç Dağlı

This publication is available for download under this QR code.

148/1-S-2019/EN
Publication: April 2019

PROJECT LEAD
Assoc. prof. Tatsuya Wakeyama
Renewable Energy Institute and Kyushu University
t.wakeyama@renewable-ei.org

Dimitri Pescia, Agora Energiewende
dimitri.pescia@agora-energiewende.de

ACKNOLWEDGEMENTS
We would like to thank all those who participated in the expert workshops for their valuable input and in particular Yukari Takamura, Professsor, Integrated Research System for Sustainability Science (IR3S), University of Tokyo Institutes for Advanced Study (UTIAS) – Yoh Yasuda, Project Professor, Graduate School of Economics, Faculty of Economics, Kyoto University, Takao Tsuji, Associate Professor, Faculty of Engineering, Yokohama National University – Tetsuo SAITO, University of Tokyo, Institute of Industrial Science – Nobuyuki Honjo, Leader, Power System Committee, Japan Wind Power Association (JWPA) – Takeaki Masukawa, Secretary General, Japan Photovoltaic Energy Association (JPEA) – Hideyuki Ohnishi, Regional General Manager, GE Renewables, North Asia – affiliations as of December 2018.

We are grateful to the support provided by Adelphi.

Please cite as:
Renewable Energy Institute, Agora Energiewende (2018): *Integrating renewables into the Japanese power grid by 2030.* Study on behalf of Renewable Energy Institute and Agora Energiewende

www.renewable-ei.org
www.agora-energiewende.de

Preface

Dear readers,

As the cost of wind and solar power generation has drastically fallen, these technologies have come to make a major contribution to the decarbonisation of power systems. In Japan, solar photovoltaic uptake has risen rapidly over the last five years, making the country one of the most dynamic photovoltaic markets outside China. While the proportion of variable renewables in the Japanese system is increasing, however, it remains rather low, at around 7%.

Concerns over whether renewables can be efficiently integrated into Japan's power grids without endangering grid stability have raised the spectre of a renewables slowdown in the country. International experience has shown, however, that a number of technical measures that are not yet widespread in Japan can be safely implemented to improve grid stability. Unfortunately, there are very few studies in the public domain on these aspects of Japan's power system.

In this study, Japan's Renewable Energy Institute (REI) and Agora Energiewende attempt to partially fill this lacuna. As well as providing new insights into grid stability in Japan, the study also promotes data transparency. We are firmly convinced that third party analysis on the basis of transparent data can contribute to a more robust discussion and ultimately raise societal awareness of the importance of the energy transition.

Yours sincerely,
Patrick Graichen,
Executive Director of Agora Energiewende
and **Mika Ohbayashi,**
Director of the Renewable Energy Institute

Key insights

1. **The Japanese power system can accommodate a larger proportion of renewables (RES) than is currently provided for in the government's 2030 targets, while still maintaining grid stability.** An annual share of at least 33% RES (22% variable renewables – VRES) can easily be integrated, while still maintaining grid stability within a tolerable range. A higher renewable share of 40% (30% VRES) could also be achieved with very low curtailment level.

2. **There already exist a number of technical measures to improve grid stability in situations where a high proportion of variable renewables could place a strain on grid operations.** Indeed, VRES can contribute to maintaining grid stability by providing fast frequency response (FFR). On conservative assumptions, this study shows that such FFR services would enable the existing Japanese transmission grid to incorporate instantaneous VRES penetration levels of up to 60% in eastern Japan and around 70% in western Japan, while still maintaining frequency stability. These assessments confirm the trends observed in 2018 in regions such as Kyushu or Shikoku, where hourly VRES penetration satisfied more than 80% of demand (corresponding to more than 55% of all power generation). By 2030, these high regional infeed levels could become the norm for the Japanese system as a whole. Furthermore, implementing additional technical measures would allow even higher penetration levels to be reached.

3. **Integrated grid and resource planning can help mitigate the impact of wind and solar PV deployment on intraregional and interregional load flows.** Increasing the proportion of VRES in the mix is expected to reduce power line loading in some regions and increase it in other parts of the system. The impact of VRES distribution on the grid must therefore be systematically taken into account in future grid development plans, in order to avoid creating line-loading hotspots.

4. **Non-discriminatory market regulations, enhanced transparency, and state-of-the-art operational and planning practices facilitate the integration of a higher proportion of variable renewables.** In particular, renewables should be incorporated into ancillary service provision, since they can contribute to frequency stability, balancing, and voltage control in tandem with other technologies (such as demand side response, conventional generation, and storage).

Inhalt

Executive summary

Independent and transparent grid integration studies contribute to factually grounded debate on the future of the Japanese power system

The task of integrating a high level of renewables into the power mix while reducing the proportion of conventional generation such as coal and nuclear presents Japan's power system with new challenges. Increased uptake of variable renewables, and particularly solar PV (49 GW total installed capacity at the end of 2017), has heightened concern over the impact of variable renewables (VRES) on grid stability. This has prompted investigations into various possibilities of incentivising sufficient system flexibility. Against this backdrop, grid integration studies have become an invaluable means of facilitating informed debate and guiding national policy.

This study, jointly conducted by Japan's Renewable Energy Institute and Agora Energiewende, investigates the impact of the integration of renewables in Japan on frequency stability and – to a lesser extent – power flows. It is based on a modelling and simulating tool chain of the Japanese power system developed for this project by Elia Grid International and Gridlab, which aims to facilitate independent third-party research. The study compares two scenarios for the year 2030: the government's target scenario, which provides for a renewables penetration level of 22–24% (64 GW solar and 10 GW wind), and a more ambitious scenario (100 GW solar and 36 GW wind). The study examines how the system responds at a number of extreme snapshots involving very high nonsynchronous renewables penetration levels (i.e. wind and solar energy). At these levels, conventional power plants are displaced, thereby pushing down the inertia limits that play a key part in ensuring the Japanese power system's frequency stability.

The study simulates frequency stability and power flows for Japan's western and eastern synchronous areas. Additional analysis was carried out on the extent to which system stability is boosted by VRES-based fast frequency response (FFR) services and by the provision of fast ancillary support using the HVDC interconnection between the eastern and western synchronous areas, which is already in place to cope with certain emergency situations.

Particular emphasis was placed on developing a transparent methodology that could address two major challenges facing countries undertaking studies on renewables integration: (1) significant constraints on data availability (despite the improvements initiated by Japan's energy regulator), and (2) the need to establish a sustainable tool chain for the purposes of modelling and simulating the power system – particularly for third parties wishing to conduct independent research. All of the input and output data generated during the course of this project are hereby made public. We intend this study to contribute to further discussion on renewable energy integration and data transparency.[1]

The Japanese system can accommodate a larger proportion of variable renewables in the energy mix than is currently provided for in the government's 2030 targets, while still maintaining grid stability.

On conservative assumptions, this study suggests that the use of renewables-based FFR services may allow instantaneous variable renewables penetration levels to rise to around 70% in western Japan and up to 60% in the eastern synchronous area, while still

1 The dynamic investigations undertaken in this project are based on the bulk power system models for Japan provided by the country's Institute of Electrical Engineers (IEE model). The IEE model used for this analysis is a simplified model of the Japanese power system. An analysis based on a more detailed model would likely improve the quality of the results.

maintaining frequency stability within tolerable ranges.[2] These figures imply that even greater renewables penetration may be possible in certain regions. In the absence of fast frequency response (FFR) services, instantaneous penetration levels would only reach around 60% in western Japan and 50% in eastern Japan. These assessments confirm the trends observed in 2018 in regions such as Kyushu and Shikoku, where hourly VRES infeed already covers 84% and 79%[3] of demand, respectively (and accounts for over 55% of production). By 2030, these high regional infeed levels could become the norm for the Japanese system as a whole.

Instantaneous infeed levels above these thresholds would begin to challenge the system's frequency stability limits. This situation would only rarely ensue in the more ambitious renewables scenario, however, and would almost never occur in the governmental scenario. One solution could therefore be to introduce instantaneous penetration (SNSP) limits and curtail renewables infeed above these thresholds. This approach would lead to curtailment levels of under 2%[4] of annual renewable generation in the more ambitious renewables scenario.

The analysis implies that, on conservative assumptions concerning renewable energy developments, the annual share of renewables in Japan can be increased to at least 33%[5] by 2030, while still maintaining grid stability within a tolerable range and without additional transmission line reinforcement.

A higher renewable share of 40%[6] could also be achieved on the same stability limit assumptions (SNSP limit of 60% VRES in eastern Japan and 70% in western Japan) with only a very small increase in the curtailment level to 4% of annual renewable generation. Such a scenario would be possible even on the assumption of a significant reduction in conventional thermal generation (i.e. coal and nuclear) by 2030. Furthermore, given the rapid growth of renewables over the last 5 years, even the 40% share would seem a conservative figure and could be reached before 2030.

In order to further expand variable renewables, it is necessary to consider the additional measures that might be adopted to maintain system stability. These should be implemented in the form of ancillary services (such as FFR or virtual inertia) and may be provided by a range of technologies such as batteries, variable renewables, conventional power plants, synchronous condensers, HVDC links, demand response, and flywheels.[7] Modifying service provision requirements for both conventional and renewable generators is also key to improving grid stability while increasing the proportion of variable renewables in Japan.

Wind and solar energy systems can contribute to maintaining grid stability in situations where high levels of variable renewables may pose a challenge for grid operations

Maintaining power system stability is one of the most critical tasks of transmission system operators. Frequency stability must be maintained at all times, even during major system disturbances.[8] In this

2 These penetration levels do not take into account any additional technical countermeasures, except the 600 MW ancillary support delivered via the HVDC lines from the western synchronous area to the eastern synchronous area.

3 When taking into account biomass energy and hydropower during these hours, renewables satisfied close to 100% of power demand.

4 Assuming that variable renewable energy generation is curtailed above the instantaneous penetration level of 70% in western Japan and 60% in eastern Japan.

5 Corresponding to 22% wind and solar energy

6 Corresponding to about 30% wind and solar energy

7 Quantifying the benefits of these various measures would require more detailed analyses than were possible in the context of this project, given the data available.

8 Other stability criteria, such as voltage stability, rotor angle stability, short circuits, and power quality, are also relevant but were not assessed in detail in this project due to the limited quantity of publicly available data.

Frequency response after loss of 1 500 MW for western Japan +RES scenario; with and without wind and solar FFR

Figure E1

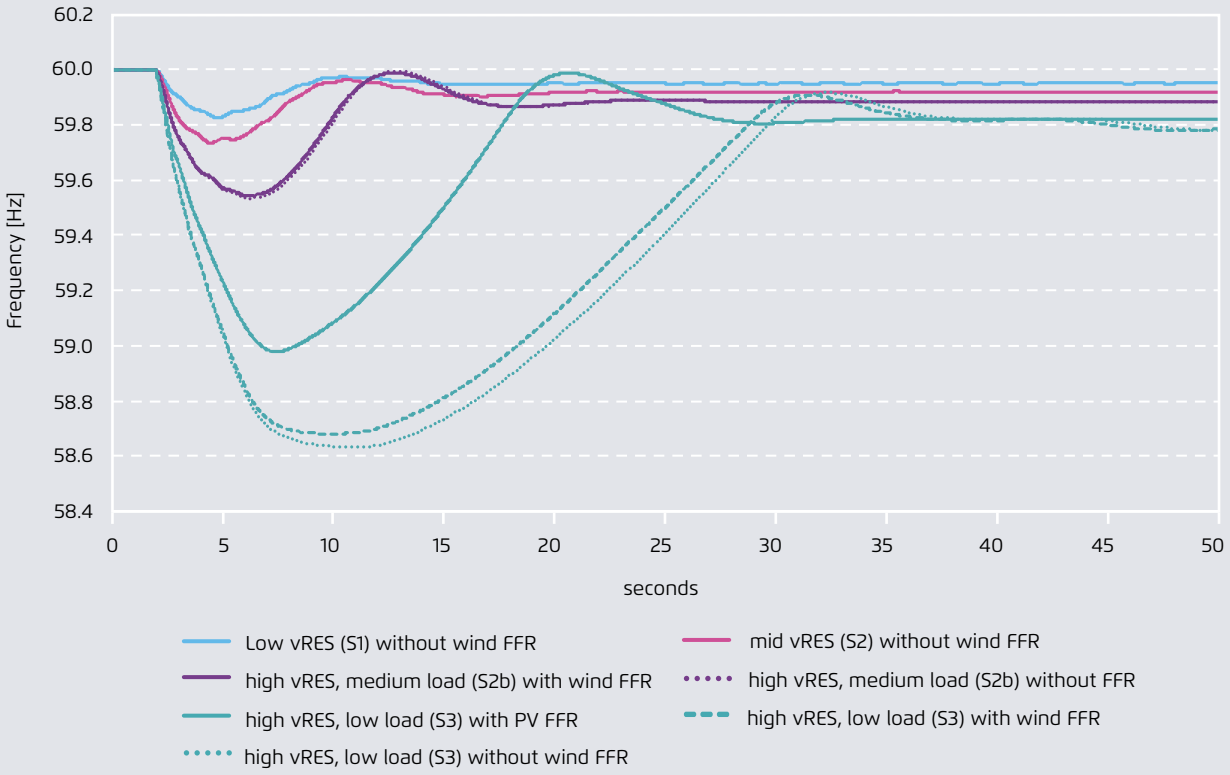

GridLab, Elia Grid International

study, frequency stability was assessed in the event of a 1.5 GW generation loss, which was identified as the extreme dimensioning reference incident. System frequency response was assessed in different snapshots involving increasing levels of variable renewables penetration (from 9% to 65%), as illustrated in Figure E1. With respect to the evaluation criteria, the system was assessed on its capacity to maintain frequency drops above 58.8 Hz in western Japan and above 49 Hz in eastern Japan (i.e. a threshold of 0.98 pu). Should the frequency nadir fall below this level, this may result in generators and loads disconnecting, which could in turn lead to local blackouts or cascade effects. Monitoring the remaining inertia in the system is important to guard against critical system states and frequency stability issues.

The results for the frequency nadir in the western area are shown in Figure E1. It can be seen here that the frequency nadir remains above the critical threshold of 58.8 Hz in snapshots S1 (9% VRES), S2 (45% VRES), and S2b (49% VRES) in the western synchronous area. This is the case when the only corrective measures applied are the remaining system inertia and primary control of thermal generators. Snapshot S3 (65% vRES) falls slightly below the critical threshold. With a minimal solar PV contribution to fast frequency service (at a total of 250 MW, which equates to only 0.75% of the actual PV infeed), however, the system can maintain the frequency nadir within the safe operating area (i.e. above 58.8Hz). This highlights the positive impact of VRES-based FFR services in this particular case.

Evaluation of the frequency nadir for the western synchronous area — Figure E2

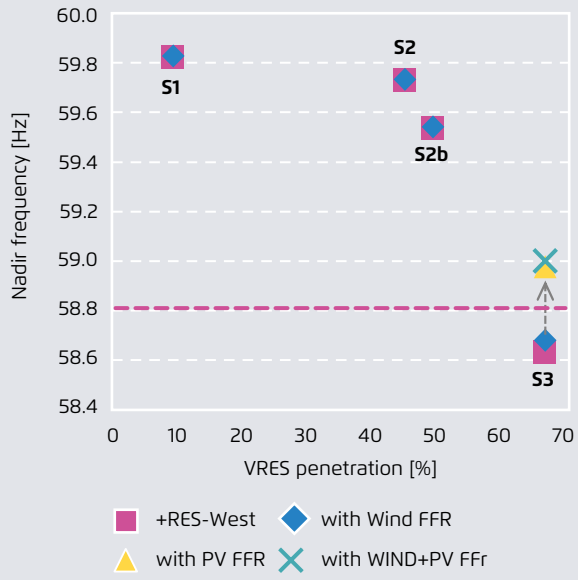

GridLab, Elia Grid International

Nadir frequency and VRES penetration in eastern Japan with and without the 600MW ancillary service — Figure E3

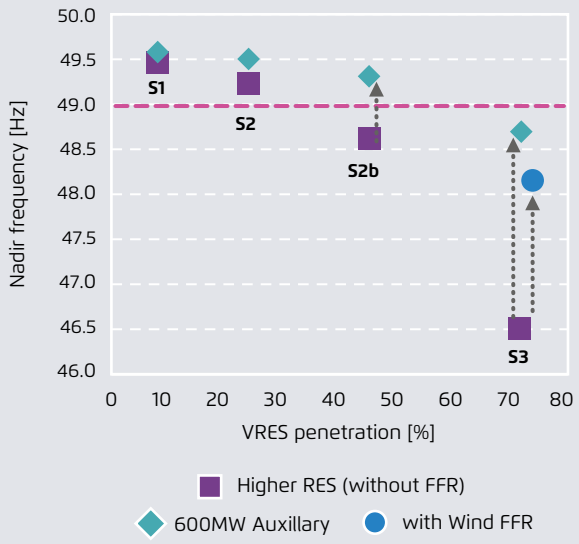

GridLab, Elia Grid International

Alongside renewables-based fast frequency response – which is not yet widespread[9] – a range of other technical solutions and modifications to service provision requirements may be implemented to improve grid stability. The technologies that may be employed include ancillary support via HVDC lines, synchronous condensers (created for example by converting decommissioned nuclear reactors[10]), demand side response, and batteries. In Japan, the existing 600MW ancillary support delivered by the HVDC lines from the western synchronous area to the eastern area help to mitigate the loss of frequency in the system. The contribution made by this service to renewable energy integration has been assessed in detail in this study, as can be seen in Figure E2.[11] Snapshot 2b again shows how critical situations can be mitigated and how the nadir can be raised above the critical threshold of 49.0 Hz. In snapshot E3, the nadir remains below the critical threshold, yet it can be raised by a remarkable 2.2 Hz. Similarly, fast frequency response from wind turbines (wind FFR) can maintain frequency levels above 48.0 Hz.

9 The technology already exists but since it is not yet required in most markets, its deployment is limited to a few systems which have very high levels of variable renewables (such as Denmark and Ireland).

10 Such a transformation was undertaken at the Biblis A power plant in Germany, after the electricity generating part of the nuclear reactor was definitively switched off.

11 In order to demonstrate the effect of this mechanism, only the eastern synchronous area was investigated. During the critical snapshots, power flowed from east to west which suggests that an additional injection from west to east would also be possible.

Wind and solar PV deployment have a significant impact on intraregional and interregional load flow. While line loading may decrease in some regions, it is expected to increase in other parts of the system.

This study also investigates the impact of increasing renewables penetration on load flows at the inter-regional and intraregional levels.[12] Aggregated results for the higher RES scenario are given in Table 1, which shows the loading tendencies for interregional lines. These tendencies are divided into three categories: increasing, decreasing and same range.[13] An increase indicates a potential need for grid reinforcement but could also highlight the benefits of improving operational practices. Indeed, higher loads could be achieved in some cases by delivering higher grid capacities (NTC values) to market participants participating in cross-regional exchange. While a detailed evaluation of grid reinforcement measures would call for further investigation,[14] our study shows that the power flow from Kyushu to Chugoku and from Chugoku to Kansai increases in response to an increase in variable renewables penetration. By contrast, power flow from Shikoku to Kansai and from Hokuriku to Kansai decreases. These trends are to be expected, since the significant solar PV installations in Kyushu, Chugoku, and Shikoku serve to reduce the import dependency of these regions' and turn them into net exporters. Finally, increased VRES penetration is accompanied by an increase in exports via the Hokkaido – Tohoku and Chubu – Tokyo HVDC links. Both links are at their maximum loading in the highest VRES penetration snapshots.

Line loading tendencies at higher RE levels — Table E1

Interconnection	Loading tendency
Western area	
Chugoku to Kyushu	Increasing
Shikoku to Chugoku	Decreasing
Chugoku to Kansai	Increasing
Hokuriku to Kansai	Decreasing
Kansai to Chubu	Same range
Shikoku to Kansai	Decreasing
Eastern area	
Tohoku to Tokyo	Increasing
HVDC links	
Hokkaido – Tohoku	Increasing
Chubu – Tokyo	Increasing

GridLab, Elia Grid International

The study further assessed the impact of greater renewables levels on the general loading on the meshed[15] transmission lines within each region. The results for the higher RES scenario are shown in Table E2. In general, we can observe that in certain regions (such as Kyushu, Chugoku, Shikoku and Tohoku), the line loadings and thus the need for energy transmission increases. This indicates a potential need for grid reinforcement. In certain regions, however, the average line loading decreases. This is due to the fact that, in these regions, consumption and generation are moving closer to each other as installed capacities and the overall share of renewables in the energy mix increase.

12 Due to a lack of data in the public domain, our load-flow analysis was only able to assess line loading tendencies.

13 A change within the same range is a loading difference of up to 100MW.

14 This would require greater transparency and improved data access.

15 Meshed lines were chosen here because they more clearly indicate the need for additional energy transportation. In contrast to feeder or generator lines, reinforcement is triggered only by additional generation capacities.

Line loading tendencies by region in response to higher RE levels — Table E2

EPCO region	Loading tendency
West	
Kyushu	Increasing
Chugoku	Increasing
Kansai	Decreasing
Hokuriku	Decreasing
Chubu	Decreasing
Shikoku	Increasing
East	
Tohoku	Increasing
Tokyo	Decreasing

GridLab, Elia Grid International

Variable renewables can deliver some of the additional ancillary services required, particularly additional reactive power

Increased penetration of inverter-based renewable technologies (predominantly consisting of wind and solar power) has the effect of displacing conventional synchronous machines (i.e. coal, nuclear and gas power plants). This displacement of thermal generation not only has implications for frequency stability but also for ancillary services that are important in ensuring system reliability, such as reactive power/voltage support, control power, short circuit currents, and system restoration. The study gives an indication of how high renewables infeed levels in Japan may affect demand for reactive power. The overall results are given in Table E3.[16]

Additional reactive power demand in the +RES scenario — Table E3

	+RES scenario			
	West		East	
	Q_L (Mvar)	Q_C (Mvar)	Q_L (Mvar)	Q_C (Mvar)
Low RES (S1)	–	1,300	–	–
Med. RES (S2)	–	1,000	–	–
High RES (S3)	220	180	740	1,960

GridLab, Elia Grid International

It can be seen here that the additional demand for reactive power remains within a moderate range of < 2GVAr in the eastern and western areas. This range is moderate to the extent that 2GVAr represents only a small fraction of the assumed renewable energy installations of 36GW of wind and 100GW of PV. State-of-the-art wind farms and PV solar parks also have a default feature that allows them to provide reactive power. On the conservative assumption that variable renewables can contribute only 10% of their installed active power in the form of reactive power (i.e. 100GW of PV can provide 10GVAr of reactive power) the additional 2GVAr of reactive power demand can easily be satisfied by VRES. Variable renewables may then actively contribute to reactive power management (along with other ancillary services such as control power).

Non-discriminatory market rules, enhanced transparency, and state-of-the-art operational and planning practices can facilitate the integration of variable renewables in Japan

In light of the experience of various other countries, a number of recommendations can be derived from our analysis. These recommendations aim to facilitate the integration of renewables at a reduced cost while maintaining a high level of reliability in the power system.

16 Q_L indicates demand for inductive reactive power; Q_C for capacitive reactive power.

Recommendations for policy planners and regulatory bodies

- **Implement non-discriminatory market rules for renewable integration:** consider the potential role of RES in ancillary services such as balancing markets and reactive power provision. This would boost the new business case for RES and allow RES to assume greater responsibilities within the power system as a whole.
- **Foster data transparency** to enable third parties to carry out meaningful studies on the Japanese energy sector. This will eventually result in more robust debate and help to raise public awareness.
- **Encourage further power system studies involving independent parties:** Integrating renewables is an interdisciplinary project and further studies should be conducted on congestion management, adequacy, market integration, operational planning adaptation, connection requirements, and system defence.

Recommendations for system operators

- **Establish inertia monitoring:** inertia is a key parameter in ensuring system stability. By monitoring it, system operators can actively limit the consequences of frequency deviation incidents.
- **Integrate renewables into ancillary service provision**: system operators can make use of the capacity of VRES to maintain frequency stability and provide balancing power and voltage control. In all such cases, system operators should diversify their portfolio of service providers.
- **Increase the transparency of the grid and power system data** required for long-term planning.

Recommendations for renewable developers

- **Anticipate grid service requirements:** the Japanese energy sector is set to undergo major changes in the near future as a result of unbundling and the establishment of new markets. Developers should actively define their role in this process and seek out new opportunities.
- **Explore the additional services renewables may provide:** renewable energy sources are already capable of providing other services beyond mere energy supply. We recommend carrying out further studies and defining use cases for services such as FFR, balancing, and reactive power. This will allow innovative solutions to be developed for the benefit of all parties.

1 Introduction and overview of the project

Japan has a reasonable share of renewable energies in its power mix: 17% of its annual electrical energy is supplied by renewables, including hydropower. While the overall proportion of variable renewables (i.e. solar and wind) is increasing, it remains rather low at 6.6% (REI, 2018). The government has set a renewables penetration target of 22–24% of power production by 2030 (METI, 2018); a 2050 target has not yet been established. Concrete plans for major electricity sector reforms, including unbundling and a transition toward market-based approaches, have been developed as a means of facilitating the policy goals. There is nonetheless concern about how efficiently the Japanese power grids will manage the integration of renewables in light of current practices for grid security assessment and grid management.

One particular concern is the impact of high levels of variable renewables (VRES) on system frequency stability. Experience has shown that this can be a critical issue in some island systems like those of Ireland, the UK, and the Nordic synchronous systems, i.e. systems with no alternating current (AC) interconnection with neighbouring systems. Several studies have been conducted on these power systems (Entso-E, 2018, Eirgrid). This situation may also pose a challenge for Japan, particularly if the country speeds up the introduction of VRES beyond its current targets. The Japanese power system is comprised of three main AC synchronous areas (eastern Japan, western Japan and Hokkaido) interconnected via a high voltage direct current (HVDC) connection, and is not yet internationally interconnected.

International experience has shown both that renewables growth can occur at an unexpected rate and that several technical grid management solutions can be safely applied to deal with this growth that are not yet widespread in Japan. While it is true that VRES pose new grid management challenges, these energy sources can also contribute to improving grid security by means of technical solutions such as fast frequency response (FFR) from solar and wind power plants. Nevertheless, there are few studies on renewable grid integration in the public domain that address these aspects of the Japanese power grid. This is mainly due to the inaccessibility of asset data and information concerning the operational practices of the incumbent grid companies that would be necessary to conduct meaningful studies. Although data transparency is constantly improving,[17] the grid data required to carry out accurate power flow simulations are not made available for third parties to conduct independent studies.[18] Despite these constraints, however, several studies[19] have attempted to reconstruct grid models in order to carry out power flow and frequency response (stability) simulations.

Against this backdrop, Japan's Renewable Energy Institute (REI) and Agora Energiewende sought to bring together various stakeholders in the Japanese

17 Data recently made public include hourly active demand (available from each electric power company's website (e.g. TEPCO, 2018)), the installation capacity of the conventional power plant fleet (FEPC, 2018) and of renewables (METI, 2018), hourly solar radiation, and wind velocity data (Japan Meteorological Agency, 2018)

18 Japanese EPCOs that own and manage transmission systems in each area, have not disclosed all the information pertaining to those systems. The EPCOs have provided this information to OCCTO which will not disclose it to third parties or support verification by independent models.

19 (Sugiyama, Komiyama, & Fujii, 2016) and (Tsujii, Tsuji, Oyama, Nakachi, & Chand Verma, 2016).

power industry[20] to gather data, validate modelling and simulation results, and apply progressive technical assessment methods for integrating renewables. As part of the study, a methodology and tool chain were established for the purposes of analysis, covering data collection and processing techniques, scenario and snapshot building, dispatch simulation, grid model construction and validation, data reformatting, transfer automation between simulation tools, and approaches to evaluating results.

Chapter 1 provides an overview of the type of analysis performed in this study, namely frequency stability analysis and load flow analysis.
Chapter 2 outlines the methodology used to establish the grid model, to derive appropriate scenarios for 2030, and to set the different VRES penetration levels for the snapshots (i.e. dispatch simulations). The tool chain constructed for this study consists of the SWITCH model[21] for dispatch simulation and a PowerFactory grid model[22] for power flow and frequency response (stability) simulations. It is expected that the tool-chain will be further refined in future as data availability improves in Japan.[23]

Chapter 3 sets out the main findings of the analysis. With respect to frequency stability, it indicates the VRES penetration levels that can be accommodated by the eastern and western synchronous areas without additional technical measures and without compromising the elements of grid security evaluated here. We simulated dynamic frequency stability and tested the system at selected snapshots involving different demand and VRES penetration levels. Chapter 3 also investigates the extent to which VRES may contribute to frequency stability, since it is expected that VRES may also support ancillary services in future. In Chapters 4 & 5, the study is brought to a close with a number of conclusions and recommendations for relevant stakeholders in the Japanese power sector.

The study aims to be transparent in terms of its methodology and data usage. The technical annexes provide detailed information allowing readers to more thoroughly investigate particular topics.[24] This information is necessary to facilitate a technical dialogue on these topics and to allow a broader audience to participate in it.

20 The stakeholder group included academic researchers who authored referenced studies, members of relevant associations in the renewables industry. Interviews were also conducted with representatives from METI, OCCTO and EPCOs.

21 http://switch-model.org/

22 https://www.digsilent.de/de/powerfactory.html

23 Due to a lack of accessible data, it was not possible to assess several important aspects of renewables integration in this study. These included the following in particular: congestions and congestion management, adequacy, short circuit power provision and protection mechanisms, local voltage stability, balancing issues in the future scenarios, the market integration of renewable energy sources, system defence and system restoration processes, and changes to operational processes and operational planning process due to higher levels of VRES. Further studies are planned in order to shed light on these issues.

24 The annexes provide detailed information on the following topics: background information on the tool chain used in this study, a description of the dispatch model (SWITCH MODEL) used, a detailed description of the scenarios developed in the study, further details on the different snapshots, remarks on methodological procedures and model validation, control strategies for VRES frequency support; remarks on the Power Factory simulation model, the VRES distribution applied in the 2030 scenarios, and dispatch rules in Japan for 2018.

2 System stability and load-flow analysis: an overview

2.1 General overview of system stability

Maintaining power system stability is one of the most critical tasks of transmission system operators. The increased use of variable renewables (VRES) in power systems worldwide has begun to raise concerns over their impact on system stability. International experience in countries such as Germany, Ireland, and Denmark has nonetheless shown that a number of technical grid management solutions can be safely applied when the proportion of renewables in the energy mix increases.

Power system stability refers to the capacity of an electric power system to regain a state of operating equilibrium after being subjected to a physical disturbance. In order to evaluate system stability, the dynamic (or transient) behaviour of the system is analysed after a triggering event for a certain period, usually lasting a few seconds (see Figure 1). Typical triggering events include short circuits, loss of transmission lines, loss of generation, and loss of loads.

Following a triggering event, a power system leaves its steady state. Key physical values such as frequency, voltage, generator rotor angles, and current then begin to change. In order to ensure stable operation, each of these values must remain within a safe operating range (i.e. between the upper and lower limits for the different values). In this case, no assets will be damaged and no serious consequences will ensue for the power system (such as local blackouts, system-wide blackouts, system splits or further asset disconnection). As Figure 1 illustrates, there are generally three possible transitional states:

Steady state transition — Figure 1

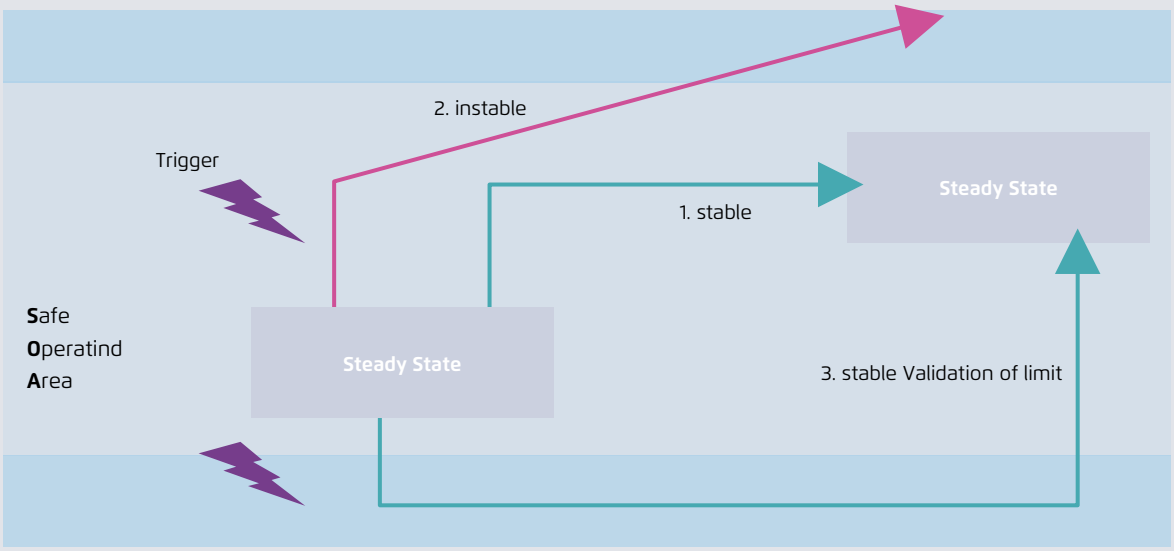

EGI (2019)

1. A transitional state in which all of the observed values stay within their defined safe operating range. In such a case, the system is considered stable.
2. A transitional state in which one or a number of values temporarily leave their safe operating range, but then return to it and remain there, allowing for steady state operation. In such a case, the consequences of the temporary boundary violation must be investigated in more detail.
3. One or more monitored values permanently leave the safe operating range. In such a case, the system is considered unstable.

System stability can be broken down into 3 categories (see Figure 2), depending on which value is monitored: voltage stability, rotor angle stability, or frequency stability. In this study, we only evaluated frequency stability, though all of the above are generally affected in the event of a power system disturbance.

Voltage stability

Voltage stability assessments evaluate the local behaviour of voltage at specific busbars in a power system. Voltage violations are critical, since they may trigger protection devices and some generation sources or consumers may be disconnected from the system. Voltage violations may be transient, as in the case of a switching event or a short circuit, or may occur in the steady state as a result of the specific load flow.

Rotor angle stability

The rotor angle may function as a monitoring value for synchronous generation units. The violation of a rotor angle limit may cause a generator to trip or may destabilise other synchronous generators nearby.

Frequency stability

Unlike voltage, frequency is a global monitoring criterion. Within a synchronous area it can generally be considered equal at each substation. It should nonetheless be noted that in larger synchronous areas such as Continental Europe, frequency can vary under certain conditions, and frequency oscillations (which should be addressed by further studies) can occur. Since the geographical extent of the Japanese synchronous systems is smaller than those of Continental Europe, this effect is not taken into account in this study.

Power system stability overview — Figure 2

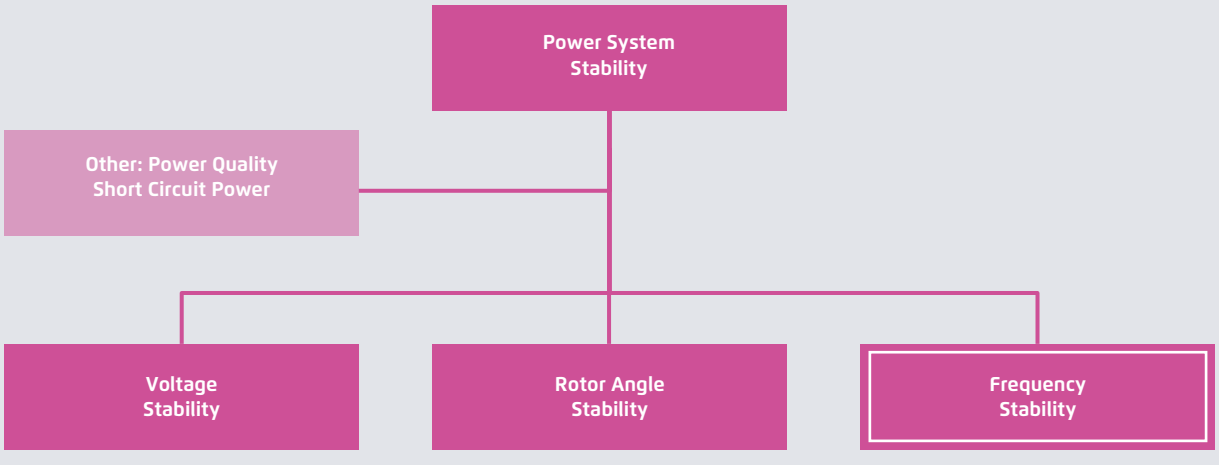

EGI (2019)

Short circuit power and power quality
In a broader sense, short circuit currents and power quality can also be considered as stability criteria.

The **short circuit** current at a specific point in the network is an important parameter when conducting protection studies (i.e. obtaining tripping thresholds for protection equipment). It needs to be ensured that, at any point in time, the online generation units are able to provide enough short circuit currents to trigger the protection devices in such events.

Power quality, on the other hand, refers to the purity of the sinusoidal voltage. In every power system, the voltage contains some harmonics, i.e. sine waves with a multiple frequency of 50/60 Hz. Up to a certain point, this is not a problem, yet if the level of harmonics becomes too high, sensitive consumers may be disconnected and the system's resonant frequency might be reached.

2.2 Frequency stability

Frequency stability is the capacity to maintain the frequency of the transmission system within tolerable ranges in the N-Situation,[25] especially after a disturbance. The electric frequency of the system is expressed in Hertz and can be measured in all parts of the synchronous area.[26] In the Japanese power system, there are 3 synchronous areas, which have a nominal frequency of either 50 Hertz (eastern Japan and Hokkaido) or 60 Hertz (western Japan).

The system operators of a given synchronous area are responsible for maintaining frequency stability by any means and under all circumstances; frequency is therefore heavily monitored. The main question at issue in this analysis is the extent to which the frequency deviates in certain incident cases. A deviation is caused by an imbalance in the current load and demand situation in the power system. Small deviations in system frequency are normal and as long as they remain within an appropriate tolerance band are not a cause for concern. Excessive deviations, however, cause generators and consumers to disconnect, which can lead to local blackouts, system splits, and in the worst case scenario a total system blackout, which has to be avoided at all costs.

Figure 3 illustrates the case of a sudden loss of generation, which is considered the worst form of imbalance that can be imposed on a system (on a par with a sudden loss of consumption). This is the triggering incident that we have chosen to analyse in this study.

Directly after the incident, the frequency begins to change. The rate of change of frequency (RoCoF, which is essentially the frequency deviation over a certain period of time in Hz/s) can usually be used to monitor the impact of the incident on frequency stability.

25 An N-Situation is a situation in which one or several generation units, transformers or transmission lines disconnect from the system. This study considers the N-1 case, i.e. the situation in which one generation unit is disconnected.

26 We assume here that the frequency remains consistent in the overall system within the time frame of a few seconds, with only minor differences between different measurement locations.

Typical frequency response behaviour in the event of a loss of generation — Figure 3

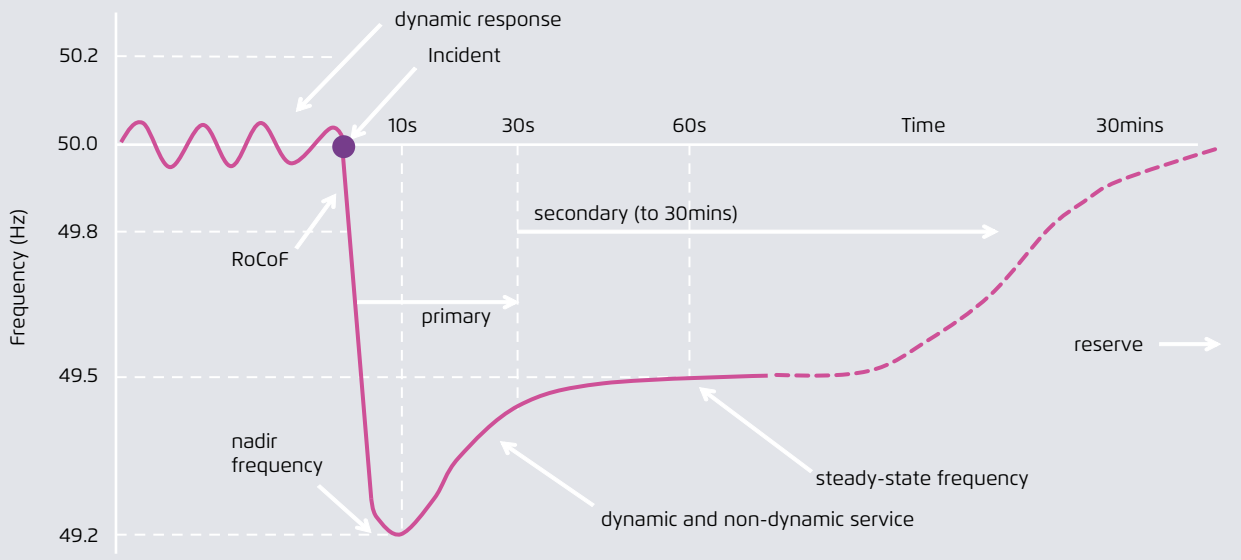

EGI (2019)

In such cases, several countermeasures usually begin to come into operation.

→ **System inertia** is a key contributor to frequency stability and constitutes the system's immediate response during the initial few seconds following an incident. Inertia is the kinetic energy stored in the rotating parts of synchronous machines. It is available permanently and can be released or absorbed instantaneously to stabilise the grid.[27] The energy exchange is inversely proportionate to the gradient of the frequency (RoCoF) and is automatically and instantaneously activated.[28] By default, non-synchronously connected generators, such as fully rated converter wind turbines and inverter-connected photovoltaic systems, do not provide this inertia. The following table provides inertia constant values for different generator types. As we can observe, condensing generators (such as nuclear and coal generators) have the highest (and similar) inertia values, which means that nuclear and coal generators make a similar contribution to frequency stability.

Inertia constant values for different generator types — Table 1

Technology	Inertia constant in GW
Steam turbines	4–9
Gas turbines	3–4
Hydro turbines	2–4
Synchronous condenser	1–1.5

EGI/Gridlab (2019)

27 For the purposes of comparison, a 1 GW turbine generator provides inertia of 3 to 9 GWs depending on the technology used.

28 All other grid stabilisation countermeasures are activated by particular triggers, which depend on a given system value such as frequency being monitored, and sometimes even on active communication between one power system monitoring system and another.

→ **Control reserves** are activated after system inertia, and serve to prevent a further drop in frequency:
  - Primary control is the fastest reserve, and is usually activated within a few seconds.
  - Secondary control is activated second. The requirements on its activation time are not as strict as for primary control and its activation period is longer.
  - Potential reserves requiring a longer activation period can also be incorporated into a system where needed (e.g. tertiary reserves or restoration reserves).

The system inertia and the activation of control reserves prevent the frequency from dropping, and the frequency turning point or nadir is usually reached during the activation time of the primary reserve. A steady state deviation point is then reached, and is usually brought back to nominal frequency by the activation of subsequent reserves. Depending on the reserve requirements in place and the size of the incident in the synchronous area, this can take up to several minutes.

2.3 Overview of load flow analysis

A load flow analysis determines the electrical flow in a power system resulting from generator infeed and the energy consumption of loads within the system. The actual load flow depends on the further physical parameters of the transmission elements, and predominantly on its impedance.

In contrast to a stability analysis that would assess the dynamic behaviour of a power system, a load flow calculation always evaluates the steady state of a power system, i.e. a single instant or snapshot in which demand and the power provision from generation units is constant. Frequency is considered constant, as is substation voltage.

In this study, we performed a power flow assessment in order to identify those line and load flow corridors that are affected by a greater proportion of renewable installations and a lower proportion of conventional generation units. We analysed both interregional line connections and intraregional lines.[29] In the intraregional line analysis, a distinction was drawn between feeder lines (coming from the generators) and meshed lines running between two substations.

Given the limited amount of data available, this analysis was subject to the following limitations:
→ The load flow simulation was only performed on selected representative snapshots, rather than on a yearly dispatch simulation.
→ Since a reduced grid model was used (see the following section) which did not include a detailed characterisation of reactive power but with a modification in terms of the installed generation fleet, the initial load flow resulted in some reactive power flow imbalances. A number of reactive power compensation elements were therefore added to obtain a convergent load flow. These elements are used to compensate for the reactive power capability loss which accompanies the displacement of thermal units resulting from increased renewables usage.
→ Since no ampacity values[30] were available for the simulation model, it was only possible to state where and in which direction the power flow changed between the snapshots.

On account of these limitations, it would be necessary to further enhance the model using the rated transmission capacities in order to obtain insights into congestion and, ultimately, specific reinforcement needs. The results are therefore only indicative.

29 The dispatch simulation was performed with certain import/export constraints between each EPCO region. This means that, where the dispatch was concerned, we assumed there was a copper-plate without any transfer constraints within an EPCO region. Transferring the result to a grid model which includes higher resolution grid constraints within the EPCO regions allowed us to identify highly loaded intraregional transmission lines.

30 Ampacity is the current in amperes that can be permanently carried on a transmission line or cable without the line or cable being damaged.

3 Overview of the model set-up and scenarios

The entire modelling and simulation process is shown in Figure 4. Further details are given in the Annex. Publicly available data was gathered to build the models and inputs for the scenarios. In order to simulate the system's power flow and frequency response at a high renewables penetration level, we selected situations expected to place the grid under stress, including those involving high demand and high levels of renewables on the one hand, and low demand and high levels of renewables on the other. While it is possible to simulate the dispatch in these situations in the grid model itself, a conscious decision was made to simulate the dispatch in a separate tool, in order to establish a robust tool chain approach. The dispatch in each scenario was therefore simulated using the SWITCH model of the Japanese power system developed by REI (2015). Four snapshots representing a range of situations expected to place the grid under stress were then selected. Demand and generation outputs corresponding to these snapshots were subsequently applied to the Power Factory grid model. On the basis of the grid model, the following aspects of each snapshot were evaluated:

- → Power flows in the transmission grid;
- → Frequency responses following the sudden loss of a large generator in Japan's eastern (50 Hz) and western (60 Hz) frequency zones;
- → The impact of ancillary service provision by wind and solar power plants on frequency response;
- → The impact of the 600 MW ancillary frequency control support provided via the high voltage direct current (HVDC) interconnection between eastern and western Japan (OCCTO, 2016).

Overall modelling and simulation procedure — Figure 4

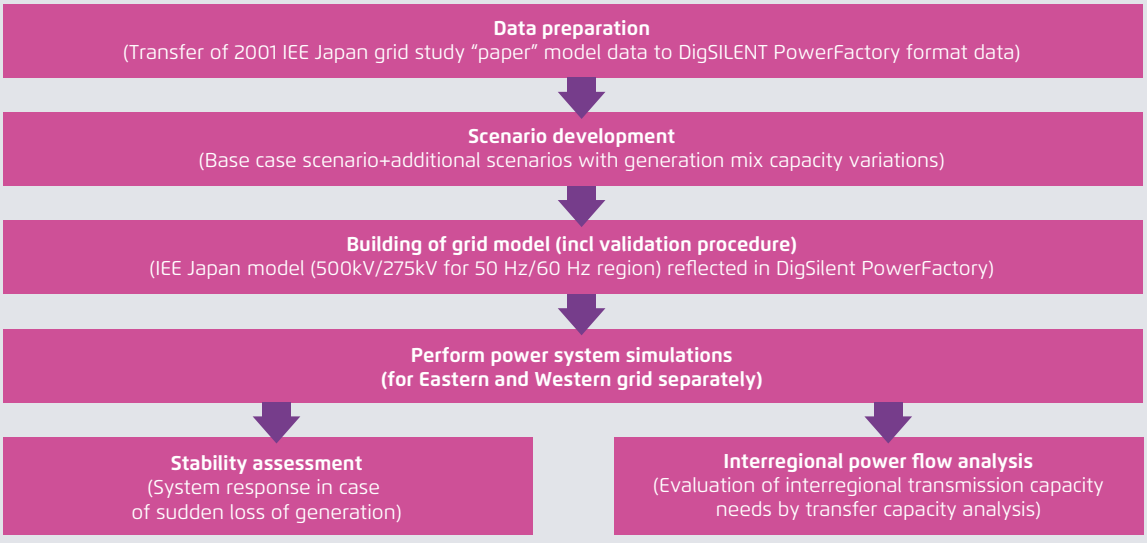

EGI (2019)

3.1 Grid model

Detailed grid data remains the property of each EPCO region and was unfortunately not made accessible for this study. In order to build a grid model from scratch, we used publicly available data from the IEE model.[31] The IEE model was first implemented in DIgSILENT PowerFactory (see Annex 5 for a detailed account). Figure 5 illustrates the shape of the study grid model for the eastern network.

3.2 The scenarios

The study compares the impact of renewables on the grid for two scenarios in 2030: the **government scenario** (GovS) and the **higher RE scenario** (+RES). GovS is based on the government's plan (METI, 2015) and assumes installed capacities of 64 GW solar and 10 GW wind, while +RES assumes a more ambitious uptake of renewables, resulting in installed capacities of 100 GW solar and 36 GW wind (see Table 5).

The government scenario represents the Japanese government's political targets for 2030 in terms of installed capacities.[32] In this scenario, renewables

31 The IEE (2001) model is a reduced grid model in which aggregated resistance and reactance values are given but do not contain individual line property data in terms of line numbers, type of line, line length, and ampacity. Grid data was enhanced by updating the capacities of the interconnecting lines between the EPCO regions.

32 The dispatch and grid operation assumptions made in this study may nonetheless differ from those contained in the government's plan.

Grid model for the Eastern Synchronous Area — Figure 5

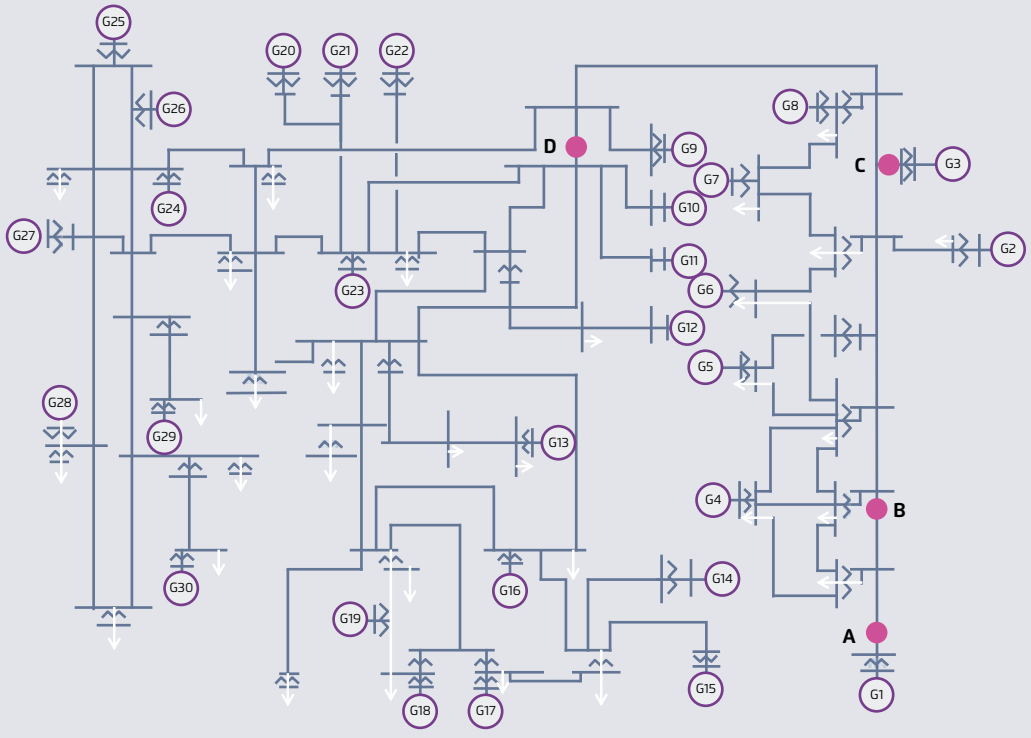

IEE Japan (2001)

would account for around 22–24% of electrical energy production.

The +RES scenario features higher installed capacities of variable renewables, which seem achievable according to the Japanese renewable energy associations.[33] These higher installed capacities result in higher instantaneous infeed situations. The scenario also assumes that there are no nuclear power plants in operation. Considered from the perspective of inertia, however, this could also correspond to a scenario in which there is a higher proportion of nuclear generation capacity in the energy mix (e.g. + 10 GW) and a lower proportion of coal (-10 GW), since both generators have similar inertial characteristics.[34] The annexes detail the methodology used to calculate the distribution of installed capacity in 2030, the operational capability of generators, and the demand levels.

Comparison of installed capacity in the GovS and +RES — Table 2

Generation type	Installed capacities [GW]		
	GovS	+RES	Delta
Solar	64	100	+34
Wind	10	36	+26
Nuclear	23	0	-23
Coal	37	37	0
Natural gas[a]	53	75	+22
Hydro[b]	52	52	0
Oil	0	0	0
Bio-energy[c]	4.7	2.1	-2.6
Geothermal	1.7	1.7	0

a. Including gas co-generation, as provided by the Advanced Cogeneration and Energy Utilization Center Japan.
b. Including pumped hydro
c. Biogas and biomass

REI (2019)

33 Japan Wind Power Association (JWPA) and the Japan Photovoltaic Energy Association (JPEA).

34 The dimensioning parameter for the frequency analysis is not the level of nuclear and coal capacities taken individually but rather the sum of both, since the inertia constants of both technologies are comparable (see Table 1). The +RES scenario is comparable to an alternative scenario in which some coal generators have been replaced by nuclear reactors located in the same area. In concrete terms, this implies that a scenario with 27.6 GW of coal-based capacities and 10.1 GW of nuclear capacities would – all other capacities remaining equal – be equivalent to the +RES scenario, in which there are 37.7 GW of coal-based capacities and 0 GW of nuclear capacities.

Figure 6 shows the installed capacities per region for each scenario. It is important to look closely at these regional capacities, since they have important implications for the simulation results. Here we can make a few initial observations:

→ In general the total installed capacities are higher in the +RES than in the government scenario, with the exception of Hokuriku, where the renewables increase does not compensate for the reduction in nuclear generation. This implies that Hokuriku may need to import more energy in the +RES than in the government scenario.
→ Solar installations are distributed relatively equally across Japan. This implies that solar power may be best used to supply local demand, rather than being transferred to serve demand in other areas and thereby burdening the transmission grid.
→ The highest concentration of wind power installations is in Tohoku in the eastern synchronous area, followed by Hokkaido (in its own synchronous area). This implies that, contrary to solar power, wind power may need to be transferred to serve demand in other areas.

3.3 Snapshot selection

In this study, we opted to evaluate representative system snapshots, i.e. individual hourly results of the dispatch simulation (SWITCH model). Situations that are expected to place the grid under stress tend to be high demand situations. In the case of renewable integration, however, high VRES penetration may also place the grid under stress, and this may occur

Installed capacities per region in the GovS and +RES — Figure 6

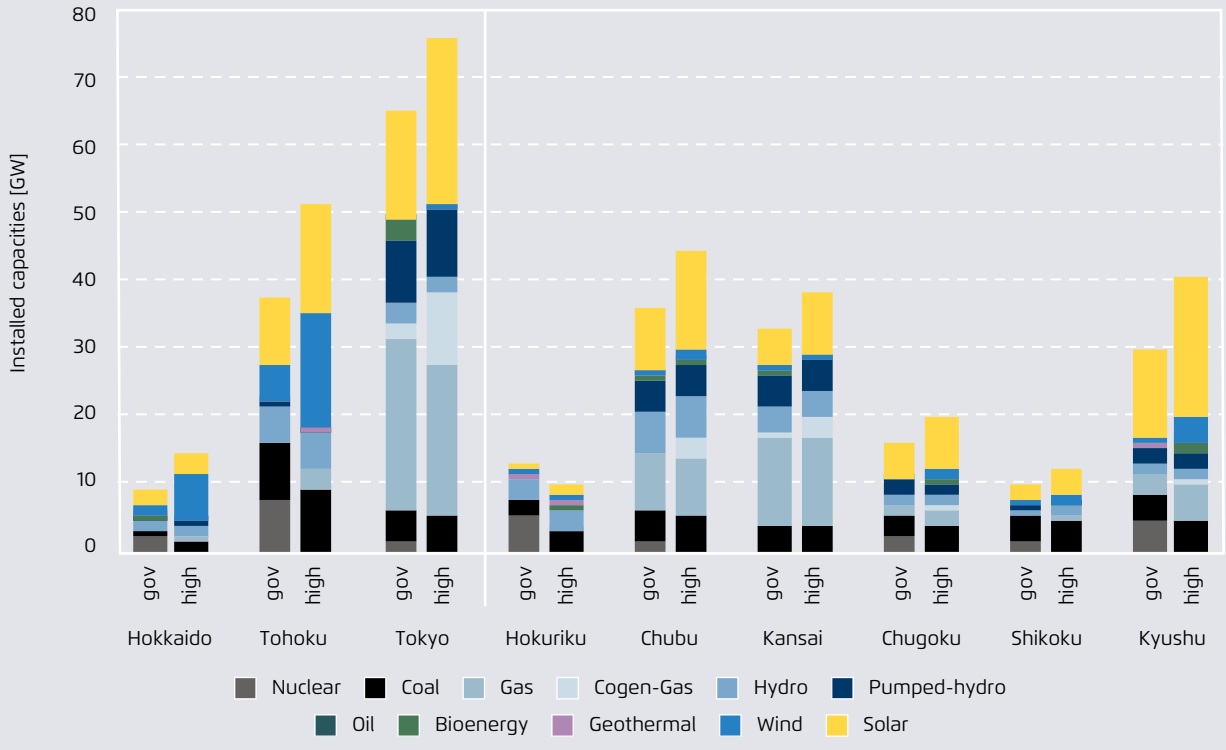

Illustration by the authors

even in a low demand situation. The following criteria were therefore applied in selecting the snapshots:

- → The snapshots should cover a wide range of VRES penetration levels
- → The snapshots should reflect different demand situations
- → The same time stamp should be selected in the different scenarios, in order to easily compare the snapshots.

The following table summarises the snapshots chosen for closer analysis:

The snapshots were chosen on the basis of an evaluation of the +RES dispatch results (288 snapshots), as illustrated in Figure 7, below. Since the +RES scenario is primarily dominated by solar power, snapshots corresponding to the peak infeed time (1 pm) were evaluated to find snapshots with high and medium VRES levels.

Snapshot 1 represents high demand and low VRES. The time of 7pm falls within summer evening peak demand, in which little contribution is made by solar power and little wind energy is generated.

Overview of the snapshots — Table 3

No.	Time stamp	Demand	RE output	RE share of consumption	VRES levelGovS	VRES level +RES
S1	Night in August 2030, 7pm	High 147 GW	Low (night)	Low	5%	9%
S2	Day in August 2030, 1pm	High 150 GW	High	Medium	22%	36%
S2b	Day in July 2030, 1pm	Medium 111 GW	Medium	Medium	–	48%
S3	Day in May 2030, 1pm	Low 90 GW	High	High	40%	69%

REI (2019)

VRES levels during peak hours (1pm) in the +RES scenario — Figure 7

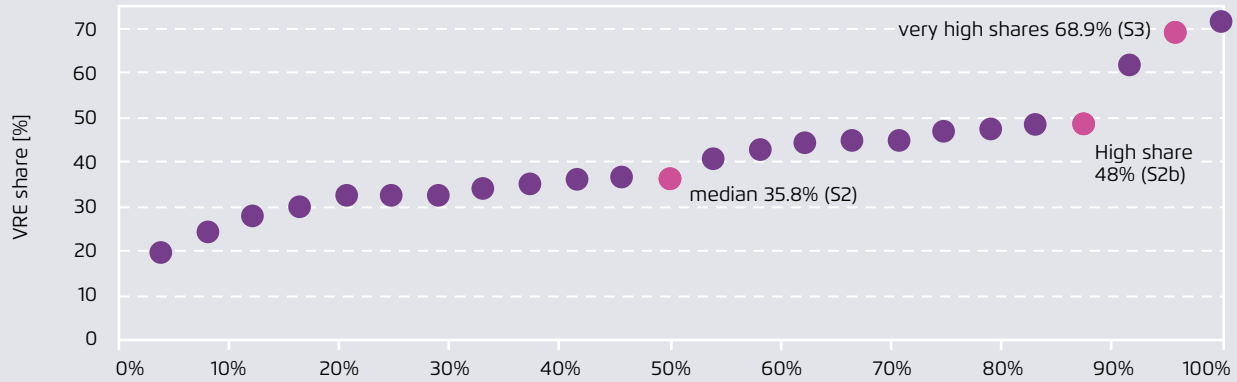

The graph shows the occurrence of snapshots below a certain renewables penetration level (in 96% of the snapshots, for example, the variable renewables penetration level is below 68.9%). The graph only shows the 24 peak hours, which is why snapshot S1 is not included, since it is in the evening

REI (2019)

Snapshot 2 represents the median of the 24 peak hour snapshots and was therefore chosen as the medium VRES snapshot. **Snapshot 3** represents a high level of VRES generation. The snapshot is in May and thus represents a probable example of very high VRES infeed in the Japanese power system. It was preferred to the snapshot where the level of renewables is highest because it better fits the higher load requirement (108 GW compared to 97 GW in the snapshot with the highest renewables level).

In addition, snapshot 2b was chosen after extensive analysis of Snapshots 2 to 3. The aim of this snapshot is to gain additional insights into system behaviour for a system state involving a VRES level intermediate between snapshots 2 and 3. Dynamic stability in snapshot 2b was assessed only in the +RE scenario.

Four snapshots provide a solid basis for our frequency stability analysis assessment, since the wide range of VRES levels (5–69%) has a direct impact on the remaining inertia, which functions as an important stability indicator. The following points are important to note concerning the snapshots in general:

- In general the infeed from VRES is higher in the +RES than in the GovS. This implies that higher VRES capacity displaces infeed from conventional power plants in all regions, and particularly affects regions with higher installation capacities (such as Kyushu and Tohoku).
- In general, instantaneous VRES penetration is higher in western Japan than in eastern Japan due to the higher number of solar installations. An exception is +RES snapshot 3, where infeed from wind power located mainly in the eastern area is also high.
- Kyushu region is by far the region with the highest VRES penetration (mainly solar). In snapshot 3, where wind power infeed is also high, Tohoku and Hokkaido reach VRES penetration levels above 80% of total regional production.
- Where present, pumped hydro is producing electricity in the low VRES snapshots while it switches to pumping mode in higher VRES snapshots.
- Higher VRES penetration snapshots result in higher import/export levels between EPCO regions. While Hokuriku and Shikoku are the only exporters in the low VRES situations, regions with higher VRES installations become exporters as VRES penetration increases.
- The missing nuclear generation in the +RES is almost exclusively replaced by VRES. This can be seen most clearly in the Kyushu and Tohoku regions. The Hokuriku region exports nuclear power in the GovS snapshots, and ceases to export in the higher +RES snapshots.

3.4 Evaluation criteria

The frequency stability evaluations consisted of time domain simulations relating to a contingency in each frequency zone (50 Hz in eastern Japan and 60 Hz in western Japan). The largest contingency was identified as a sudden loss in generation of 1.5 GW. Eastern and western Japan were evaluated separately, since they are not synchronised and have different system frequencies. The impact of fast frequency response provision by wind and solar power plants was also assessed. This provision is important in situations where a high level of renewables penetration results in low system inertia.

One of the key aims of the analysis is to evaluate the maximum RES penetration that can be assimilated by the Japanese power system by 2030 without compromising grid stability. The frequency responses were evaluated on the basis of several key criteria: **system inertia, RoCoF, and nadir frequency:**

- **System inertia** is the kinetic energy stored in the rotating parts of synchronous generators such as coal, hydro, gas, and nuclear power plants. It is a countermeasure that is always available on an ad hoc basis. The amount of energy available, however, can vary. To this extent, it is an

important measure of normal, pre-fault system operation, since the effects of frequency deviation become more drastic when there is less inertia in the system.

→ **The rate of change of frequency (RoCoF)** for a specified time window (here 1000 ms) is also important in assessing stability. The RoCoF is a parameter that can be set as a trigger value in protection devices. Here it serves as an additional layer of security. The underlying idea is that if the RoCoF is high directly after the fault, the nadir (see description below) will also likely be high. Nevertheless, the RoCoF information is available earlier, which allows remedial actions to be triggered earlier. For further information on how the RoCoF was determined in this study, see Annex 5. In consultation with stakeholders, the critical threshold for the RoCoF value was set at 0.2 Hz/s.

→ **The frequency nadir (i.e. the largest deviation from the nominal value)** is considered here as the most important evaluation criterion. Should the frequency drop below a certain value, both generators and loads within the transmission system may disconnect. This can lead to local blackouts or cascade effects, such as when a generation unit disconnects in cases of under frequency. The worst case scenario would be a system-wide blackout. In consultation with stakeholders, the critical threshold for under frequency was set at 0.98 p.u.[35] (i.e. 49 Hz for eastern Japan and 58.8 Hz for western Japan). The 0.98 p.u. limit plays a similar operational role in Germany, since other countermeasures such as load-shedding mechanisms are activated at this point.

35 The per-unit (p.u.) system is an expression of electrical system parameters (such as frequency) in relation to a defined base value.

4 Results

This chapter presents the results of the frequency stability analysis (4.1 and 4.2), the load-flow analysis (4.3), and the reactive power evaluation (4.4).

The frequency response analysis is performed in two stages. Section 4.1 provides a detailed analysis of the frequency response (within the time domain) in key snapshots in the two scenarios. Section 4.2 draws a number of general conclusions on the basis of this analysis and seeks above all to identify critical values concerning the minimum inertia required in the system to accommodate very high renewables penetration levels.

4.1 Frequency response assessment: time-domain analysis

4.1.1 Analysis of key snapshots in the government scenario

Three snapshots were evaluated for the government scenario: low, medium, and high VRES. Eastern and western Japan were assessed separately. Each snapshot in the eastern and western areas had a unique dynamic response to the contingencies. Tables 4 and Table 5 present the snapshot results in the government scenario (GovS). The tables show that as VRES penetration increases, system inertia decreases. They also show that while wind power penetration is low in both scenarios, it is higher in the east than in the west, while solar power penetration is significantly higher in the west than in the east.

Eastern Japan's dispatch situation in the government scenario snapshots — Table 4

No.	Snapshot	Conv. gen (GW)	VRES level (%)	Wind (GW)	PV (GW)	Load (GW)	System inertia (GW*s)
S1	Low VRES | 1st Aug, 7pm	59.8	3.0	0.74	1.1	60.3	314
S2	Med VRES | 1st Aug, 1pm	53.7	13.9	0.53	8.1	61.5	281
S3	High VRES | 2nd May, 1pm	23.2	38.4	2.2	12.3	37.5	117

REI, EGI, GridLab (2019)

Western Japan's dispatch situation in the government scenario snapshots — Table 5

No.	Snapshot	Conv. gen (GW)	VRES level (%)	Wind (GW)	PV (GW)	Load (GW)	System inertia GW*s)
S1	Low VRES | 1st Aug, 7pm	79.2	5.8	0.1	4.7	82.5	444
S2	Med VRES | 1st Aug, 1pm	62.6	28.2	0.1	24.4	85.1	349
S3	High VRES | 2nd May, 1pm	30.1	41.3	0.1	21.1	48.5	162

REI, EGI, GridLab (2019)

The system frequency response (time-domain analysis, RoCoF, and nadir) following the loss of 1,500 MW of generation is given in Figures 8 and 9. Each coloured line represents a different snapshot. The simulations were performed on both the eastern and western networks with and without wind-based fast frequency response (FFR[36]). The tables below the graphs summarize the RoCoF and nadir values in the different snapshots. Values that remain within tolerable ranges are highlighted in green. Values that exceed these tolerable limits are highlighted in red.

36 This study only considers FFR and not virtual inertia.

a. Eastern network (Figure 8)

In eastern Japan, the frequency drop is maintained above the lower limit of 49 Hz in the low and medium VRES snapshots (snapshots 1 and 2, respectively). In these cases, the frequency drop is reduced even further when wind FFR is activated. In the low and medium VRES snapshots, there is active power support of approximately 73 MW and 53 MW, respectively, from wind FFR. In these cases, the frequency reaches a stable operating point after 30 seconds. It can be concluded that the available primary frequency response from conventional generators and the additional support from wind turbines is sufficient to ensure that the system returns to a stable operating point following the 1,500 MW loss of generation.

Frequency response after a 1,500 MW generation loss in eastern Japan in the government scenario

Figure 8

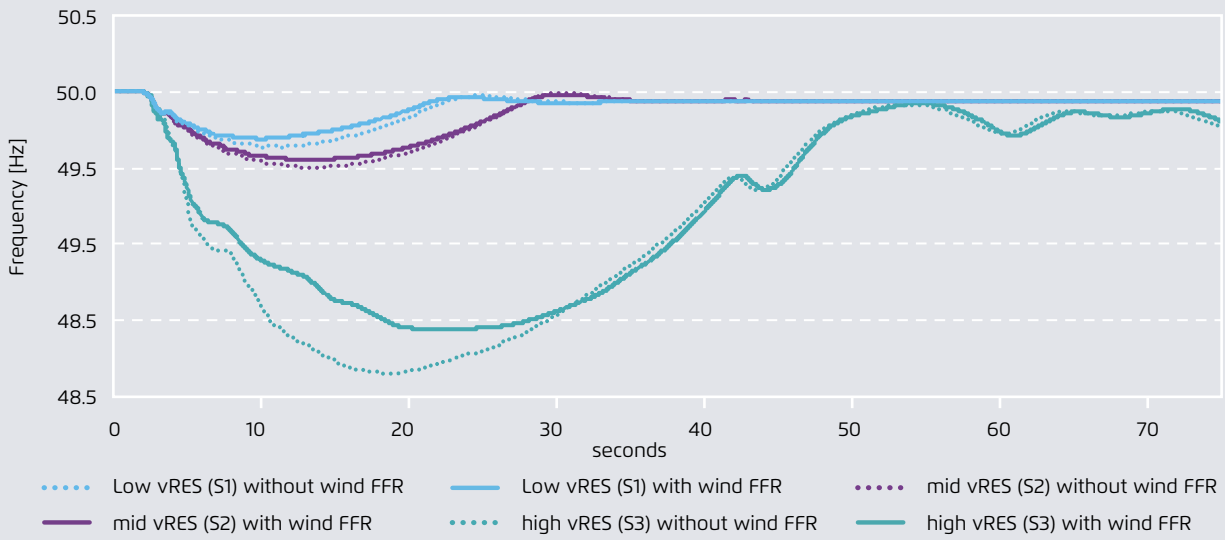

		RoCoF (Hz/s)		Frequency nadir (Hz)	
No.	**Snapshot**	**No FFR**	**Wind FFR**	**No FFR**	**Wind FFR**
S1	**Low_VRES**	-0.044	-0.037	49.64	49.695
S2	**Med_VRES**	-0.058	-0.052	49.507	49.558
S3	**High_VRES**	-0.136	-0.105	48.154	48.447

Gridlab (2019)

In the high VRES snapshot (snapshot 3), the frequency drop is significantly larger and the operational limit of 49 Hz is crossed. The RoCoF is also higher, but remains within an acceptable range. Due to the higher levels of wind penetration in the high VRES snapshot, greater FFR support is also available. Additional active power totalling approximately 216 MW is fed into the system by wind turbines. Nevertheless, the frequency does not return to a completely stable operating point, but operates at a quasi-stable level after 60 seconds. This is because the governor response from conventional generators reaches its limit, which means that there is insufficient frequency response to make the system completely stable.

a. Western network (Figure 9)

When compared with eastern Japan, it is evident that the frequency drop in western Japan is lower. This is because the level of installed conventional generation in the western area is higher. The available rotating mass and the primary reserve from these generators is therefore higher. In all three renewables penetration snapshots, the frequency drop remains above the lower limit of 58.8 Hz. The RoCoF value also remains within the tolerable range. Wind-based FFR is not significant, since wind power penetration in the western network is low. In all cases, the system reaches a stable operating point 30 seconds after the 1,500 MW generation loss.

Frequency response after a 1,500 MW generation loss in western Japan in the government scenario

Figure 9

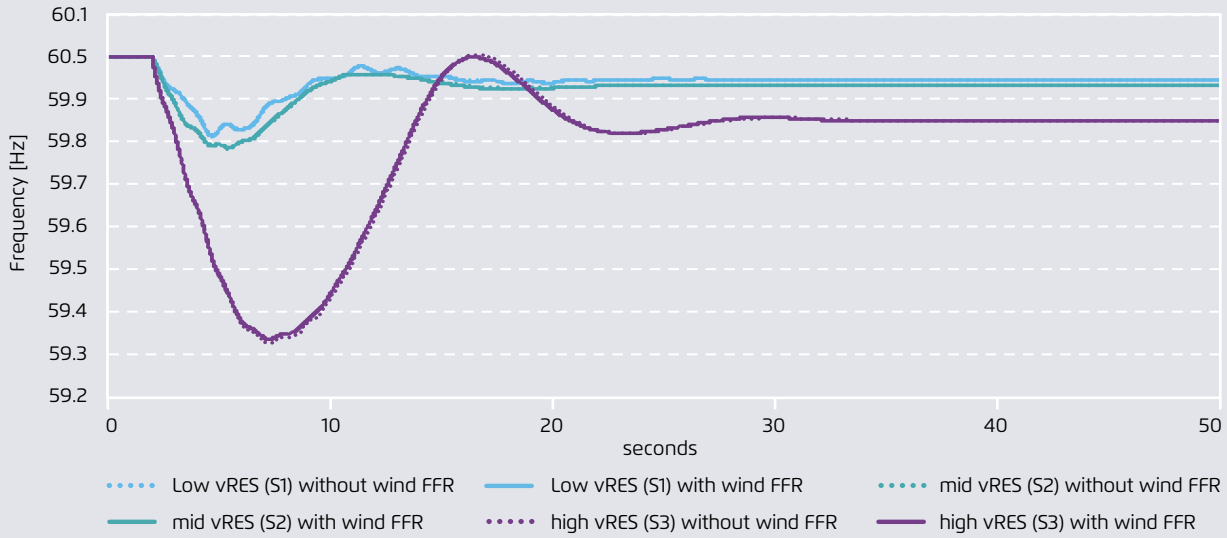

		RoCoF (Hz/s)		Frequency nadir (Hz)	
No.	**Snapshot**	**No FFR**	**Wind FFR**	**No FFR**	**Wind FFR**
S1	**Low_VRES**	-0.069	-0.068	59.812	59.813
S2	**Med_VRES**	-0.063	-0.061	59.783	59.786
S3	**High_VRES**	-0.128	-0.126	59.326	59.34

Gridlab (2019)

4.1.2 Analysis of key snapshots in the higher renewables scenario

Four snapshots were evaluated in the higher renewables scenario: low, medium, high VRES with high load and high VRES with low load. Eastern and western Japan were assessed separately. Each snapshot for east and west had a unique dynamic response to the contingencies.

Tables 6 and Table 7 provide an overview of all the snapshots in the +RES. The tables show that as VRES penetration increases, system inertia decreases. VRES penetration in the +RES is significantly higher than in the GoVS. This results in a significant decrease in system inertia.

Eastern Japan's dispatch situation in the higher RE scenario snapshots — Table 6

No.	Snapshot	Conv. gen (GW)	VRES level (%)	Wind (GW)	PV (GW)	Load (GW)	System inertia (GW*s)
S1	Low VRES | 1st Aug,7pm	56.6	7.2	2.66	1.70	60.3	298
S2	Med VRES | 1st Aug, 1pm	47.8	23.4	1.92	12.7	61.5	250
S2b	High VRES, medium load 2nd July, 1 pm	24.5	45.3	0.42	19.9	44.4	124
S3	High VRES, low load 2nd May, 1pm	10.5	72.0	7.80	19.2	37.5	57

REI, EGI, GridLab (2019)

Eastern Japan's dispatch situation in the higher RE scenario snapshots — Table 7

No.	Snapshot	Conv. gen (GW)	VRES level (%)	Wind (GW)	PV (GW)	Load (GW)	System inertia (GW*s)
S1	Low VRES | 1st Aug,7pm	75.5	9.4	0.41	7.4	82.5	422
S2	Med VRES | 1st Aug, 1pm	47.6	44.8	0.41	38.2	85.2	265
S2b	High VRES, medium load 2nd July, 1 pm	33.5	49.2	0.52	31.9	63.1	185
S3	High VRES, low load 2nd May, 1pm	18.1	64.9	0.42	33.0	48.5	97

REI, EGI, GridLab (2019)

Figures 10 to Figure 13 show the results of the system frequency response analysis (time domain analysis, RoCoF and nadir) following the loss of 1,500 MW of generation. The simulations were performed for both eastern and western Japan (i) without fast frequency response (FFR) from wind and PV, (ii) with FFR from wind and PV, and (iii) with FFR from both wind and PV.

a. Eastern network

In the low and medium VRES snapshots (snapshots 1 and 2, respectively), the frequency drop is maintained above the lower limit of 49 Hz. When wind FFR is activated in these cases, the frequency drop is further reduced. In the low and medium VRES snapshots, wind FFR provides active power support totalling approximately 266 MW and 191 MW, respectively. In these snapshots, the frequency returns to a stable operating point after 40 seconds.

In the high VRES snapshot (snapshot 3), the frequency drop is significantly larger (below 46.5 Hz) and the RoCoF rises to 0.34 Hz/s. In the high VRES/low load snapshot, higher FFR support is available due to the higher level of wind penetration. Additional active power totalling approximately 780 MW is fed into the system by wind turbines. In the high VRES snapshot with FFR support, there is a sudden change in the frequency response curve at 23 seconds. This is due to the restoration period of the wind turbines, as discussed in the FFR section (Annex 5). During the restoration period, the wind turbines lower their output by 390 MW. Finally, in snapshot 2b (high VRES/high load), the RoCoF and the frequency drop are reduced as a result of the higher levels of conventional generation and the high system inertia.

Frequency response after a 1,500 MW generation loss in eastern Japan in the higher RE scenario, with and without wind FFR

Figure 10

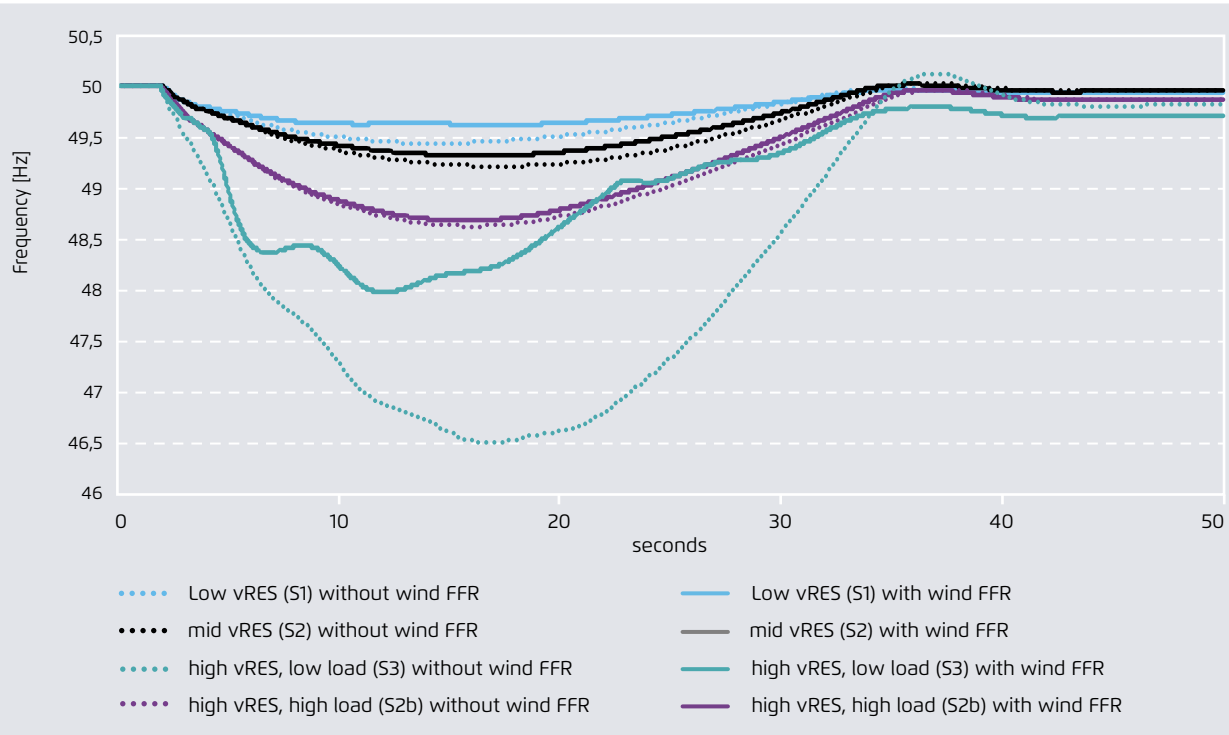

GridLab (2019)

In light of the higher frequency drop in snapshot 3 (high VRES, low load), we also considered additional frequency support from PV systems. A number of PV systems close to thermal power stations in substations in Akita, Hirono, Hitachinaka, Onagawa and Somakyodo were assumed to participate in the frequency support. To achieve the appropriate power balance, the output power of these PV systems was reduced by 20% and the additional power required was dispatched from the nearby thermal power stations. This 20% reduction corresponds to the 102 MW of active power available from the PV systems for the purposes of frequency support. Figure 11, below, compares the frequency response with and without FFR support from wind and PV systems.

Frequency response by FFR technology after a 1,500 MW generation loss in eastern Japan in the higher RE scenario

Figure 11

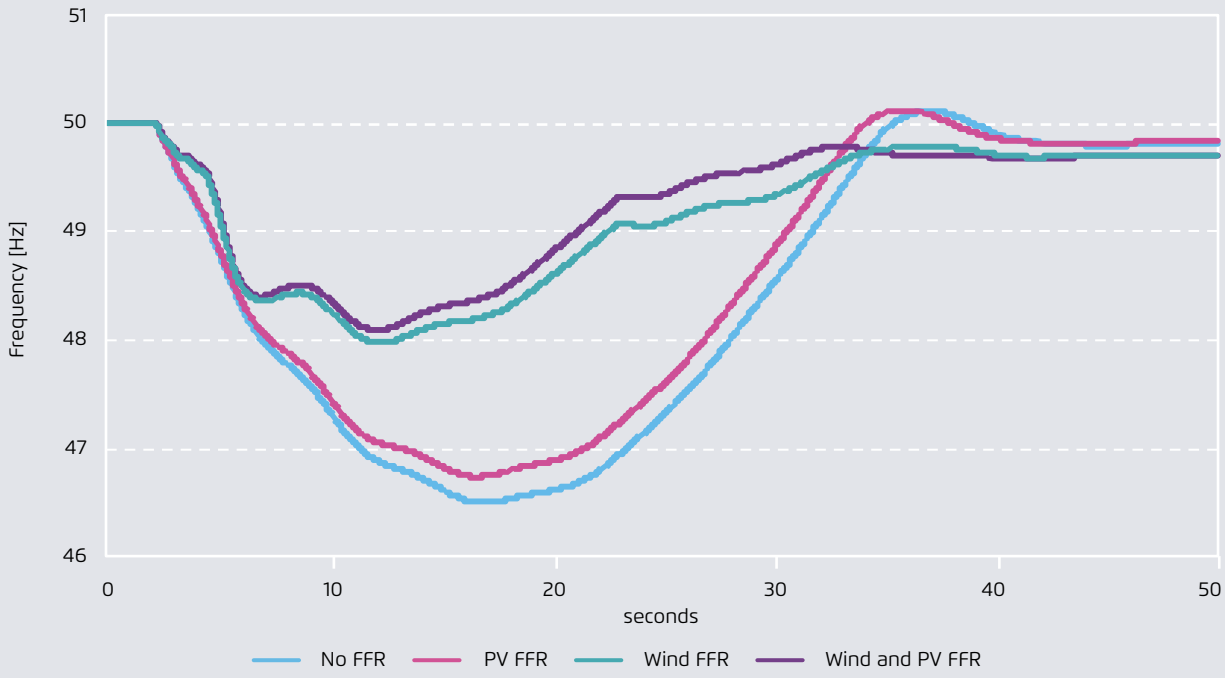

No.	Snapshots	RoCoF (Hz/s)				Frequency nadir (Hz)			
		No FFR	Wind FFR	PV FFR	Wind & PV FFR	No FFR	Wind FFR	PV FFR	Wind & PV FFR
S1	Low_VRES	-0.063	-0.046	–	–	49.439	49.617	–	–
S2	Med_VRES	-0.079	-0.072	–	–	49.213	49.32	–	–
S2b	High_VRES high load	-0.146	-0.135	–	–	48.626	48.68	–	–
S3	High_VRES low load	-0.342	-0.222	-0.324	-0.208	46.498	47.974	46.739	48.091

GridLab (2019)

b. Western network

The frequency drop in the western network is lower than in the eastern network. This is because the level of installed conventional generation in the west is greater, so that the available rotating mass and the primary reserve from these generators is also greater. In snapshots S1, S2 and S2b, the frequency drop remains above the lower limit of 58.8 Hz. In snapshot S3 (high VRES, low load), however, the frequency drops below 58.7 Hz. Since wind penetration in the western network is lower, wind FFR is not significant, at only around 42 MW. Nevertheless, in all of the snapshots the system reaches a stable operating point within 40 seconds of the 1,500 MW generation loss.

Frequency response after loss of 1,500 MW for western Japan +RES scenario; with and without wind and solar FFR

Figure 12

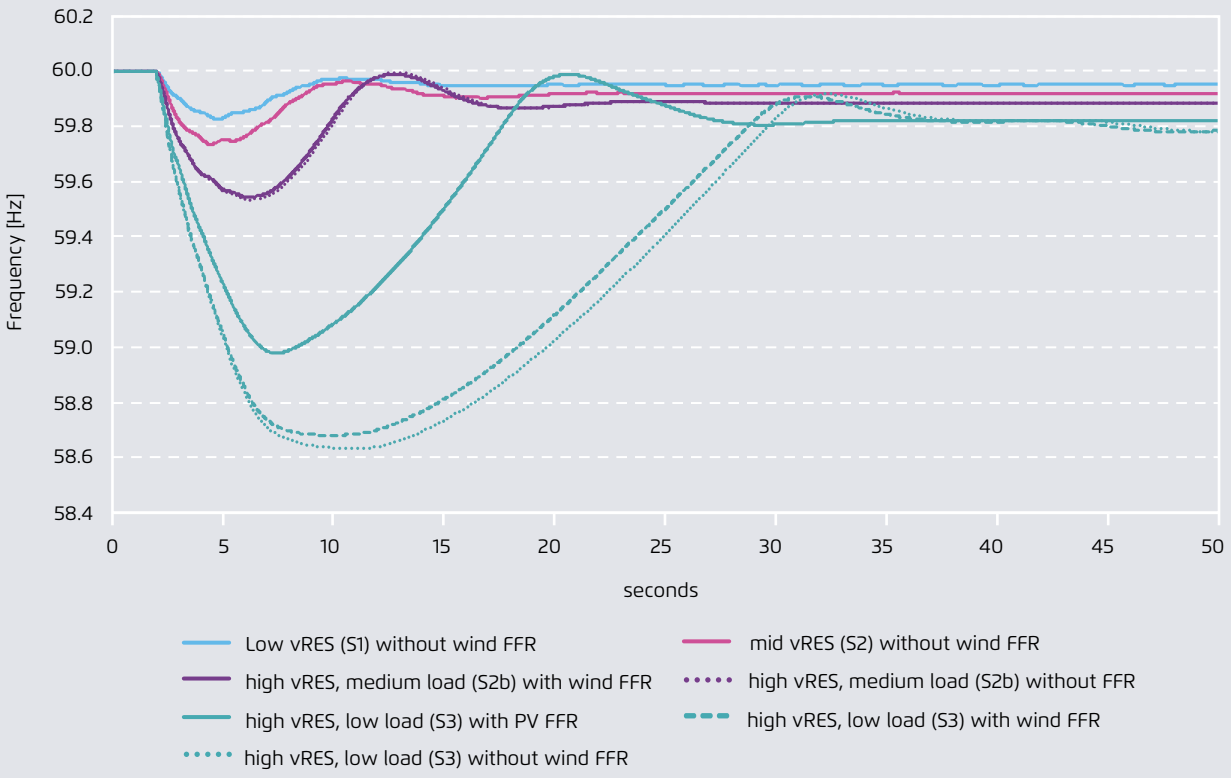

GridLab, Elia Grid International

On account of the higher frequency drop in snapshot S3 (high VRES, low load), we also considered additional frequency support from PV systems. As in the case of eastern Japan, the PV systems close to the thermal power stations were assumed to participate in the frequency support. In order to achieve a power balance, the output of these PV systems was reduced by 10% and the additional power required was dispatched from the nearby thermal power stations. The output from thermal power plants and PV systems connected to the following substation locations were adjusted : Anan, Atsumi, Kawauchi, Kitanosho, Maiduru, Misumi, and Shika (see annex 2 for a more detailed description of how power plants were aggregated at substation level).

The western area had higher installed capacities of PV. 248 MW of active power was available from the PV system for the purposes of frequency support. The figure below compares the frequency response from PV and wind individually, and from PV & wind combined. It is clear that additional FFR functionality from PV systems can push the frequency drop back over the 58.8 Hz lower limit.

Frequency response by FFR technology after a 1,500 MW generation loss in western Japan in the higher RE scenario

Figure 13

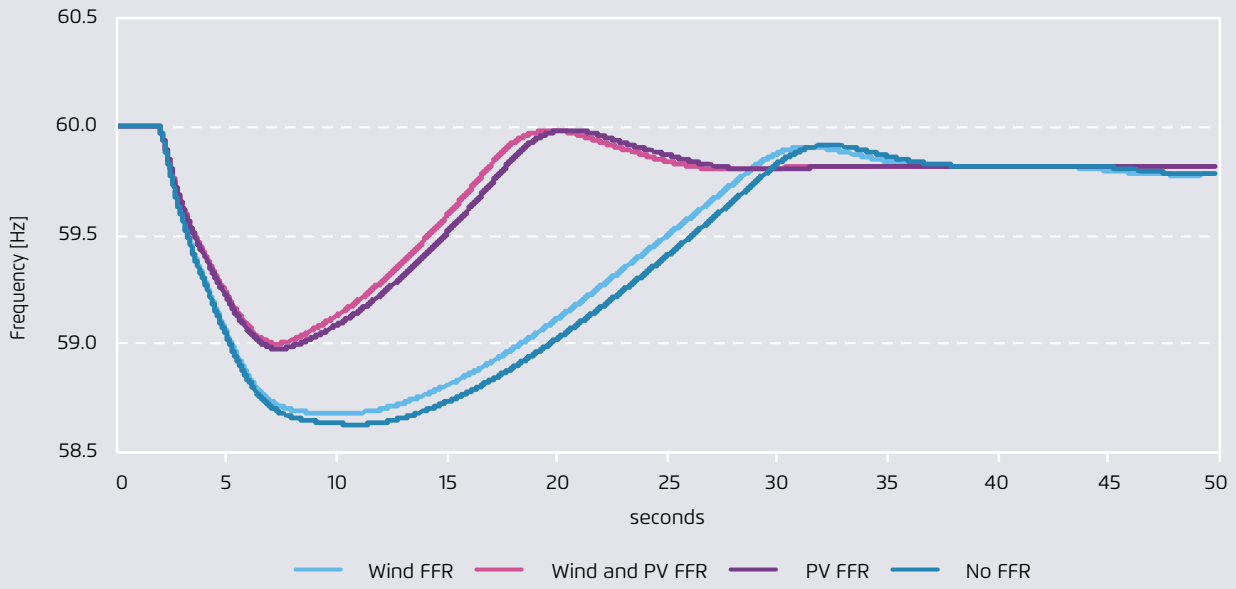

No.	Snapshots	RoCoF (Hz/s)				Frequency nadir (Hz)			
		No FFR	Wind FFR	PV FFR	Wind & PV FFR	No FFR	Wind FFR	PV FFR	Wind & PV FFR
S1	Low_VRES	-0.064	-0.061	–	–	59.824	59.829	–	–
S2	Med_VRES	-0.111	-0.106	–	–	59.727	59.734	–	–
S2b	High_VRES high load	-0.112	-0.109	–	–	59.534	59.543	–	–
S3	High_VRES low load	-0.24	-0.232	-0.186	-0.18	58.632	58.682	58.978	59.002

Gridlab (2019)

4.2 Aggregated results of the frequency response assessment

This section draws a number of overall conclusions from the modelling results presented in section 4.1. In particular, it discusses system inertia (4.2.1), RoCoF (4.2.2), and the frequency nadir (4.2.3).

4.2.1 System inertia

System inertia is provided by synchronous generators such as coal, hydro, gas and nuclear power plants. Whether a generator is online or not depends on the dispatch outcome. In turn, the dispatch outcome is optimised for each EPCO region. This means that inertia in the grid depends on the location of these power plants.

In both the GovS and +RES, system inertia is reduced in the higher penetration snapshots (Figure 14). This is because these snapshots result in higher VRES infeed, which displaces the infeed from synchronous generation. It can also be seen that eastern Japan has lower system inertia than western Japan, despite having lower VRES penetration. This is because demand in eastern Japan, and therefore the amount of generation online in the region, is lower than in western Japan.

Figure 14 shows the distribution of system inertia in the eastern and western grids in the representative snapshots. For the +RES and high VRES penetration snapshots (S3), inertia is concentrated in Chubu, Kansai and Tokyo,

System inertia and VRES penetration in the GovS and +RES snapshots — Figure 14

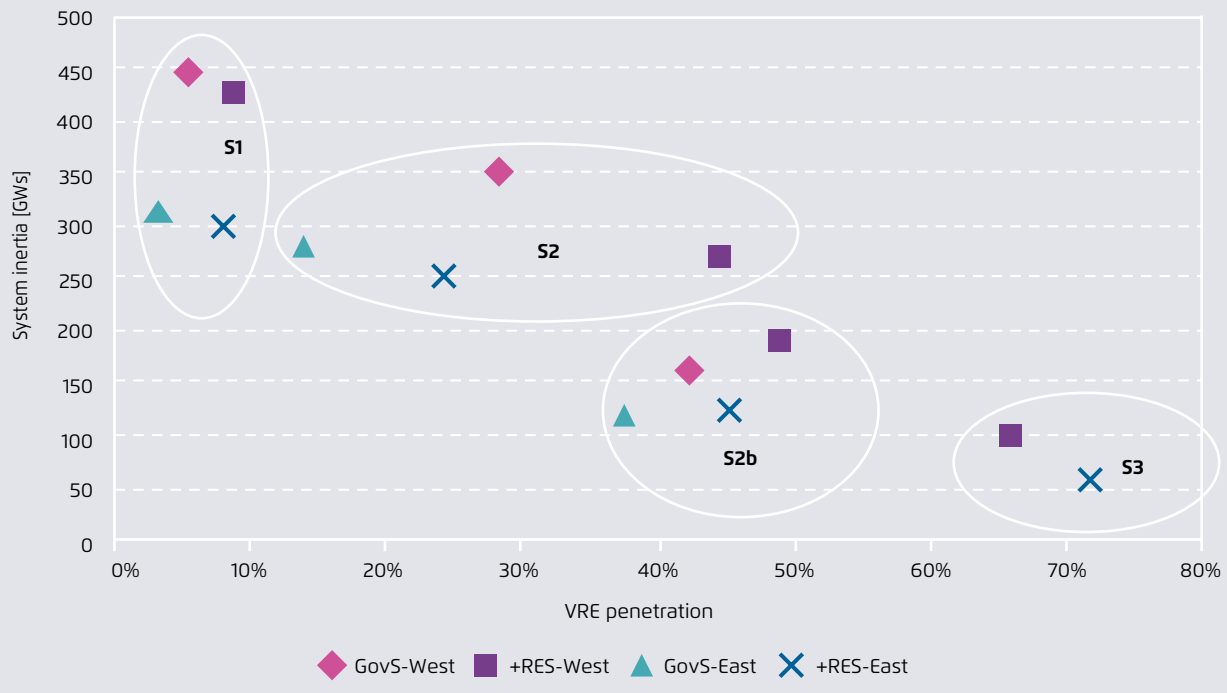

Illustration by the authors

and is very low in regions such as Kyushu and Hokuriku. This is due to the assumption that some thermal power plants will be decommissioned by 2030, and some regions will have high levels of VRES installations. In the GovS, for example, it is assumed that nuclear power plants in Hokuriku and Kyushu are in operation, while in the +RES they are assumed to be decommissioned.

Furthermore, significant levels of solar power are assumed to be installed in Kyushu by 2030, resulting in high VRES infeed and a concomitant displacement of the dispatch of synchronous generation. S3 also results in low inertia in eastern Japan, where significant wind power infeed in Tohoku displaces the inertia contribution made by thermal power plants.

System inertia by region in different snapshots — Figure 15

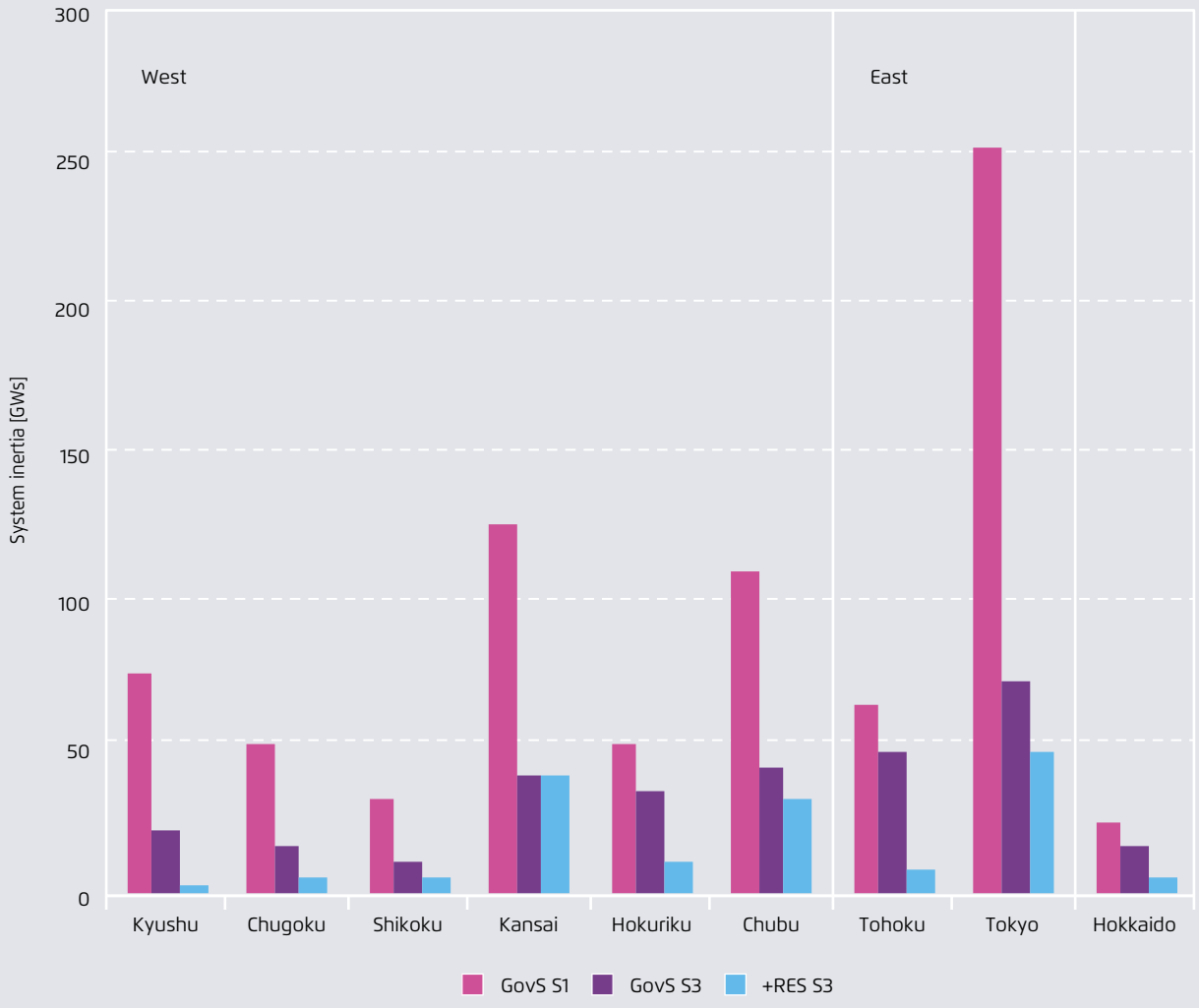

Illustration by the authors

Table 8 compares the inertia values (i.e. the available kinetic energy) in the Japanese system in 2030 (based on our simulation results) with the inertia values of several other power systems today. The results for Japan are based on the extreme 2030 snapshots (S1 for higher inertia and S3 for lower inertia).

Here we can observe that, in 2030, the maximum inertia values for the eastern Japanese synchronous area (298 GWs, +RES Scenario, low RES, S1) are comparable with those of the European Nordic synchronous area (240 GWs). The values for the western Japanese synchronous area are comparable with those of the ERCOT System in the USA. These two zones may therefore serve as a potential benchmark for Japan where the assessment of grid stability is concerned. The table also shows that, by 2030, both of the Japanese systems will still have much higher inertia than can be observed today in Ireland, and a similar level of inertia to Quebec. Furthermore, it is important to note that the variation between the high and low inertia values in Japan in 2030 (factor 4 to 5) is about twice as high as the difference between these inertia values at present in the other power systems.

Minimum and maximum inertia available in different synchronous areas — Table 8

Synchronous area or company name	Countries	Min. load [GW]	Max. load [GW]	Min. kinetic energy [GWs]	Max. kinetic energy [GWs]
Faroe island	Denmark	0.02	0.1	NA	NA
Tasmania	Tasmania	0.9	1.7	4	10
Transpower	New Zealand (South Island)	1.3	2.2	11	25
Transpower	New Zealand (North Island)	1.7	4.5	20	41
Eirgrid	Ireland	2.3	6.4	20	46
Australia	Queensland, Victoria, New South Wales, and South Australia	14	30	72	50
Hydro-Quebec TransEnergie	Canada	15	39	60	160
National Grid (NG)	Scotland, Wales, England	17	53	130	NA
ERCOT	USA	24	70	152	389
The Nordic power system	Norway, Eastern Denmark, Sweden, Finland	25	70	125	240
Japan East*	Tokyo, Tohoku	39.5	61.3	53	298
Japan West*	Kyushu, Shikoku, Kansai, Chubu, Chugoku, Hokuriku	50.4	83.4	91	422

* Whereas the values for the Japanese system are the result of our 2030 simulation which assumes high RES instantaneous penetration (69%), the values given for the other synchronous areas are the output of a 2015 assessment that does not provide information on VRES penetration levels in each case.

ENTSOE (2018), GridLab/EGI (2019)

4.2.2 RoCoF

The rate of change of frequency (RoCoF) is an output of the PowerFactory model. A high RoCoF can indicate low system inertia, as can be seen in Figure 16. If the RoCoF is high, the primary response may not activate quickly enough to arrest the frequency drop.

This means that at the same quantity and quality of primary response, a higher RoCoF would result in a lower nadir. In Japan, a RoCoF below -0.2 Hz/s is considered a critical threshold for maintaining system stability.[37] Figure 16 also shows that the RoCoF is below the critical threshold of -0.2 Hz/s in the high VRES infeed snapshot (S3) in the higher RES scenario. Without additional technical measures to improve frequency response, such a situation would be considered unacceptable according to Japanese power system security standards.

4.2.3 Frequency nadir

The frequency nadir following a sudden loss of generation is one of the most important criteria in evaluating frequency stability. The RoCoF value – as assessed in the previous section – is particularly important in relation to protection device settings for electrical grid infrastructures (see section 3.4).

Following the sudden loss of a large generator, frequency begins to fall. The amount of inertia in the system influences just how fast it does so

37 This is not a limit set by means of technical regulations, but rather a 'rule of thumb' used by EPCOs. It falls within the range used by other island systems such as Ireland and the United Kingdom.

RoCoF and system inertia in the GovS and +RES snapshots — Figure 16

Illustration by the authors

(i.e. the rate of change of frequency). The level and speed of the primary response in the system (i.e. generator governors and FFR) affects how quickly the fall in frequency can be stopped. If there is sufficient inertia and primary response, the frequency will fall to a low point (nadir), before returning to a stable frequency. The nadir in this sense is a key measure of whether there is sufficient inertia and primary response in the system.

Ideally, the nadir frequency should not be below the load-shedding frequency. Although in Japan there are no hard, static load-shedding frequency limits (Shinichi Imai, 2004), it is considered a critical situation if the frequency falls below 58.8 Hz in western Japan and below 49 Hz in eastern Japan (which corresponds to 0.98 p.u.). A frequency below this level would trigger further operational counter-measures within the real system to mitigate the fall. Figure 17 shows the frequency nadir as a function of the remaining inertia in the higher renewables scenario. The results for eastern Japan are given both with and without fast frequency reserve capabilities from wind energy systems. Since only four snapshots were analysed in this scenario, the results are interpolated to estimate intermediate values. On this basis, it is possible to derive a tripping point for the system inertia required to maintain the nadir above a certain level without additional operational measures. As Figure 17 shows, the tripping point is around 120 GWs for the western area and 180 GWs for the eastern area. The figure also shows how wind FFR contributes to maintaining system inertia (in eastern Japan).

Frequency nadir: System inertia characteristics in the higher RE scenario — Figure 17

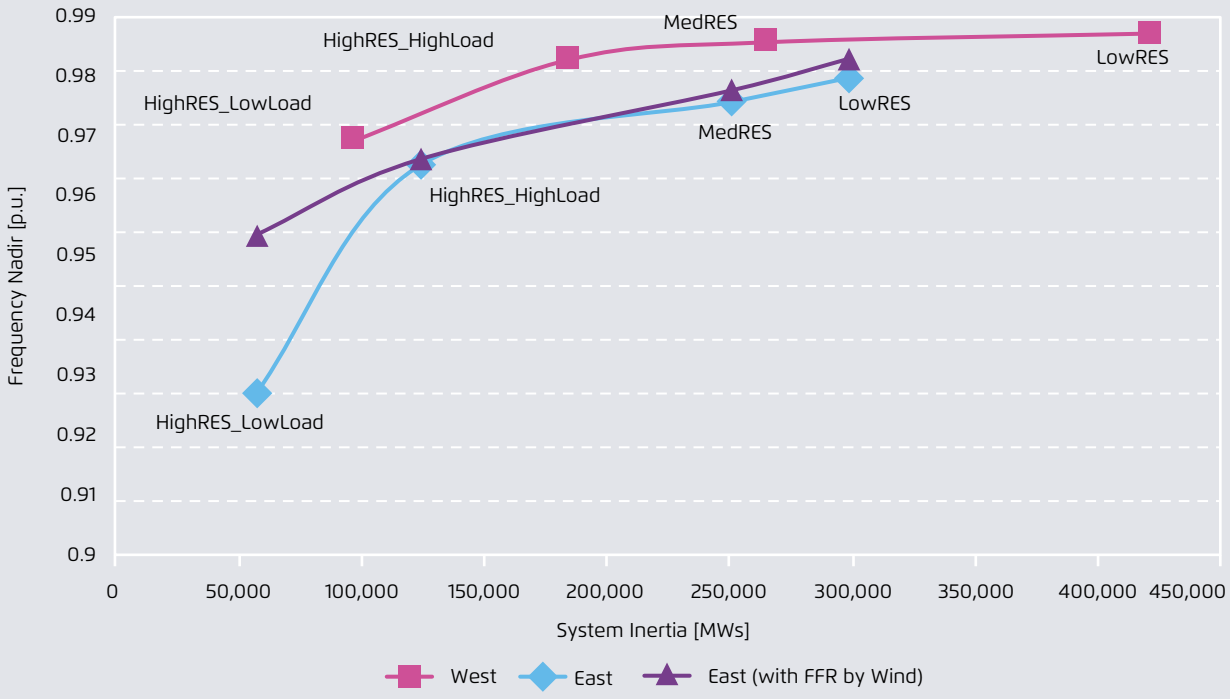

Illustration by the authors

Figures 18 and 19 show the frequency nadir as a function of the instantaneous penetration level of variable renewables. Results are given with and without wind-based FFR. For the eastern region, the impact of a further operational measure already in existence, namely frequency support using the HVDC interconnection between western and eastern Japan, is also shown (scenario East+).

The following figures show how the frequency nadir drops as VRES penetration increases. Without taking into account any additional technical measures, the evaluation shows that, despite a significant reduction in conventional thermal generation (i.e. coal and nuclear) by 2030, instantaneous variable renewables penetration levels of up to 62% in western Japan and 53% in eastern Japan (scenario East+ taking into account the ancillary interconnected support from western to eastern Japan) can be achieved without compromising grid security, as evaluated here. When FFR capability from wind turbines in eastern Japan is taken into account, the tripping point can be raised above 60% in eastern and western Japan. In the absence of additional technical measures to improve frequency response, variable renewables penetration above this threshold would result in an unacceptably large frequency drop.

Figure 20 also illustrates the contribution made by the ancillary service using the HVDC interconnection between western and eastern Japan. This existing ancillary control ensures a stepwise active power injection of up to 600 MW when a frequency threshold of 49.6 Hz is reached. This shows the potential for increased RES penetration if we take into account a more comprehensive set of operational measures that are already available for use.[38] In snapshot 2b, the nadir can be raised above the critical 49 Hz (0.98 p.u.) threshold. In snapshot 3, the nadir can be raised by an impressive +2.1 Hz.

38 In this study's simulations, the 600 MW ancillary support is considered only in one direction, since the east-west-interconnection line loading in our snapshots only allows for a power flow increase in this direction.

Frequency nadir as a function of variable RES shares in the higher RES scenario — Figure 18

Illustration by the authors

Frequency nadir as a function of variable RES shares in the higher RES scenario (with wind FFR) Figure 19

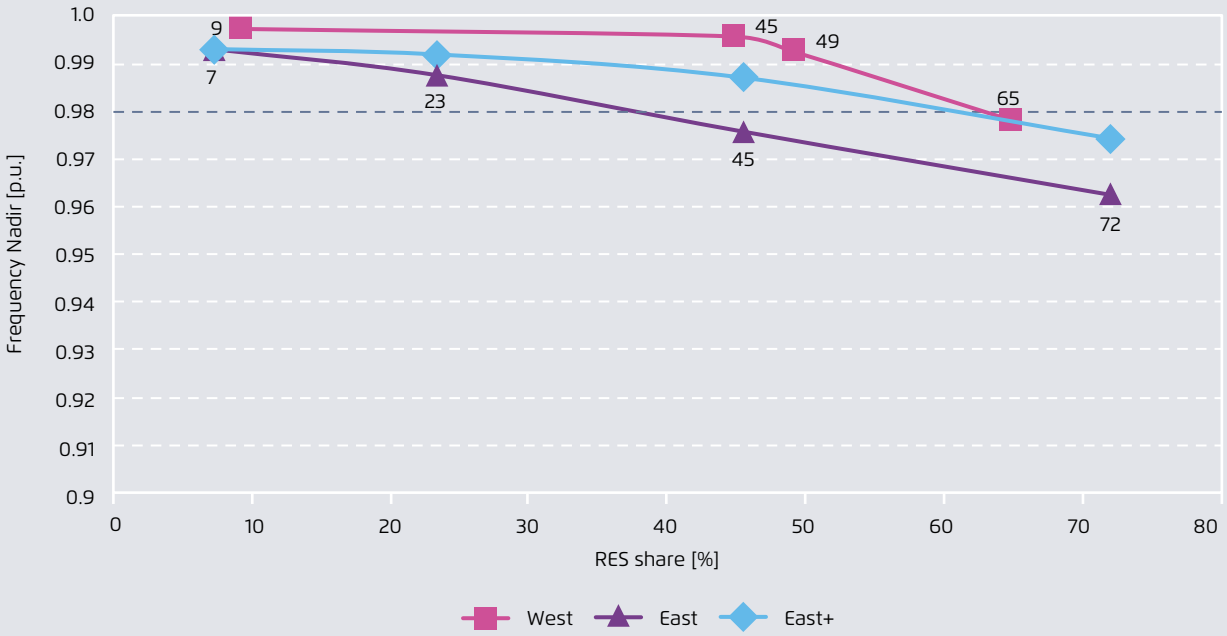

Illustration by the authors

Nadir frequency and VRES penetration in eastern Japan with and without the 600MW ancillary service Figure 20

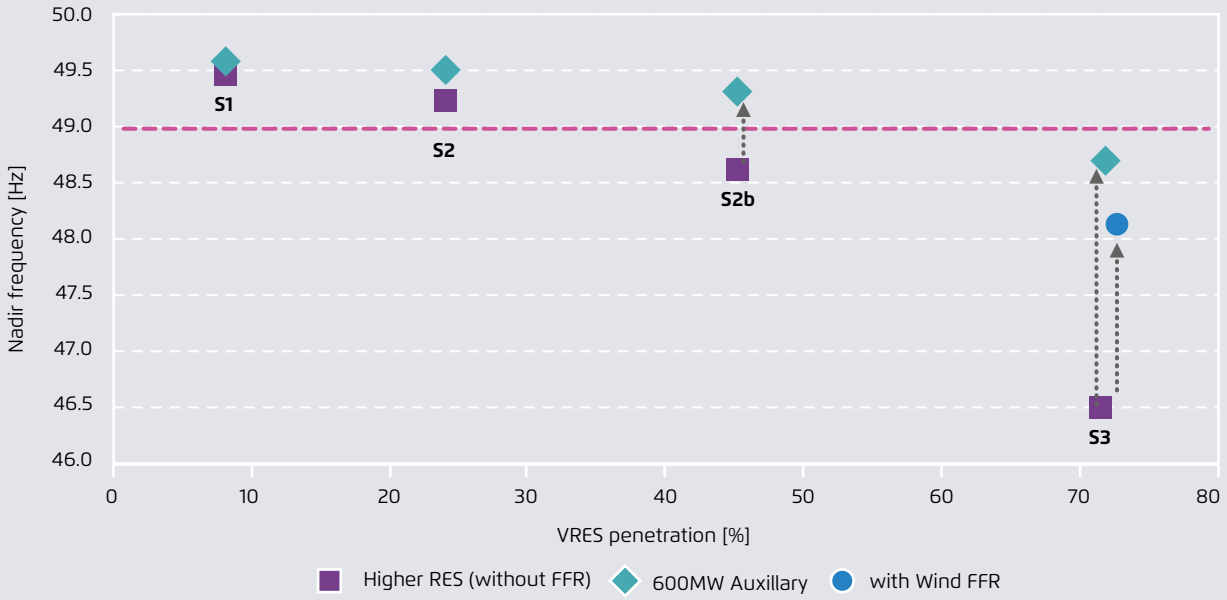

GridLab, Elia Grid International

The analysis shows that in all cases the western grid can more robustly withstand internal incidents than the eastern grid. There are several reasons for this difference:

→ Variation in grid topology: the eastern grid is smaller than the western grid in terms of its number of nodes and – disregarding the Tokyo area – its level of intermeshing.

→ Variation in the size of the power demand: as can be seen in the system overview (section 4.1.2), the load or residual load in the higher-RES scenario is much smaller in the eastern area than in the western area.

→ Variation in remaining system inertia: the remaining system inertia, which promotes frequency stability, is significantly higher in western Japan than in eastern Japan. In our 2030 scenarios, the reduction in conventional generation (i.e. coal and nuclear) in eastern Japan is indeed proportionally higher than in western Japan. The remaining system inertia is thus around 40% lower in the eastern grid than in the western grid (in snapshot 3). In addition, it is also worth noting that the distribution of thermal generation with low inertia constant values (such as gas cogeneration power plants) is higher than in the western area.

Comparison of factors influencing stability between the eastern and western synchronous areas Table 9

Contributor to system stability	Reason	East	West
Grid			
Grid topology	Better meshed, more lines → more stable	–	+
Grid size	More transmission lines / More damping	–	+
Remaining system inertia	Less inertia → less stable		
Generation technologies	Different technologies have different inertia constants	○	○
Generator operating points / dispatch	If load distributed to more generators with less loading, inertia is higher	–	+
Peak load / load level in general	For higher loads, the same level of SNSP means more system inertia	–	+
Pumped hydro & hydro installations	pumped hydro & hydro is always on and always provides inertia	–	+
Counter measures			
Amount of primary control	More primary control, more stability	○	○
Response time for primary control	More ancillary support more stability	○	○
Auxiliary support services (600MW)	More ancillary support more stability	○	○
Fast frequency response services	The more RE installed, the greater	–	+
Event			
Dimensioning incident	The bigger the incident event [in GW], the bigger the impact on frequency stability	○	○
Incident location		○	○

EGI/GridLab (2019)

4.2.4 Provision of VRES-based FFR

This section illustrates the impact of ancillary service (FFR) provision by wind and solar power plants. In contrast to conventional generators, wind turbines and solar photovoltaic (PV) panels are connected to the grid via power electronics converters. These converters electrically decouple the power sources from the grid. Any change in grid conditions during an incident is not then inherently communicated to the power source. FFR can be provided by a controller that is specifically designed to sense the grid conditions and provide an appropriate response signal to the power source controllers. RE-based FFR provision is rather new (though technically possible) and is not yet widespread. Further technical details on such provision are given in Annex 5.

Since most of the wind power plants are located in eastern Japan and solar power plants are found in both regions, FFR provision by these two technologies affects eastern and western Japan in different ways. If we take into account FFR from wind power plants alone, the effect is more visible in the east than in the west. The combined effect of FFR provision by both wind and solar power plants is more dramatic compared than that of FFR provision by wind plants or solar plants alone. The effect is more visible in snapshots with a high level of VRES, and particularly in snapshot 3 (S3). The example of snapshot S3, illustrated in Figure 21 for western Japan, shows that FFR can help to mitigate a low nadir situation by restoring the nadir to an acceptable level. From a frequency stability perspective, we can extrapolate from this result to gain an insight into the highest levels of instantaneous VRES penetration that can be reached in western Japan when taking into account wind and solar PV FFR. As illustrated in Figure 25, the tripping point could then be increased to around 70% (compared to a threshold of around 60% without FFR from renewables).

Nadir frequency and VRES penetration in western Japan by snapshot — Figure 21

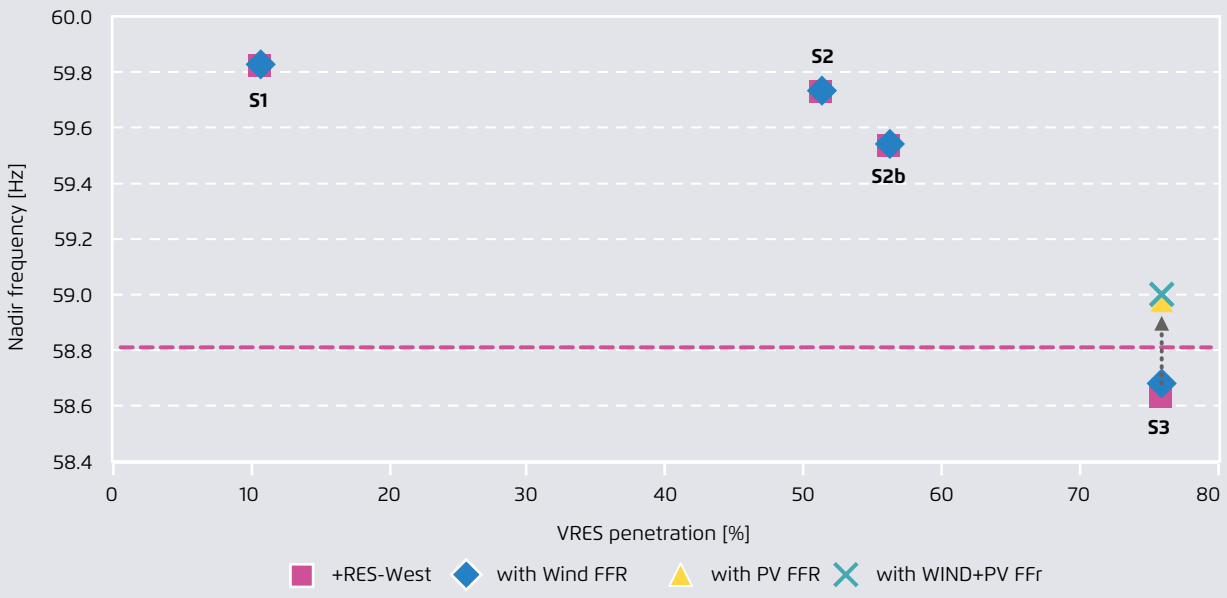

GridLab, Elia Grid International

4.3 Load flow analysis

In this study, we performed a power flow evaluation to identify lines and load flow corridors impacted by increasing numbers of renewable installations and decreasing numbers of conventional power plants. Since no ampacity values were available for the simulation model, we can only state where and in which direction power flow changes between the snapshots. Power flow evolution is calculated according to a generation distribution explained in Annex 4.

Our evaluation of the power flow values does not consider the direction of the flow in detail, since from the perspective of the power transmission line, the capacity reinforcement needs remain the same whether it is import or export power flows that are increasing. The analysis focusses on whether the line loading increases or decreases as the renewables infeed increases. Some aggregated information is nevertheless given concerning the direction of the flows between regions. It is important to state that an increase in line loading does not necessarily entail a need for grid reinforcement. Indeed, such higher loadings could also be achieved if higher NTC values (i.e. the amount of grid capacity effectively available in real time for power flow exchanges between regions) were delivered to market players.

Since the load situation is not equal in all of the snapshots, a linear regression approach[39] was applied to meaningfully classify the power flow tendency as either 'decreasing' or 'increasing'. Where the linear regression tendency is marginal (< 100 MW), the tendency is characterised as 'remaining in the same range'. The threshold of 100 MW was chosen to generate more precise, higher-resolution information concerning the development of power flow tendencies. All of the results and data on power flow values on all lines in both scenarios are available as an attachment to this report.[40]

The power flow tendency on each line is indicated by means of colors: red means increasing power flow, green decreasing, and blue no clear tendency.

Interregional power flows in the government scenario — Table 10

Interregional power flows	Low RES (S1) [MW]	Med RES (S2) [MW]	High RES (S3) [MW]
Chugoku to Kyushu	-76	-748	-2,524
Shikoku to Chugoku	614	1,022	-30
Chugoku to Kansai	-392	811	1,979
Hokuriku to Kansai	4,950	3,126	3,744
Kansai to Chubu	3,062	1,146	862
Shikoku to Kansai	537	489	228
Tokyo to Tohoku	-2,086	-1,312	-6,046

EGI, GridLab (2019)

In both scenarios, there is a noticeable increase in the power flow from Kyushu to Chugoku and from Chugoku to Kansai as VRES penetration increases. By contrast, power flow from Shikoku to Kansai decreases in both scenarios. Kansai exports less to Chubu in the GovS and Hokuriku exports less to Kansai in the +RES scenario. These trends are to be expected, since the significant number of RE installations in Kyushu, Chugoku and Shikoku mean that these regions are less dependent on imports, and can even increase their exports. The absence of nuclear power and slow growth in renewables in Hokuriku in

39 This means that for each single line a regression line is calculated between the power flow value (first data point) belonging to the snapshot with the lowest VRES penetration and the power flow value (third data point) belonging to the snapshot with the highest VRES penetration level. This allows an overall trend to be observed for all lines in all situations.

40 Table 14 contains the interregional power flow values for the three selected snapshots in the governmental scenario, and Table 15 presents the values for the higher RE scenario.

the +RES means that the region has less capacity to export energy. In the eastern network, the flow on the interregional line between Tokyo and Tohoku in the high RE snapshot (S3) is double that in the low RE snapshot (S1), although no clear trend can be observed throughout all of the dispatch situations. From the results of this study, it remains inconclusive whether high numbers of wind power installations in Tohoku result in greater power flows to Tokyo. More snapshots should be investigated in order to better understand the relevant implications and trends. In addition, we also analysed power flow on the intraregional lines. Here we distinguished between meshed lines and generator (feeder) lines.[41] We chose an aggregated result representation in order to gain concise information on the loading tendencies in each EPCO region.[42]

Interregional power flows in the higher RE scenario — Table 11

Interregional power flows	Low RES (S1) [MW]	Med RES (S2) [MW]	High RES (S3) [MW]
Chugoku to Kyushu	-178	-2,064	-3,256
Shikoku to Chugoku	1,136	1,238	128
Chugoku to Kansai	133	1,521	2,727
Hokuriku to Kansai	1,370	118	-146
Kansai to Chubu	352	-444	-416
Shikoku to Kansai	289	127	-6
Tokyo to Tohoku	-38	1,014	-2,876

EGI, GridLab (2019)

Line loading tendencies by region in the government scenario — Table 12

EPCO region	Loading tendency	
	Meshed lines	Generator lines
West		
Kyushu	Increasing	Decreasing
Chugoku	Increasing	Decreasing
Kansai	Decreasing	Decreasing
Hokuriku	Decreasing	Decreasing
Chubu	Decreasing	Decreasing
Shikoku	Increasing	Decreasing
East		
Tohoku	Increasing	Decreasing
Tokyo	Decreasing	Decreasing

EGI, GridLab (2019)

Line loading tendencies by region in the higher RE scenario — Table 13

EPCO region	Loading tendency	
	Meshed lines	Generator lines
West		
Kyushu	Increasing	Decreasing
Chugoku	Increasing	Decreasing
Kansai	Decreasing	Decreasing
Hokuriku	Decreasing	Decreasing
Chubu	Decreasing	Decreasing
Shikoku	Increasing	Decreasing
East		
Tohoku	Increasing	Increasing
Tokyo	Decreasing	Decreasing

EGI, GridLab (2019)

41 Generator lines connect conventional generators to the meshed grid. Meshed lines are part of the meshed grid and connect different grid nodes.

42 The results for each line can be downloaded from the REI website.

In some EPCO regions (such as Kyushu, Chugoku, Shikoku and Tohoku), the loading on the meshed lines tends to increase. In regions such as Kansai, Hokuriku, Chubu, and Tokyo, by contrast, meshed line loadings tend to decrease as renewable generation increases in the grid, which can be explained by the distribution of renewable sources in relation to the loads within the system. The distribution of renewables across the Japanese system, particularly solar energy, is more uniform in our scenario, in order to minimize transmission needs. This conforms to Japan's stated aim of selecting locations for RES installations that are close to the load centers. Our results prove that a more homogeneous distribution that avoids renewables hotspots can indeed minimize the need for transmission grid reinforcement in some regions.

Furthermore, in our model, the loading on the generator lines that connect the conventional generators to the grid tends to globally decrease in all regions (if not necessarily at each node), which reflects a decrease in conventional generation in our 2030 scenarios. In Tohoku, however, generator line loading increases, since there is a high level of renewable generation on the conventional generator nodes.

4.4 Reactive power evaluation

While the IEE grid model used in this study is not designed for a detailed reactive power assessment,[43] it is possible to obtain model-specific results concerning reactive power on the basis of data concerning line elements, transformers, loads, and the generators' P-Q-capability.[44] These results are described in this section.

Table 14 provides an overview of the maximum amount of available reactive power in our different scenarios.[45] The loss of reactive power provision capability by conventional generating units can also be seen by comparing the scenario values with the original capacity under the 2001 network conditions. As expected, there is a continuous reduction of Q and a significant difference of up to 21 Gvar between the eastern and western networks in terms of the reactive power reserve available from conventional generators when comparing the figures for the base case.

43 Since it is an aggregated grid study model designed for frequency stability evaluations.

44 P stands for quantity of active power; Q for reactive power.

45 Based on the IEE grid model with 30 generators per region (east and west).

Available reactive power from conventional generators — Table 14

Region	Scenario	Snapshots			
		Low RES (S1) [Gvar]	Med RES (S2) [Gvar]	High RES (S3) [Gvar]	Base case [Gvar]
EAST	GovS +RES	46.0 43.5	41.2 36.6	17.1 8.5	56.3
WEST	GovS +RES	61.3 58.4	48.2 36.4	22.6 13.5	77.3

EGI, GridLab (2019)

Where the activation of reactive power to compensate the lines' Q demand is concerned, we can observe from the simulation model and the power flow results that in some cases a higher level of RES leads to lower transmission needs because the RES installations are more widespread and closer to the load locations (which also reflects the Japanese planning approach). This implies that the transmission lines are not very heavily loaded, which means that the voltage drops are reduced. Finally, this leads to lower reactive power consumption.

In the first stage of the simulation, adapting the conventional capacities to 2030 conditions while keeping the load locations constant causes higher reactive power demands. Table 15 presents the reactive power compensation requirements (in addition to the reactive power consumed in the IEE 2001 model). It shows that, in the western grid, the additional (external) reactive power compensation required is greatest in the low RES snapshot[46] (for the above reasons).

In the Western system, high capacitive reactive power is required in both scenarios in the low RES and medium RES snapshots. This is due to high load in the Atsumi area (Chubu EPCO) at 3800 MW and very low generation of 180 MW, which leads to significant inductive losses and large voltage drops. In the western grid (high RES), relatively little reactive power compensation is required due to increased local generation dispatch in Atsumi (500 MW) and there are therefore lower transmission needs. In the eastern area, no reactive power compensation is required in the low and medium RES snapshots in both scenarios. In the high RES case, however, the compensation is distributed across the entire network.

The additional demand for reactive power remains within a moderate range of < 2 GVAr for both the eastern and western areas. This range is moderate insofar as 2 GVAr represents only a small fraction of the assumed renewable energy installation capacity of 36 GW of wind and 100 GW of PV. State-of-the-art wind farms and PV solar parks are also equipped with a default feature which allows them to provide reactive power. On the conservative assumption that variable renewables can contribute only 10% of their installed active power in the form of reactive power (i.e. 100 GW of PV can provide 10 GVAr reactive power), this additional 2 GVAr of reactive power demand can easily be provided by VRES.

46 Q_L denotes inductive reactive power demand; Q_C capacitive reactive power

Quantification of additional reactive power compensation requirements — Table 15

	WEST				EAST			
	+RES		GovS		+RES		GovS	
	Q_L (Mvar)	Q_C (Mvar)	Q_L (Mvar)	Q_C (Mvar)	Q_L (Mvar)	Q_C (Mvar)	Q_L (Mvar)	Q_C (Mvar)
Low RES (S1)	–	1,300	–	1,400	–	–	–	–
Med RES (S2)	–	1,000	–	1,300	–	–	–	–
High RES (S3)	220	180	–	–	740	1,960	–	100

EGI, GridLab (2019)

5 Further study insights

5.1 Yearly shares of renewables considering stability limit

As discussed in Chapter 4, the instantaneous infeed of variable renewables (SNSP[47]) above certain levels would potentially require additional measures to guarantee grid stability in eastern and western Japan. On the basis of our analysis, these thresholds are around 60% in western Japan and 50% in eastern Japan (without FFR from wind turbines and solar PV). The thresholds could be increased to 70% in western Japan and 60% in eastern Japan when taking into account FFR capabilities from wind turbines and solar PV. This section puts these stability thresholds into perspective by means of an annual estimate of how much renewable energy would potentially be fed in above those thresholds. This estimate assumes that there is no change in the demand profile and in the proportional distribution of VRES installations between 2013/2014 and 2030.[48]

The results of the analysis are summarized in Table 16 below.

47 System non-synchronous penetration

48 The estimate was derived using the following three-stage process : (1) wind and PV profiles from 2017 were upscaled using the ratio of the installed capacities from 2017 (31st March) and the 2030 target values for the +RES scenario (100 GW PV and 36 GW Wind); (2) the upscaled VRES values were compared to the load profiles from 2013 (corresponding to the demand used in the Switch model) and the hourly VRES level was calculated; (3) the level of VRES above the system non-synchronous penetration (SNSP) levels of 60% and 70% was calculated.

Annual RES levels in 2030 Table 16

	JAPAN ~33% RES			JAPAN ~ 40% RES		
	JAPAN	EAST	WEST	JAPAN	EAST	WEST
Annual demand (TWh)	916	412	503	916	412	503
PV (GW)	100	44.7	55.3	125	44.8	80,2
Wind (GW)	36	24.9	11.1	54	37.5	16.5
Pumped hydro (GW)	22.3	8.9	13.3	22.3	8.9	13.3
SNSP limit*	60% for East 70% for West	60%	70%	60% for East 70% for West	60%	70%
Annual VRES share	22.1%	28.4%	16.9%	28.9%	34.7%	24.1%
Annual RE incl. hydro share	33.0%	38.9%	28.3%	39.8%	45.2%	35.5%
Annual VRES curtailment	1.8%	3%	0%	3.9%	5.1%	2.5%

* The SNSP limit is defined as the hourly upper limit of variable renewables penetration.
REI (2019)

From a grid stability perspective, one approach would be to curtail the amount of VRES exceeding the above thresholds, in order to maintain system stability within a tolerable range. This would maintain sufficient inertia in the system and ensure frequency stability without the need for additional technical measures. This would represent a rather conservative approach to grid stability, though it would be worth assessing its costs and benefits in more detail, particularly in comparison with other means of ensuring grid stability. As Table 17 shows, this approach would result in a very low curtailment rate of about 2% of annual VRES production in 2030 in the +RES scenario (100 GW PV and 36 GW wind). This shows that on conservative assumptions, renewables in Japan can easily satisfy at least 33% of annual demand. while still maintaining grid stability within a tolerable range. A higher renewables share of 40% could also be achieved on the same stability limit assumptions (SNSP limits of 60% VRES in eastern Japan and 70% in western Japan) with only a very small increase in the curtailment level to 4% of annual renewable generation. Furthermore, the curtailed energy from renewables could be used for upward frequency response in order to ensure further system stabilisation. This would require the introduction of a dedicated market mechanism to remunerate this service. Such a scenario would require a total installed capacity of about 125 GW solar and 54 GW wind. Given the rapid growth of renewables over the last 5 years, such a 40% share is realistic and could be met even before 2030. Renewables levels in excess of 40% may require additional technical measures to ensure grid stability and maintain the level of VRES curtailment at acceptable levels. The following section discusses some of these technical solutions.

5.2 Additional measures to ensure system stability

In Chapter 4, we considered the frequency behaviour of Japan's power systems, focussing particularly on primary control power. Further sensitivity analysis was conducted on the contribution VRES may make to FFR and the 600MW ancillary support provided by another control area. Several other mitigation measures may nonetheless be implemented to overcome low inertia and critical system states. These are measures that could be activated very quickly, i.e. within the time range necessary to overcome critical disturbance events, and are described in this section.

→ **Stricter primary control requirements / FCR-N**
In many power systems, primary control reserve or frequency containment reserve (FCR, or sometimes FCR-N, where N stands for normal operation) is the kind of reserve that has the fastest response time. It is permanently available. Nevertheless, primary reserve requirements can differ with respect to the activation time and the activation threshold. Dimensioning is usually done by synchronous area and different dimensioning incidents or criteria may be applied. Increasing the amount of, and the requirements on, primary control – for example by reducing the activation time – can promote system stability and help overcome low inertia and therefore critical situations.
As a price indication, we can consider the results from Finland. In 2018, 72.6 MW of FCR-N was acquired for the Finnish system in the annual auction at a price of 14.0 €/MW,h (Fingrid, 2018).

→ **Frequency containment reserve for disturbances (FCR-D)**
The introduction of a special, fast-acting reserve dedicated to overcoming disturbances is another potential mitigation measure. This additional reserve might be tendered and procured independently from classical FCR – in a situation, for example, where low inertia can be predicted. This measure has been implemented in Finland. In 2018, 435 MW of FCR-D was acquired for the Finnish system in the annual auction at a price of 2.80 €/MW,h (Fingrid 2018).

→ **Synchronous condensers (created, for example, by retrofitting decommissioned nuclear power plants)**
A synchronous condenser is an electrical machine connected to the power system with a freely spinning shaft. It is mainly used to provide and compensate reactive power, yet since it is technically identically to a synchronous machine it helps stabilise the grid by using the stored kinetic energy in its rotating parts. Furthermore, it is possible to retrofit old power plants and use them as synchronous condensers, as illustrated by the example of the former Biblis nuclear power plant in Germany.

→ **Ancillary support from HVDC-linked synchronous areas**
Where a power system is at risk, it is possible to provide ancillary support from another control area linked via HDVC. This is the case between Japan's eastern and western synchronous areas, and the impact of this support has been evaluated in this study. The drawback of this measure is that a certain amount of capacity needs to be reserved on the interconnector if permanent availability is to be granted, and this capacity cannot then be used for market coupling.

→ **Frequency-triggered shedding from pumped-hydro power plants in particular**
The last measure that might be implemented to prevent a system blackout is the automated shedding of load, pumps, or generators. Depending on the kind of event in question (i.e. over or under frequency), generation or load can be shed. This is achieved via frequency-relays, which continually measure system frequency and can trigger switching events. Pumped hydropower is a special case here, since it can either act as a load or as a generator. When hydropower plants are pumping (i.e. behaving as a load) they are subject to preferred shedding, since this does not entail a power outage for consumers.

5.3 The contribution made by renewables to ancillary services

Increased penetration of inverter-based renewable technologies (predominantly wind and solar power) serves to displace classical synchronous machines (i.e. coal, nuclear and gas power plants). This displacement of thermal generation not only has implications for frequency stability but also for the other ancillary services that are critical for ensuring system reliability, including reactive power/voltage support, control power, short circuit currents, and system restoration. As we shall discuss in this section, however, renewables can also contribute to several ancillary services, and thereby mitigate the loss of thermal generators.

Reactive power / voltage support

The loss of reactive power capacity (see section 4.4.1.) can be compensated to some extent by means of VRES. Reactive power provision is essential to maintain voltage within a predictable tolerance band. Many grid codes require de facto reactive power support from VRES. Quantifying this support in the case of Japan nonetheless requires further analysis and more detailed models.

Control power

Control power refers to the ancillary services traditionally labelled as primary, secondary, and tertiary control reserves or control power. In general, VRES sources can be used to provide balancing services. The preconditions of this usage are high quality forecasts and a non-discriminatory market design that allows for VRES participation.

Short circuit currents

A synchronous machine can provide short circuit currents at a multiple range of its nominal current. Where faults arise in the power system, this is necessary in order to trigger protection equipment and prevent equipment from damage. VRES sources such as wind and solar usually cannot drive such high currents, which means that protection planning may need to be reviewed.

System restoration

By itself, a VRES system is incapable of providing black start functionality. A black start means energising part of the power system, providing stable frequency and voltage conditions, and allowing other generators/consumers to synchronise to the power system. Nevertheless, it is possible to perform a system restoration using other ancillary technologies such as batteries.

5.4 The experience of renewables-based frequency response and synthetic inertia requirements in other synchronous areas

Denmark / Energienet DK

In Denmark, wind farms connected at voltage levels above 100kV must provide a control feature allowing the wind farm to provide upward control power in cases of under frequency. It should then be possible to limit the output of the wind farm to a certain percentage of the theoretically possible output. This mechanism can be used to bolster stability in cases where there is a high level of renewables penetration.

Figure 20 illustrates such a case. The solid line shows the behaviour of the wind farm in a 'normal' case, without additional curtailment. Where there is a stable frequency of around 50 Hz, the wind farm feeds in 100% of the electricity produced. At frequency deviations which rise significantly above 50 Hz and thus leave the deadband, the turbine curtails itself in order to ensure system stability. This response to over-frequency events (i.e. automatic curtailment at certain settings) is a standard mechanism that is already widely used.

The **dashed line** represents behaviour in the event of the wind mill's control feature being activated. Where there is a stable frequency, the wind farm feeds in only 50% of the energy it could theoretically provide. This holds true for all wind speeds. The over-frequency behaviour is similar to the 'normal' behaviour insofar as it triggers additional curtailment. The under-frequency behaviour gives the wind mill the possibility of delivering new services to the system. Since energy is constantly held back, it can then be released in response to under-frequency events triggered by a loss of generation. The under-frequency feature is provided by many manufacturers, yet is not yet widely used.

Excerpt from Danish regulations for wind farms connected at a voltage level above 100kV — Figure 22

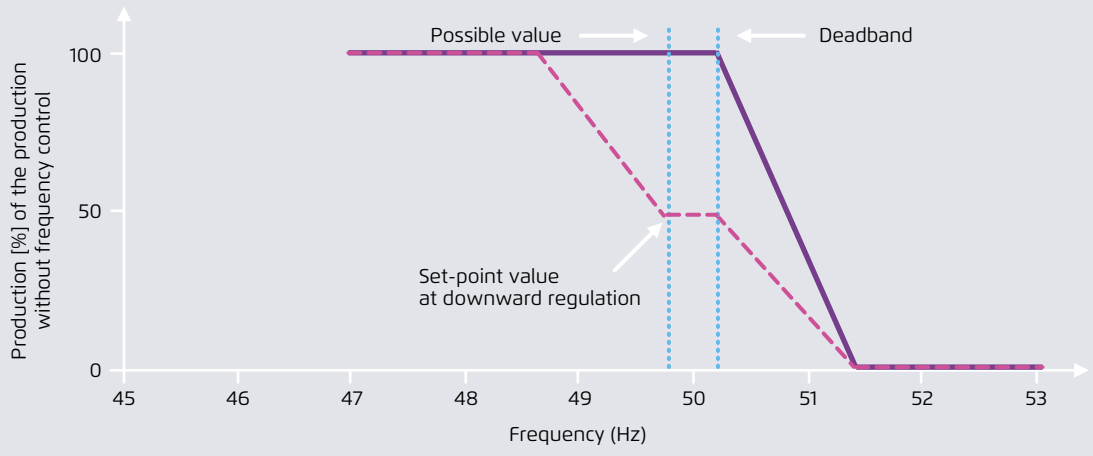

DEA (2004)

Ireland / Eirgrid

Eirgrid has similar requirements to Energienet DK, which are referred to as wind following mode. As in Denmark, wind farms are required in certain situations to run at a particular percentage of their available active power (around 85% in Figure 23) in order to be able to provide upward reserve in the event of under frequencies. The publicly available information on the relevant test procedures would appear more advanced than in the Danish case and the parametrisation of the actual frequency response is more flexible.

Grid following mode configuration from the Irish frequency response tests — Figure 23

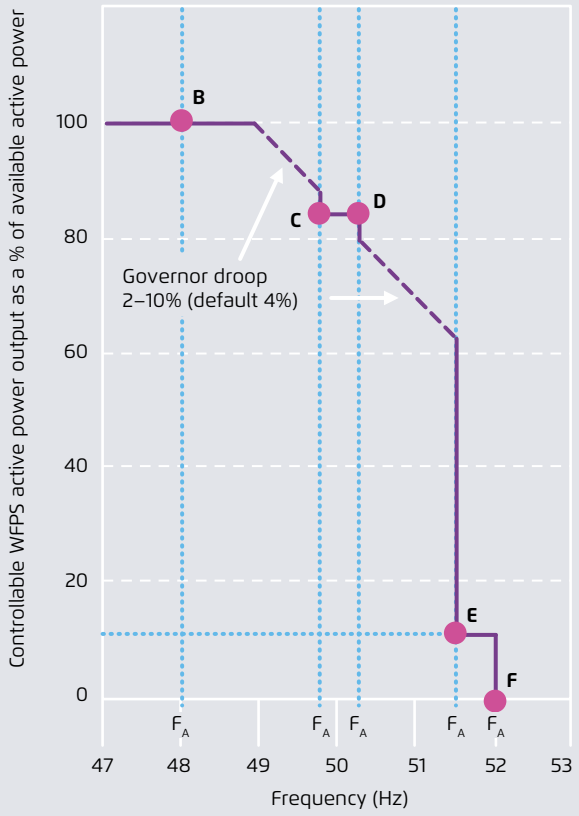

Note: (i) Droop is calculated with respect to registered capacity
(ii) The frequency deveiation is calculated from nominal frequency, not the deadband edge

Eirgrid

Canada / Hydro Quebec

In 2005, Canada's system operator added the following requirement for wind generation to its connection codes (see Hydro-Québec):

"The facilities of a wind generating plant whose rated output is greater than 10 MW must be designed to be able to be equipped with a frequency control system. The manufacturer must design this system and install it as soon as it is available. This frequency control system shall help reduce large (> 0.5 Hz), short-term (< 10 s) frequency deviations on the power system.

The frequency control system must reduce large, short-term frequency deviations at least as much as does the inertial response of a conventional generator whose inertia (H) equals 3.5 s. This target performance is met, for instance, when the frequency control system varies the real power dynamically and rapidly by about 5% for 10 s when a large, short-term frequency deviation occurs on the power system."

This functionality is mandatory and means that wind farms help to stabilise the grid during under-frequency events.

6 Conclusions

A number of conclusions can be drawn from the analyses performed in this study.

→ The study showed that it is possible to achieve a higher level of variable renewables penetration than is provided for in the government's plan, without compromising the elements of grid security evaluated here and without additional technical measures. This is true on conservative assumptions concerning instantaneous penetration levels of variable renewables (i.e. solar PV and wind energy) of up to 60% in western Japan and 50% in eastern Japan (in the event of a 1.5 GW loss of generation). These figures imply that renewables penetration could be even higher in certain regions. Our assessment was conducted on the basis of conservative assumptions that consider only the inertial response and primary response control of thermal generators and the 600 MW ancillary support provided by the HVDC link from eastern Japan to western Japan. Other technical solutions, such as synchronous condensers, HVDC links, demand response, batteries, and modifications to service provision requirements for conventional power plants can also improve grid security at higher RE penetration levels.

→ Inertia is a critical measure of system stability. We assessed several snapshots in which high levels of renewables served to push down system inertia to its limits. The study identified inertia stability limits of around 180 GW for eastern Japan and 120 GW for western Japan, below which additional technical measures may be required to safeguard grid stability. These figures were derived from an approximation between the snapshots selected and should form an initial basis for further studies.

→ Fast frequency response from renewables can help overcome inertia issues and increase the proportion of renewable energy sources in the Japanese system. The use of FFR services can mitigate critical frequency nadirs in times of emergency. In the +RES, it was possible to elevate the frequency nadir from 0.93 p.u. to 0.96 p.u. in the eastern synchronous area and from 0.977 p.u. to 0.983 p.u. in the western synchronous area. This positive effect could help to avoid blackouts, or at least to limit blackouts to certain areas. VRES-based FFR is nonetheless still a very new technology and is not yet widespread.

→ The analysis shows that on conservative assumptions concerning grid stability, renewables in Japan can easily satisfy more than 40% of annual demand (or 30% if hydropower and biomass are excluded), while still maintaining grid stability within tolerable ranges and maintaining the surplus/curtailment of variable renewables at a low level of around 4%. This is significantly higher than the official target government target of 22% RES, which includes 8.7% variable renewables. Renewables penetration levels over 40% may require additional technical measures to ensure grid stability and maintain VRES curtailment at acceptable levels.

→ Our evaluation of the rate of change of frequency (RoCoF) values for the system in 2030 allowed us to derive recommendations for potential FFR requirements. Since the maximum RoCoF value in our assessment was -0.34 Hz/s (i.e. a critical frequency drop of around -1Hz in 3 seconds) in the worst case scenario, FFR mechanisms should be able to respond within these first 3 seconds.

→ Our study shows that there is a noticeable increase in the power flow from Kyushu to Chugoku and from Chugoku to Kansai as the level of variable renewables penetration increases. By contrast, power flow from Shikoku to Kansai and from Hokuriku to Kansai decreases. These trends are to be expected, since the high levels of solar PV in

Kyushu, Chugoku and Shikoku reduces the import dependency of these regions, and turns them into net exporters. Finally, the Hokkaido–Tohoku and Chubu–Tokyo HVDC links exhibit a higher export tendency when VRES penetration increases. Both links are at their maximum loading in the snapshots with the highest VRES penetration. A detailed evaluation of grid reinforcement measures would nonetheless call for more in-depth investigation.[49]

→ In general, it can be seen that in certain regions the line loading and hence the need for energy transport increases in certain regions, such as Kyushu, Chugoku, Shikoku and Tohoku. This indicates a potential need for grid reinforcement. In other regions, however, the average line loading goes down. This is due to the fact that, in these regions, consumption and generation are moving closer to each other as installed capacities and the overall share of renewables in the power mix increase.

→ As wind and solar power penetration increases, ancillary services (and particularly reactive power/voltage support and control power) traditionally provided by thermal generators may need to be replaced by renewables themselves. Several technical solutions are already available for this. Their introduction into the market requires non-discriminatory regulation on renewables integration.

→ The methodology and tool chain developed in this study have been successfully applied to renewables penetration scenarios to evaluate frequency stability and power flows in the Japanese power system. Making the model and all the input/output data public is intended to pave the way for further studies.

49 This would require greater transparency and data access.

7 Recommendations

In light of the experience of other countries, several recommendations can be derived from the above analysis of the Japanese power system. These recommendations seek to facilitate renewable energy integration in Japan. They address three different stakeholder groups: policy makers and regulatory bodies, system operators, and renewable energy developers.

Recommendations for policy makers and regulatory bodies

→ **Foster energy sector data transparency** in order to facilitate third party studies on renewable energy integration. By continually building on existing models, power system evaluations can contribute to ongoing and future discussions concerning renewables integration in Japan. They can also foster understanding of the relevant technical issues and facilitate factually grounded debate on energy policy and regulatory decisions by a broader range of stakeholders across the industry and beyond.

→ **Implement non-discriminatory regulations for renewable integration.** Consider the potential of renewables in ancillary services such as balancing markets and reactive power provision when designing these market services. This would allow renewable producers to assume greater responsibility in ensuring system reliability. It would also provide them with new business opportunities and foster technological innovation.

→ **Encourage further power system studies involving independent parties.** Such studies are required to better capture the specific challenges of integrating renewables in Japan. The following topics would be of particular interest:

- Congestion and congestion management in relation to contingency analysis
- Advanced adequacy analyses
- Analyses of the impact of higher levels of renewables in different scenarios ranging from low to high demand for each synchronous area
- Short circuit power provision and protection measures
- Local voltage stability issues
- Balancing in the above scenarios
- Integrating renewable energy sources into the market
- System defence and system restoration processes with increased renewable integration
- Changes to operational processes and operational planning processes due to high VRES levels
- Connection requirements for renewable generation
- Countermeasures for disaster situations (as seen in Hokkaido 2018)

Recommendations for system operators

→ **Establish inertia monitoring.** Inertia is a key parameter in ensuring system stability. By actively monitoring it, system operators can limit the consequences of frequency deviation incidents. Monitoring should be undertaken at the regional level and requirements should be set for minimum inertia provision, taking into account the impact on the synchronous area. Further in-depth analysis may provide useful insights and inertia management might be enhanced by means of additional technical mechanisms such as fast frequency response services and synthetic inertia provision.

→ **Integrate renewables into ancillary service provision.** As this study has shown,[50] VRE sources are capable of providing FFR services. System operators can make use of these services to ensure frequency stability. VRES may also be harnessed for services such as reactive power provision and balancing services. In all cases, system operators can diversify their portfolio of service providers by including renewable generators as well as demand-side management solutions.

→ **Increase the transparency of the grid and power system data required for long-term planning.** In many countries, especially in Europe, there are strict requirements to publish grid data, including grid parameters, generation data, and real-time data. In general, this approach has facilitated many studies by scientific researchers and other third parties, which have resulted in innovative proposals such as business case validation for new technologies. Transparency is key when establishing wholesale and control power markets if new players are to test their business case

50 See esp. Chapter 5 and Annex 6.

Recommendations for RES developers / the industry

→ **Anticipate grid service requirements.** The Japanese energy sector will go through major changes in the near future as a result of unbundling and the establishment of new market segments. Renewable developers should actively define their role in this process and seek out new opportunities.

→ **Explore the additional services that renewables can provide.** The renewables industry should evaluate its readiness to provide services beyond mere energy provision. As technological development progresses, control algorithms and technical capabilities for VRES technologies will improve. Systems can therefore be developed to provide other services beyond energy provision, such as:

- Fast frequency response / virtual inertia
- Balancing services
- Reactive power provision
- Grid use optimisation (where the RE developer owns/operates the grid assets)
- Assessments of the impact of policy decisions and TSO operation procedures on potential curtailment

Annex 1: Generic information on how to establish a simulation tool chain

Simulation toolchain

As a basis for our analysis, a toolchain was developed for this project that covers data collection and conditioning techniques, scenario and snapshot building, dispatch simulation, grid model construction and validation, data reformatting, and transfer automation between simulation tools. The different steps of the toolchain are displayed in the following picture:

Once in place, the advantages of this process are obvious, since it ensures:

1. **Easy implementation of sensitivity analysis**
   The toolchain gives the user an easy means of conducting a sensitivity analysis in which sensitivities can be implemented in every step of the chain. Political targets can be represented as changes in the scenario development phase (e.g. the phasing out of a certain technology), different dispatch priorities can be assessed in the dispatch modelling, and grid topologies can be varied within the grid modelling.

2. **The interchangeability of different steps**
   This means that a different tool can be used after each step has been completed. For example, the dispatch modelling tool can be exchanged for a different tool that allows for a more advanced market model.

3. **Reproducibility and traceability**
   By applying the same input parameters to the toolchain and using the same models the results should be 1 to 1 reproducible. Changes in parameter or input data can be traced in order to explain changes in results or even unexpected results.

Representation of the simulation toolchain — Figure 24

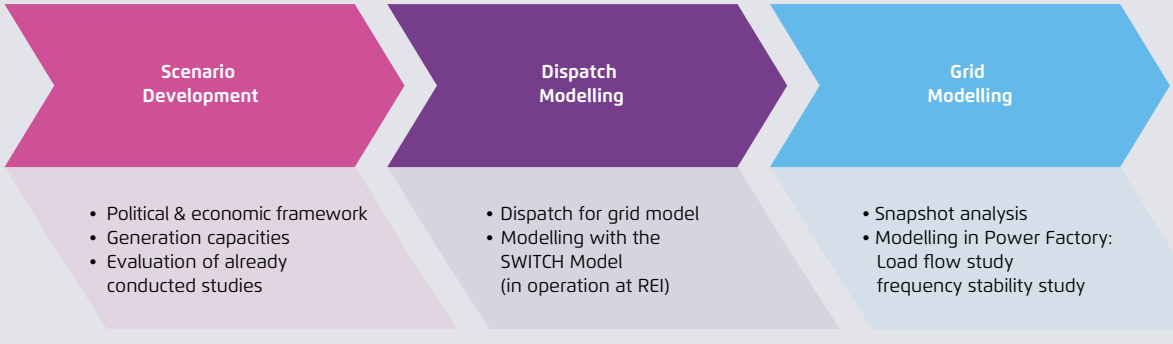

Elia Grid International

Scenario development

In this step, the fundamental parameters of the power system study are derived. These fundamental parameters and assumptions may depend on various factors, such as the political and economic framework in place (on the government scenario, for example) or assumptions concerning adequacy studies on future generation capacities. This first step enables a sensitivity analysis (e.g. "+RES scenario").

The fundamental parameters elaborated in the scenario development include:

- **Installed capacities by technology** for both conventional power plants (coal, nuclear, gas) and renewables, including assumptions concerning pumped hydro, other storage (electric vehicles, home storage, and large scale electrochemical batteries), and demand side management.
- **Geographical distribution of installed capacities.**
- **Market areas and the net transfer capacities (NTCs) between them.**
- **Demand profiles.** Assumptions need to be made concerning future electricity consumption (e.g. decreases due to energy efficiency programmes or increases due to the introduction of new energy uses).
- **Wind and solar profiles.** Realistic variable renewables infeed is generated on the basis time series of solar radiation and wind speed. Ideally, these profiles should be available year round at a high geographical resolution. Simplifications are possible.
- **Assumptions concerning reserve capacities.** Power systems require adequacy and balancing reserves. As these reserves are usually provided by the same units that satisfy power demand, specific constraints can arise for the dispatch model.
- **Assumptions concerning must-run availability** that can also result in constraints for the dispatch simulation. Must run means there is a minimum operation point for a power plant (such as 40% loading), which needs to be considered in the dispatch.

Dispatch modelling

In dispatch modelling, the actual generation of different power producers is determined according to the rules in place (either market-based dispatch or central dispatch). This is an essential input for the grid model. The dispatch modelling has a defined time resolution (such as every hour, every two hours, every 30 minutes). The essential parameters in dispatch modelling are:

- **Dispatch priority.** Certain rules may be applied to determine which technologies are allowed to feed in first to the grid. The rules could state, for example, that all renewable energy sources have priority over other thermal power plants.
- **Curtailment priority.** Curtailment priority rules may also be implicitly included in the dispatch priority. Wind generation, for example, may be curtailed before solar energy, and solar energy before biomass energy.
- **Reserve constraints.** A fixed or variable capacity value may need to be available over time as an additional reserve in certain types of generation units. Reserve can be understood as an adequacy reserve, balancing reserve or emergency reserve.
- **Rules for the use of interconnectors.** These rules define whether interconnection capacity is reserved through long-term contracts by thermal generation units or if it can be used more flexibly in short-term markets.

The dispatch model is mainly used in systems with a central dispatch, which means that the system operator sets the rules for the dispatch. In systems with a spot market (i.e. self-dispatch), the dispatch model is replaced by a market model. A market model adds an economic dimension to the dispatch model. In such cases, the market rules should be mapped on to the model (following a merit-order approach, for example, in which power plant technologies are dispatched on the basis of their marginal generation cost).

Grid modelling

The grid model is the physical representation of the power system which is subject to analysis. It is often the most complex part to be modelled and hindered by a lack of information disclosure. It often contains at least the following data:

Grid data:

- Type of grid assets (transformers, transmission lines/cables, HVDC), their topology, and their parameters (length of lines, impedance, and so on).
- Substations (topology, such as how many busbars there are and how they are operated, number of couplers in place).
- Compensation units, such as inductors and capacitors for reactive power provision.

Generators (including RES):

- Location and grid connection points of installed capacities (where and how much)
- Types and parameters of generation (such as the safe operating zone for reactive power, depending on the active power)

Demand:

- Type of load (consumer, industrial, commercial).
- Aggregation principles (usually not every single household is modelled).
- Reactive power behaviour of loads.

The data given above are the minimum required to run rudimentary load flow analysis. Where more sophisticated analyses are performed (such as dynamic fault analysis), additional data must be provided, such as protection settings, unit overcurrent capabilities, fault ride through controls of generation types or settings for over/under frequency relays.

The level of detail in the dispatch model (e.g. the level of aggregation of rooftop PV infeed) should match that of the grid model.

Annex 2: Description of the SWITCH model

In this study, power plant dispatch was simulated using the SWITCH model of the Japanese power system developed by Wakeyama. The SWITCH model was designed by Dr. Matthias Fripp, now at the University of Hawaii, when he was at the University of California, Berkeley. It works on AMPL: A Mathematical Programming Language.

The SWITCH model was used to determine a realistic dispatch for the 2030 scenarios with specific constraints. The SWITCH Model simulates regional dispatch at the level of the 9 EPCO regions (Hokkaido, Tohoku, Tokyo, Chubu, Kansai, Hokuriku, Shikoku, Chugoku, Kyushu). Okinawa is not considered in the Switch model and hence not in the grid model.

In the second stage, the results of the dispatch at EPCO level needed to be mapped at the substation level in order to make them compatible with the grid model and usable in Power Factory. This procedure is described in Annex 4.

The Switch model calculates dispatch for two representative days every months, consisting of:

1. A day with a low demand profile.
2. A day with a high demand profile.

For each day, the dispatch is calculated in a 2 hour resolution, resulting in 12 snapshots per day and 288 over the whole year.

The assumptions underlying the SWITCH modelling are detailed in the following sections.

Renewables distribution in the scenarios

Information on the currently installed RE capacity and future installation plans is publicly available.[51] The future installations considered in this study are projects with already approved construction plans. Public data is available in the form of installation capacity *by prefecture and municipality*. Nevertheless, *capacities by dispatch region (EPCO[52] region)* are needed for dispatch simulation, and capacities *by substation* are needed for the grid model. Capacities by dispatch region were derived by summing the capacities of the prefectures covered by an EPCO. Capacities by substation were derived by aggregating the capacities by municipality serviced by a particular substation. The total sum of installed capacities across the 9 EPCO regions including present and future installations was then scaled up to match the total installed capacities of VRES defined in the scenarios. This means that the distribution of the VRES capacities remains fixed for the two scenarios, and only the magnitudes of installations are scaled. Potential accelerated growth of a specific technology in a specific region was not considered. The results are given in Chapter 3.

Installed thermal capacities in 2030

Information on installed thermal power plant capacity and future installation plans is also made publicly available by each EPCO. Most of the thermal power plants in 2030 already exist in today's power system; the challenge is therefore to determine which plants may be retired by 2030 and which may still be operating. To determine this, the typical lifespan of

51 METI, "なっとく！ 再生可能エネルギー," 2018. [Online]. Available: http://www.enecho.meti.go.jp/category/saving_and_new/saiene/statistics/index.html. [Accessed April 2018].

52 An EPCO is an electric power company, such as TEPCO, which serves as the grid owner/operator for a specific geographical region of Japan. There are 10 EPCOs in total, 9 of which are interconnected across the main islands of Japan.

power plants was assumed (Table 17). The only new thermal power plants considered in this study were projects with already approved construction plans.

For new coal power plants, only projects that have passed the environmental assessment and are currently under construction were considered in the 2030 scenario.

Where the nuclear power plants are concerned, an approach was taken for the 2030 government scenario (GovS) which is in line with the reported figures from Japan's Ministry of Economy, Trade and Industry (METI, 2017). This approach results in an installed capacity of about 23 GW of nuclear generation in the GovS. No nuclear generation was assumed in the +RES scenario.

The assumption about which thermal power plants exist in the scenario has an important impact on the study results because it affects the amount of support they give to the grid. The generation type (e.g. nuclear, coal, gas) and the location of the power plant affect the amount of inertia, primary response, and proportion of infeed in the snapshots.

Assumed power plant lifespan — Table 17

Generation	Lifespan assumed
Coal	Decommissioned after 40 years of operation
Natural gas	Decommissioned after 40 years of operation
Gas co-generation	Decommissioned after 30 years of operation
Hydro	Decommissioned after 40 years of operation for new hydro
Geothermal	Decommissioned after 40 years of operation
Solar, wind, biomass	Decommissioned after 20 years of operation

REI (2019)

Approach to and constraints on net transfer capacities (NTCs)

The net transfer capacity is the maximum exchange capacity between two areas that remains compatible with security standards in both areas, while also taking into account technical uncertainties concerning network conditions (ENTSO-E, 2001). In this sense, it serves as a relevant input parameter for the dispatch model.

In a dispatch simulation, the NTCs regulate the maximum power exchange allowed between two regions. By definition this is already an important constraint that prevents transmission line overloading on interconnections between regions. The NTCs between two regions are determined through a committee discussion organized by OCCTO and can be different in absolute values in each direction.

The NTC used in the SWITCH simulation in both the GovS and the +RES are given below, along with the corresponding peak demands for each EPCO region in August 2016. The NTCs represent the current state of the art and do not include any potential future grid reinforcements, except for an update to the Hokkaido-Tohoku HVDC[53] corridor, which was increased

53 In the ENTSO-E System, HVDC interconnectors are treated as normal interconnectors when it comes to capacity allocation. This means that both TSOs linked by the interconnector need to agree on an NTC (yearly, quarterly, monthly, and daily). TSO can curtail the NTC capacity, i.e. setting it below the installed capacity of the interconnector, in case system security is endangered.

At the time of writing, it is not common practice to use HVDC interconnectors within the ENTSO-E for other purposes than market coupling. Nevertheless, the ENTSO-E Guideline on Electricity Balancing (ENTSO-E, 2017) in principle also allows for the use of interconnection capacities (AC as well as DC) for balancing purposes. Chapter 5 outlines the conditions which have to be met to use cross-zonal capacity for balancing services. In general, this is possible if socio-economic efficiency is proven for such a case.

NTC Values assumed in the SWITCH simulation

Figure 25

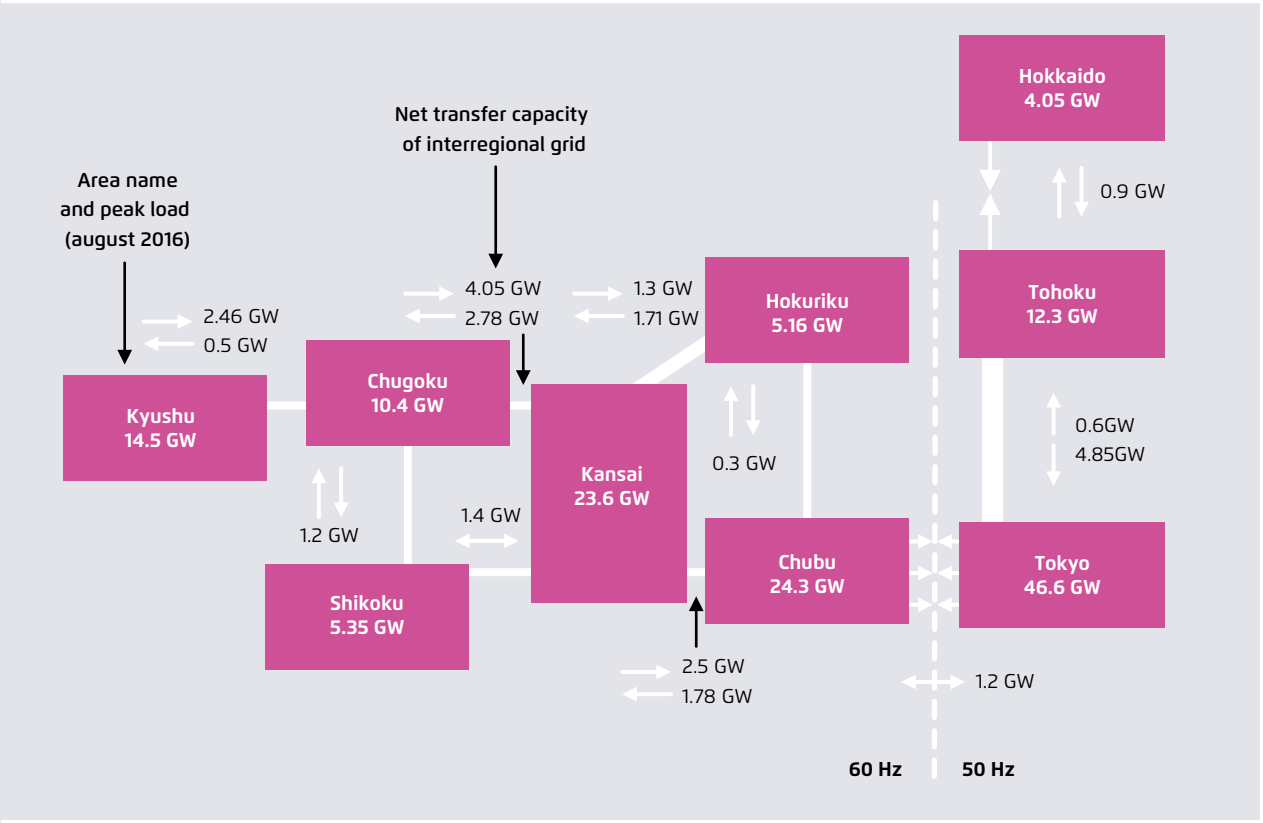

EGI (2019)

from 600MW to 900MW. As NTC restrictions have a direct impact on the dispatch, in high RES snapshots they could contribute to 'dispatch-based' RES curtailment. This was only the case for Hokkaido in snapshot 3 of the +RES , where there was a curtailment of 500MW.

Demand assumptions

Demand is considered the same in both scenarios. Despite a forecasted increase in energy efficiency and a population decrease, it is assumed that new power demand will be driven by an uptake in e-mobility, domestic battery installations, and electric space heating/cooling. In this study, we therefore use 2030 demand values similar to those of the 2013/2014 fiscal year without any modification in profile or magnitude. No demand response or load-shedding schemes were considered. The demand aggregated per EPCO region was distributed to substations in the grid model according to the repartition key applied in the IEE model. Extreme (maximum and minimum) demand situations are important for security assessments, while the hourly profile is important for year-round energy evaluation and ramp rate testing.

The days with the maximum and minimum midday peaks per month were identified and used as a basis for the SWITCH simulation. The demand curve is shown in 26. The figure shows the minimum and maximum demand days for each month consecutively. It can be seen that the absolute demand varies through the year between 75GW and 160GW and peaks in August.

Demand curve used in the SWITCH model

Figure 26

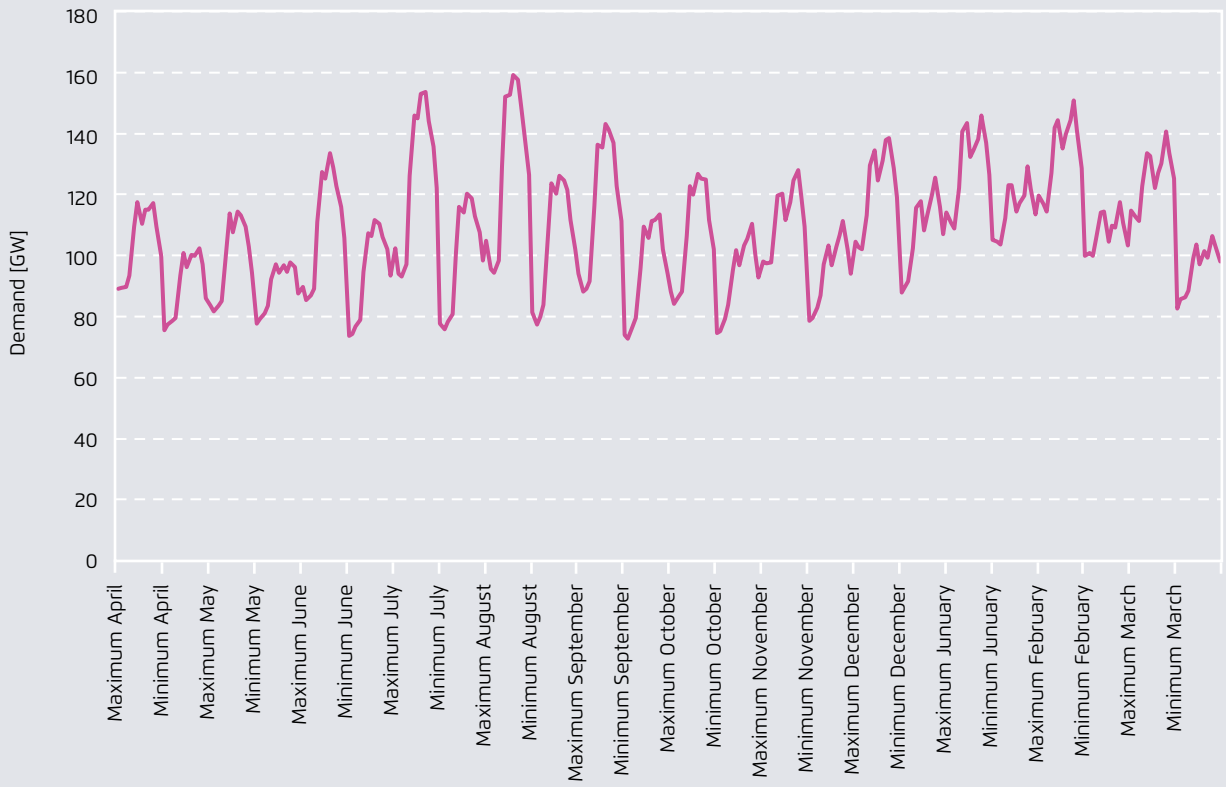

EGI (2019)

Dispatch rules and constraints applied in the SWITCH model

The following dispatch rules were applied in the SWITCH model:

→ Nuclear power plants (if present in the scenario) have dispatch priority and always run at 100% output power (this reflects current practices regarding nuclear dispatch in the Japanese system)
→ Other power plants are dispatched according to their variable costs (essentially their fuel costs)
→ Variable renewables are dispatched at fuel costs below all other technologies. They therefore have priority after nuclear generation facilities.

Additional constraints were implemented in the SWITCH model that have a direct impact on the dispatch results and potentially on stability and inertia:

- Each area must keep an (upwards) reserve generation capacity of 8% over the hourly demand. This means that the amount of primary reserve available to stabilise frequency depends on the demand. Such an approach is different from that adopted in Europe, for example, where a static amount of primary reserve is ensured regardless of the magnitude of demand. It is prudent to ensure this reserve size is in line with Japanese regulations and practice (which may change in future when transitioning to a market-based approach).
- Where a conventional power plant is dispatched in a given area, the infeed must be at least 10% of its generating capacity, ensuring some base level of

inertia and ancillary service provision to maintain grid security. Assessing whether this technical minimum sufficiently meets grid security requirements was nonetheless considered beyond the scope of this study.

- Import/export levels are limited to the net transfer capacities (NTCs – see Figure 25). The NTCs between two regions are determined through a committee discussion organized by OCCTO and can be different in absolute values in each direction.
- HVDC interconnection capacity can be used to the full for power exchange. No limitations (such as a reserve margin for emergency support) are considered.[54]
- Thermal power plants are categorised according to different levels of flexibility (baseload, intermediate, intermittent, hydropower, and storage). This means that ramp rate limitations on specific generation types are considered as constraints in the optimisation process. Nuclear power, for example is considered as inflexible baseload.

In light of these constraints, where generation exceeds demand, generation output is suppressed in thermal power plants first, then for hydro, bioenergy, and finally VRES power sources.

These dispatch constraints affect the number of units in operation and the amount of infeed from conventional power plants. This in turn affects the amount of inertia in the system and the amount of primary reserve available to support frequency. It also affects the amount of VRES that may need to be curtailed to ensure sufficient frequency support is available in the system.

54 Except when snapshots were tested with the 600 MW ancillary support at HVDC converter stations between eastern and western Japan.

Annex 3: Generation output and snapshot description

Generation output in both scenarios

Government scenario

Figure 27 shows how the load (as depicted in Figure 24) is supplied by different types of generation technologies in the government scenario. As indicated in Annex 2, the dispatch is performed for 288 snapshots (2-hourly dispatch for two days each month at maximum and minimum demand).

The following insights can be drawn from the figure:

- → Solar power infeed shows characteristic behaviour and peaks around noon. The highest hourly PV infeed is 40 GWh/h in June, and covers more than a third of demand during that hour.
- → Wind infeed is higher in the winter months and peaks at 5 am in March, at 7 GWh/h.
- → Nuclear is running baseload (priority dispatch), which results in a constant output of around 22 GWh/h.
- → Coal is operating more flexibly, with instantaneous output varying between 14 GW and 37 GW.
- → Gas operates even more flexibly, with output ranging between 8 GW and 50 GW.
- → Hydro (running water and swell water) output varies between 4 GW and 16 GW.
- → Pumped-hydro provides significant flexibility, ranging from 16 GW (pumping) to 14 GW (generating electricity).

Overview of generation output in the Government scenario — Figure 27

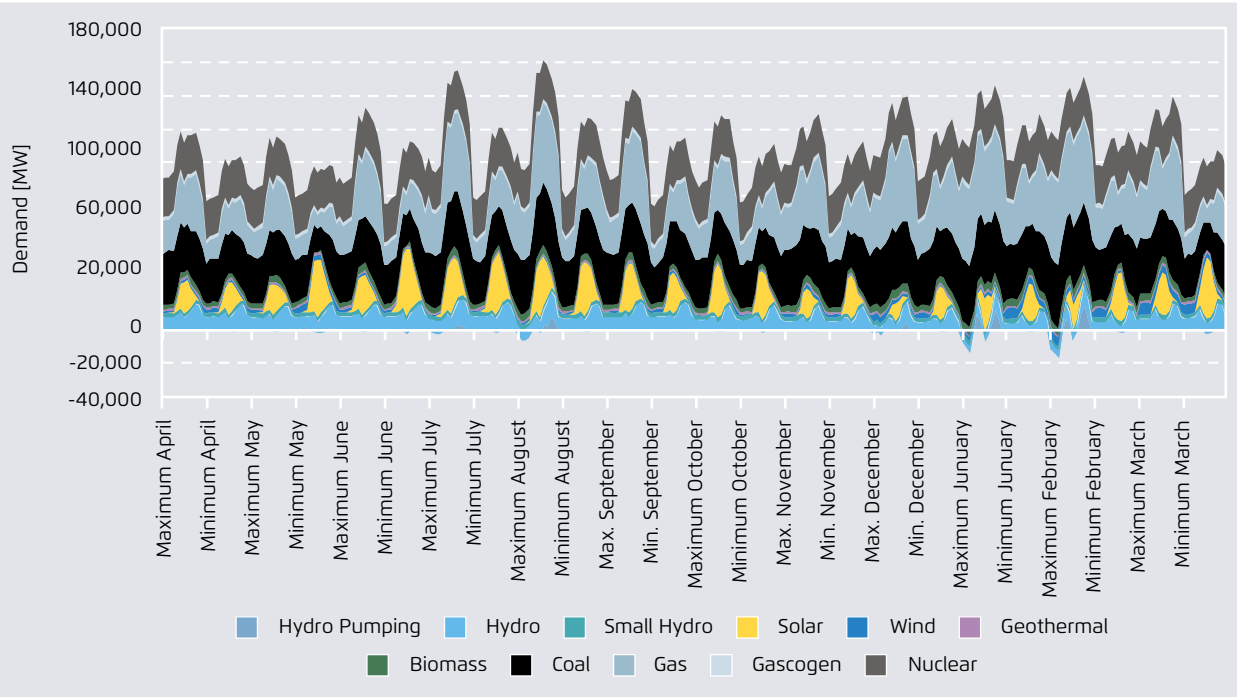

EGI (2019)

Annual generation comparison between the SWITCH model dispatch results for the Government scenario and actual government target values Table 18

Energy source	SWITCH model	Government target
Coal	28%	26%
Gas	26%	27%
Hydro	10%	8.8–9.2 %
Nuclear	21%	20–22%
Solar	7.1%	7%
Wind	1.7%	1.7%
Geothermal	1%	1.0–1.1%
Bioenergy	3.3%	3.7–4.6%
Total RE	**23%**	**22–24%**

REI (2019)

Annual generation in this scenario very much reflects the generation required to meet the official government targets for 2030, as can be seen in table 18.

+RES scenario

Figure 28 presents the generation output in the +RES scenario. The noticeable differences between this scenario and the government scenario are listed below:

- → There is no more nuclear power
- → The highest instantaneous wind infeed is multiplied by 3.7 and peaks at 26 GWh/h (in the same hour as in the government scenario).
- → The highest solar infeed is multiplied by 1.6 and peaks at 64 GWh/h (in the same hour as in the government scenario)
- → The minimum coal output is pushed down to 6 GW (compared to 14 GW in the government scenario)
- → The maximum gas output is increased to 55 GW (compared to 50 GW in the government scenario)

Overview of generation output in the +RES scenario Figure 28

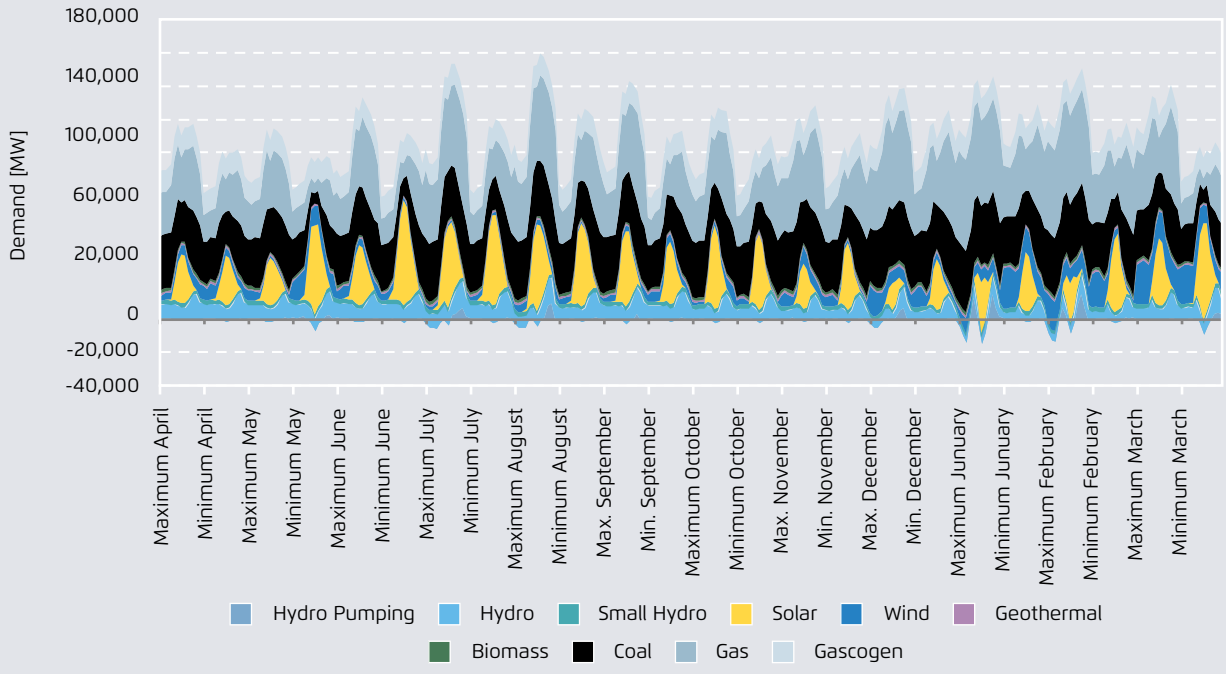

EGI (2019)

Annual generation comparison between the GovS and the +RES — Table 19

Energy source	Government scenario	+RES scenario
Coal	28%	28%
Gas	26%	31%
Hydro	10%	10%
Nuclear	21%	–
Solar	7.1%	11.1%
Wind	1.7%	6.2%
Geothermal	1%	1%
Bioenergy	3.3%	1.1%
Total RE	**23%**	**30%**

REI (2019)

Table 19 compares the annual shares of different energy sources in the GovS and the +RES.

Detailed snapshot description

This section illustrates regional dispatch in a number of snapshots analysed in this study (all of the snapshot data can be downloaded from the REI website).

Snapshot 1: High demand / low VRES

Figure 29 shows, for both scenarios, electricity generation in snapshot 1 (high demand / low VRES) in each EPCO region.

Two points can be highlighted:

→ The use of transmission capacity is moderate. The main exporters are Hokuriku and Shikoku (negative values for transmission).

→ Pumped hydro is generating.

Infeed snapshot 1 — Figure 29

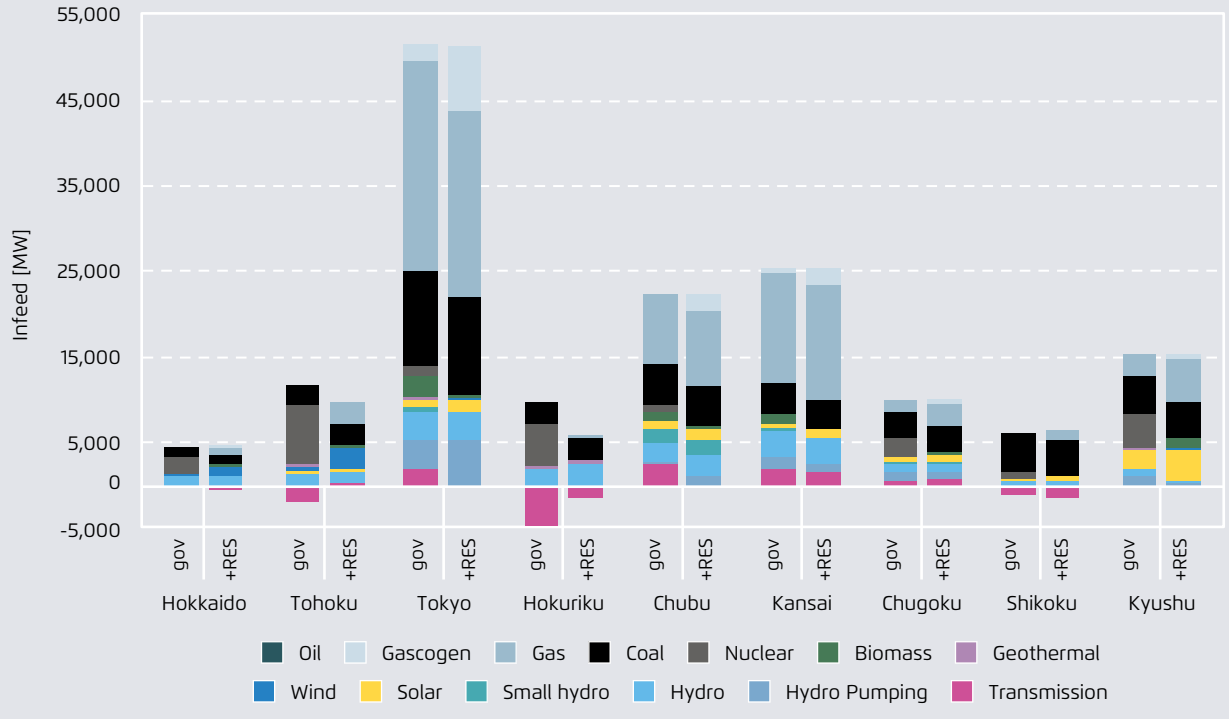

REI (2019)

Snapshot 2: High demand / medium VRES

Figure 30 shows the results of the SWITCH model for snapshot 2. A number of observations can be made:

- → The VRES share, especially solar power, is significantly higher than in the Low VRES snapshot.
- → In the +RES, the pumped hydro units are pumping.
- → There is a tendency toward higher transmission capacity usage.
- → VRES generation in Kyushu is far above the Japanese average.
- → VRES from wind only plays a significant role in the Hokkaido and Tohoku regions, i.e. the eastern part of the Japanese power system.

Infeed snapshot 2 Figure 30

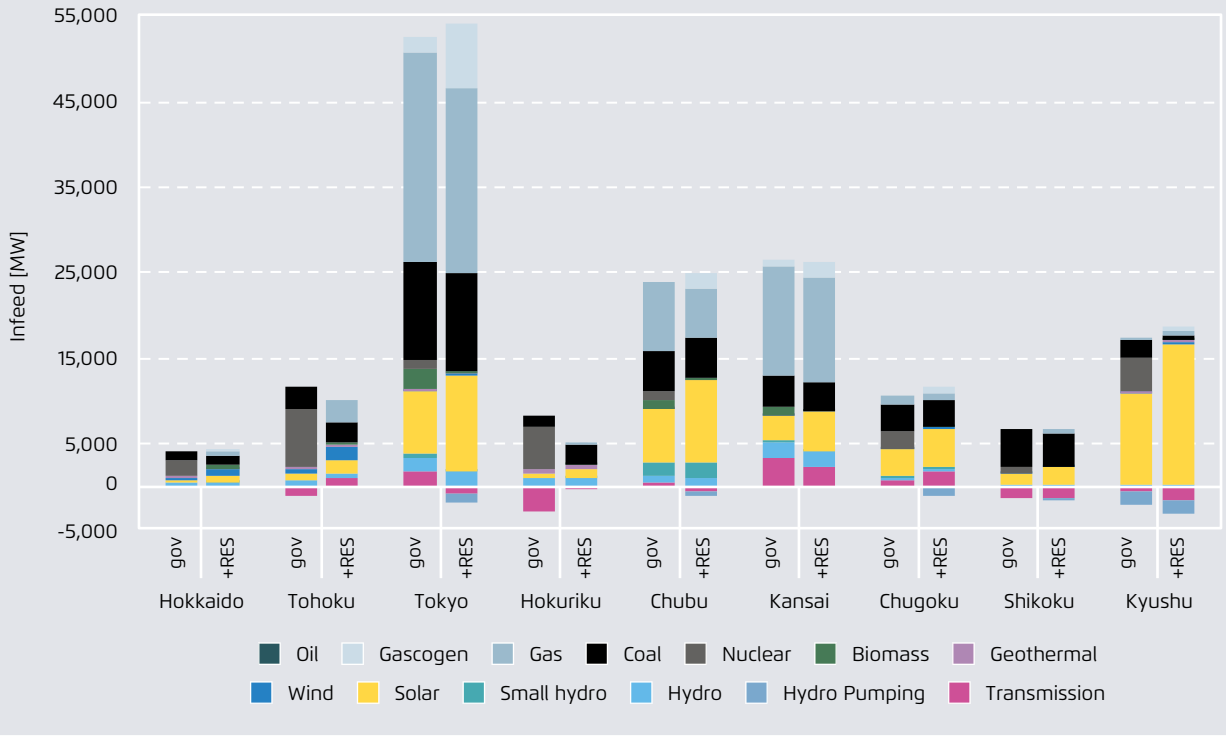

REI (2019)

Snapshot 3: Low demand / high VRES

Figure 31 shows the dispatch in snapshot 3 (high VRES / low demand).
Here we can observe the following:

- → Renewables dominate, especially in the +RES
- → Wind generation almost exclusively takes place in the eastern synchronous area of Japan (Hokkaido, Tohoku, Tokyo)
- → The missing nuclear in the +RES scenario is almost exclusively displaced by VRES. This can be seen most strikingly in Kyushu and Tohoku.
- → Pumped hydro is pumping at its maximum, especially in the Tokyo region.
- → There are very high shares of VRES, particularly in the +RES scenario for Kyushu, Shikoku, Hokkaido and Tohoku.

Infeed snapshot 3 — Figure 31

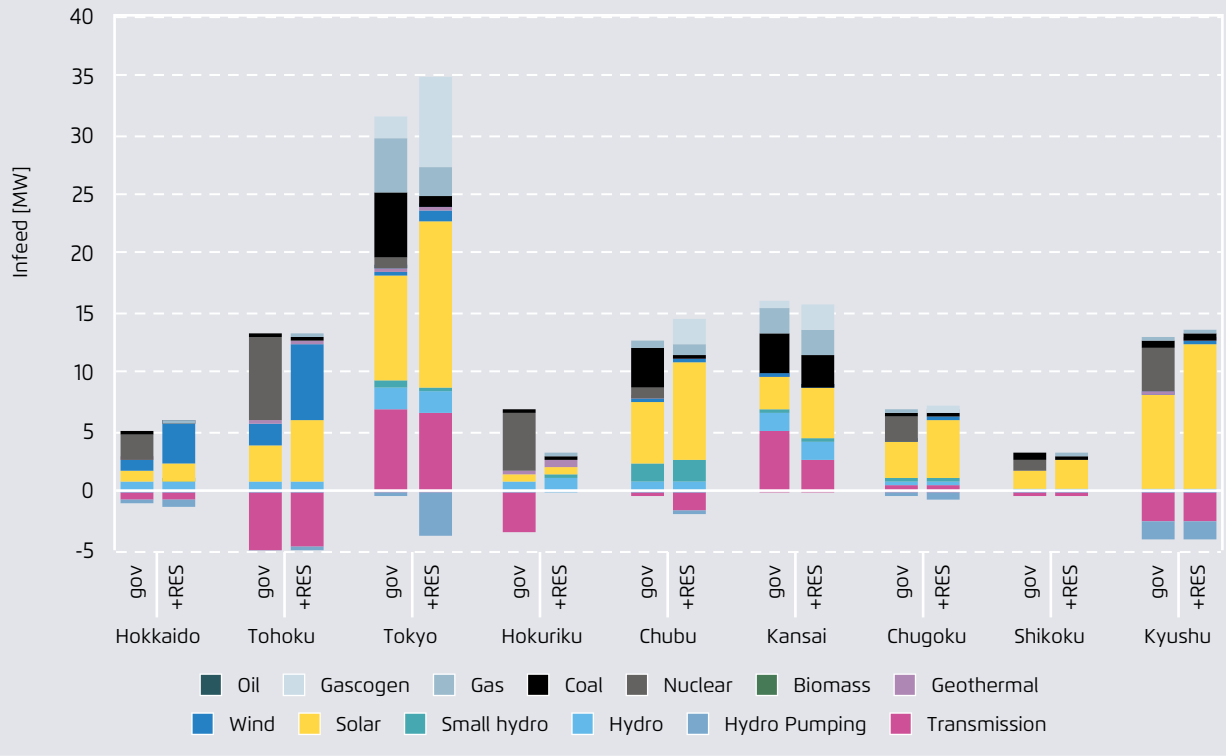

REI (2019)

Annex 4: Grid modelling assumptions

General remarks on the IEE model

The dynamic investigations undertaken for this project are based on the bulk power system models for Japan published by the Institute of Electrical Engineers in Japan (IEE).[55] The Japanese power system consists of two networks – the eastern Japan grid (50 Hz area) and western Japan grid (60 Hz area). Due to the different characteristics of these networks, two different power system models were developed. The original eastern model consists of 107 nodes with 191 branches and the original western model consists of 115 nodes with 129 branches. The entire set of conventional generation is aggregated and represented by 30 generators per network. These 30-machine system models are reduced and anonymised, representing only the 500 kV and 275 kV voltage level. Further descriptions and characteristics can be found by following the IEE website link provided.

This chapter describes how this bulk model (the 'paper model') and its apparatus including governors and automatic voltage regulators was implemented and validated in a PowerFactory grid model. The IEE bulk power system model was developed and optimised with the aim of evaluating system stability and assessing the impact of any further system control technologies within the network. In this study, the large scale 30-machine models provided by the IEE are used.

55 The original IEE simulation models are publicly available and can be downloaded from: http://www.iee.jp/pes/?page_id=141

Overall modelling and simulation procedure — Figure 32

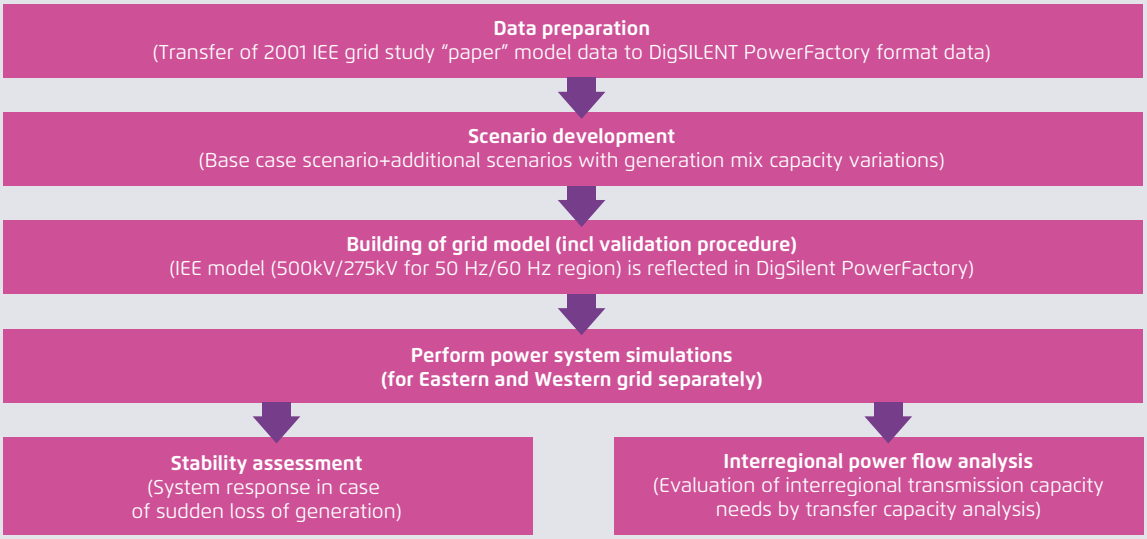

EGI (2019)

These kinds of simulation models aim to provide engineers with commonly agreed standard models that reflect the dynamic behaviour of the Japanese power system in a way that comes very close to reality. Several simplifications and compromises had to be made in creating these models. In order to ensure that the results reached via these models are robust, the dynamic behaviour of the IEE model is generally slightly more sensitive than the real system behaviour (this means that it reacts more strongly to severe conditions). The models were optimised for the investigation of fault events at selected points in the grid. This means that the model's system response (and its ability to reach stable conditions after performing a fault event) is dependent on the fault location (IEE Japan, 2018b). In this analysis, several fault locations were therefore analysed and the worst-case scenario was considered.

Modelling methodology

Figure 32 shows the entire process for the modelling and simulation procedure.

In the first stage, the 2001 IEE grid study model, which is available in paper format, was pre-processed and transferred into the DIgSILENT PowerFactory simulation environment. The latter was chosen here as the best means of generating the intended stability analysis results. The individual steps of this data preparation process are described in this annex. Figure 33 shows the shape of the original 2001 IEE study grid model for the eastern Japan network.

In the second stage, scenarios were developed and dispatch situations (snapshots) were selected. The third step is the core of the grid model simulation.

Outline of the IEE EAST 30-machine system model (IEE Japan) Figure 33

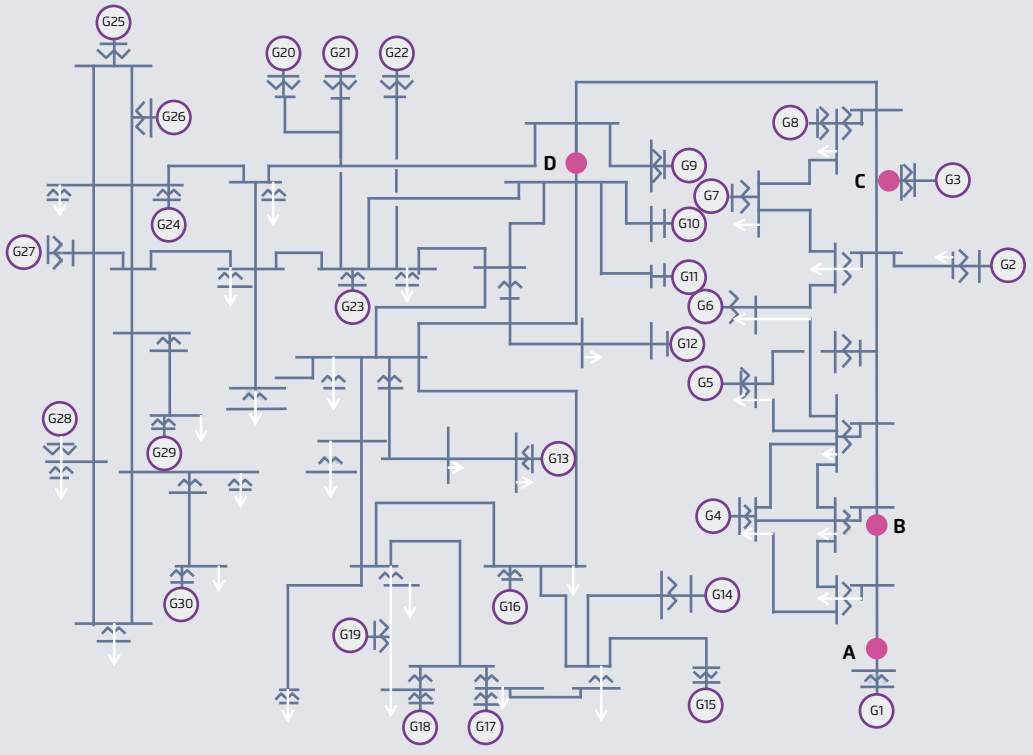

IEE (2001)

This step included a model validation procedure to show conformity between the transferred network model and the original IEE model which served as a reference. The grid simulation was then run for all scenarios under different infeed/load situations in the eastern and in the western grids. Finally, a frequency stability analysis and a load-flow analysis were performed. The stability assessment was performed to show the system response to a sudden loss of generation, and included subsequent evaluation and the derivation of important conclusions. The power flow analysis indicates certain tendencies regarding the development of line loadings by changing the RES infeed situation to determine possible grid reinforcement needs.

Grid model set-up and validation procedure

Steady-state modelling

This section provides a detailed description of the system modelling. A text document is available within the IEE models which gives the detailed steady state parameters of the network in Y-method format. The Y-method is based on the standard parameters of the CRIEPI's power system dynamics analysis program, which is widely used in Japan.

Basic system data for IEE East and IEE West — Table 20

	IEE EAST system	IEE WEST system
Frequency	50	60
Sbase	1,000 MVA	1,000 MVA
Ubase	500 kV	500 kV
Nodes	107	115
Branches	191	129

IEE (2001)

In this format, all the data concerning lines, transformers, generators and nodes are in p.u. system with base power of 1000 MW. To implement the network in DIgSILENT PowerFactory, the p.u. data has to be converted into SI unit system. The Y-data format file describes how to use and interpret the Y-data for the system.

The base voltage for all the nodes in the east and the west is taken as 500 kV. The basic system data is summarised in table 20.

Figure 34 shows the process used to import the steady state Y-method data into PowerFactory.

Import procedure for steady state Y-method data into PowerFactory — Figure 34

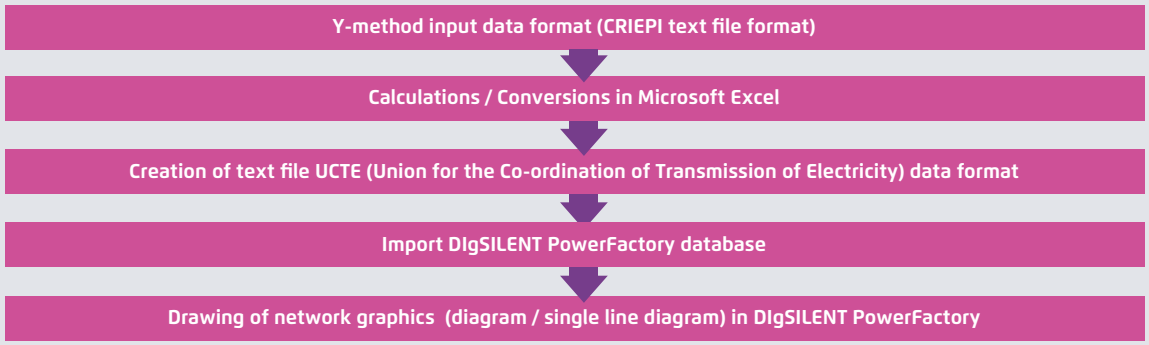

GridLab (2019)

Following an intermediate stage involving the UCTE format, the data is imported into PowerFactory. Once the data has been imported, the network graphic is drawn.

Later on, the data is assigned to network elements and components. This process is carried out for both the eastern and western network models. An additional Hokkaido EPCO region is added to the IEE 2001 East model. The final PowerFactory network graphics are shown in Figure 35 and Figure 36.

Final PowerFactory network graphic for the eastern Japan grid (50 Hz area) Figure 35

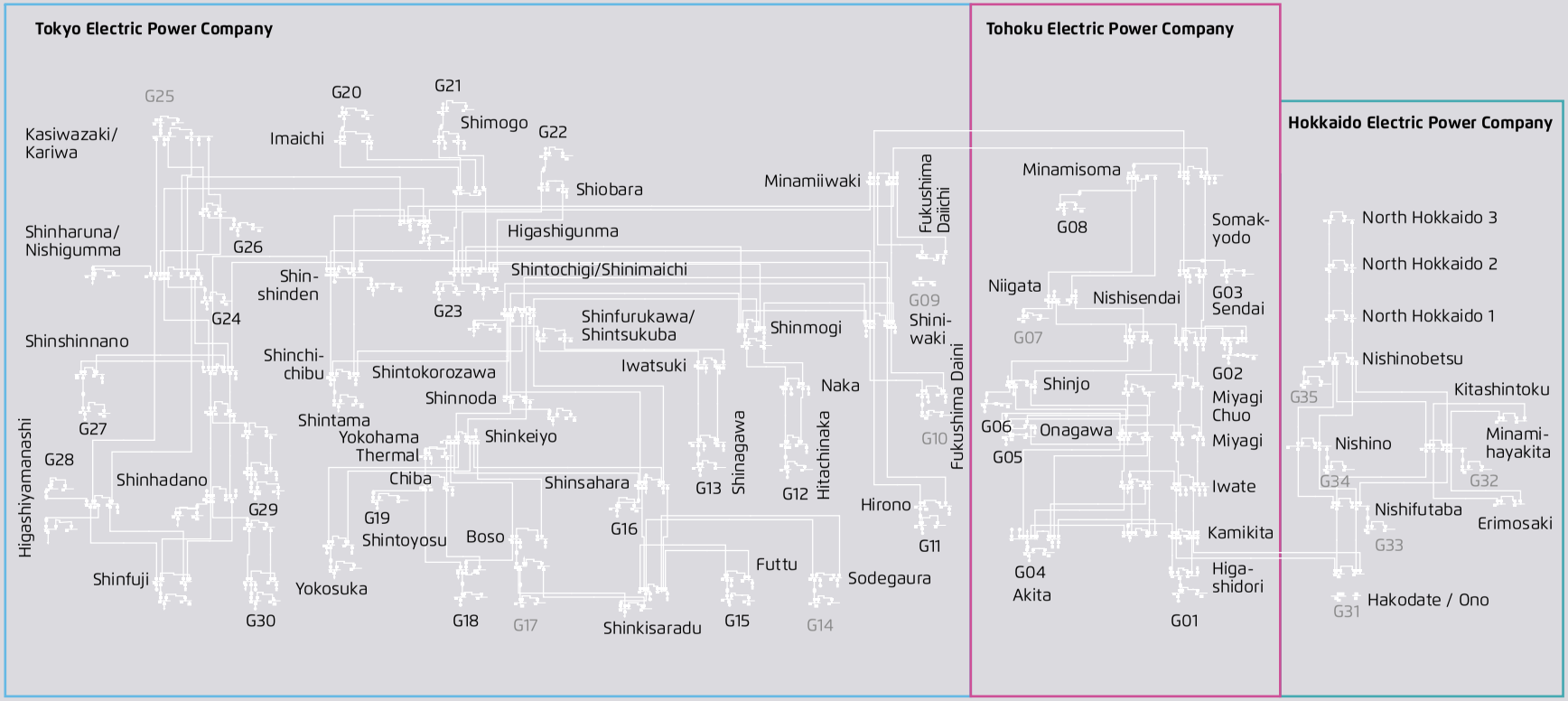

IEE (2001), GridLab (2019), REI (2019)

Figure 36

Final PowerFactory network graphic for the western Japan grid (60 Hz area)

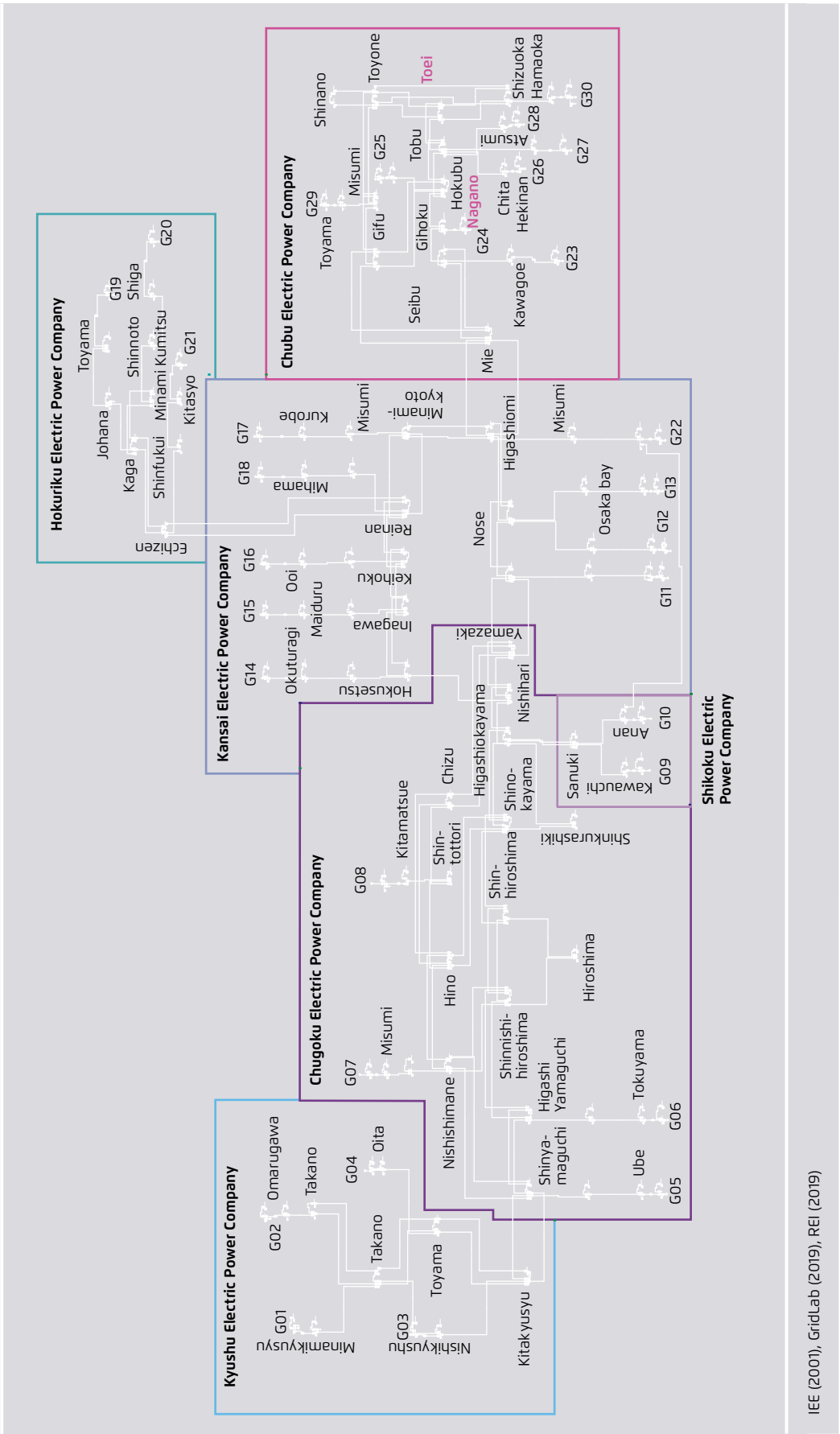

IEE (2001), GridLab (2019), REI (2019)

Dynamic system modelling

In this section, we discuss the modelling of generators' automatic voltage regulators (AVR).

a. Automatic voltage regulator (AVR)

An AVR is a device used to regulate the generator terminal voltage at a constant value during any change in load and system operating point. An error signal is generated by comparing the terminal voltage to a reference value and is then used to adjust the generator's exciter field current. The AVR model (LAT=1) documented in the IEE documentation is used to harness the accurate and legitimate behaviour of the Japanese system. It is known as a rotating exciter model and is shown in Figure 37.

b. Governors

A governor is a device used to maintain the constant speed of the generator, i.e. typically 50 Hz or 60 Hz. It ensures that the generator keeps rotating at a constant speed by opening or closing the fuel throttle of the turbine during any change in load. In thermal and nuclear power plants, it will adjust the flow of steam to the turbine. Similarly, in hydropower plants it will adjust the flow of water to the hydro turbine runner. The governor control is responsible for activating the primary control reserve (spinning reserve). In order to harness the accurate and legitimate behaviour of the Japanese system, the governor model (LPT=1, LPT=3 and LPT=4) documented in the IEE documentation is used. Figure 38 shows the governor models.

The input signal to the governor is the speed deviation. This is computed by comparing the actual generator speed to its rated speed. This speed deviation is converted into the torque signal. In Figure 39, 65M is the initial reference value at which the governor is loaded. Where the governors are not operated at 100% but at 90%, the 65M is set to 0.9 p.u. This means that during

AVR model according to the IEE documentation — Figure 37

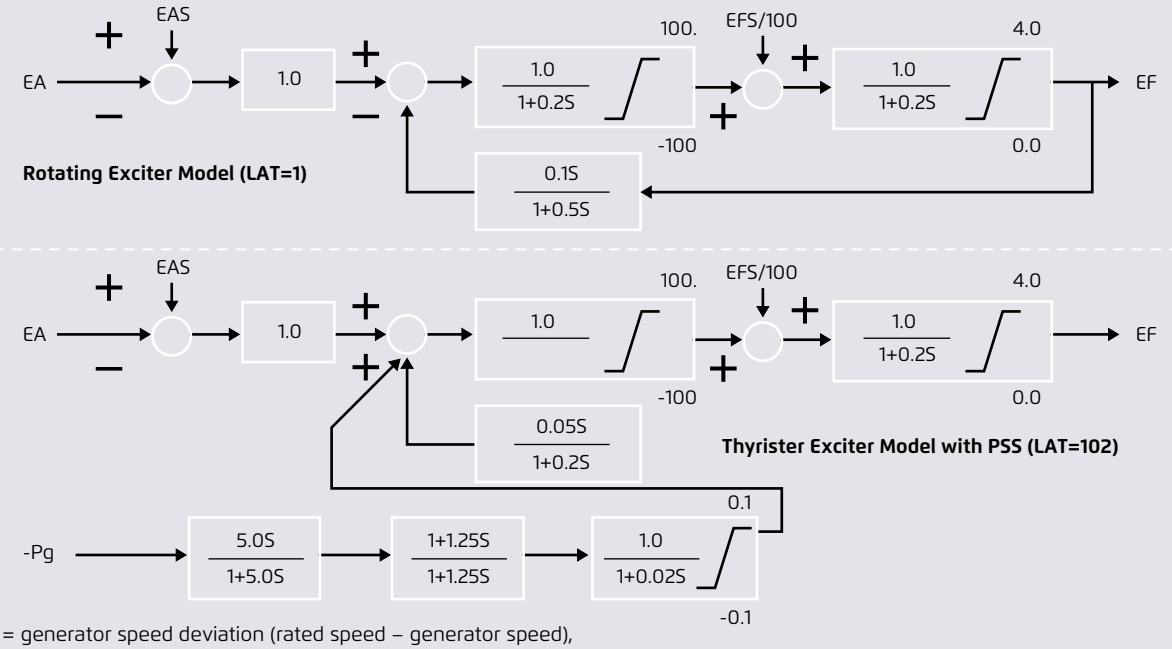

Sg = generator speed deviation (rated speed – generator speed),
TQT = turbine torque, 65M = turbine load reference, 77M = turbine load limiter

IEE Japan

Governor models according to the IEE documentation (IEE Japan, 2018) Figure 38

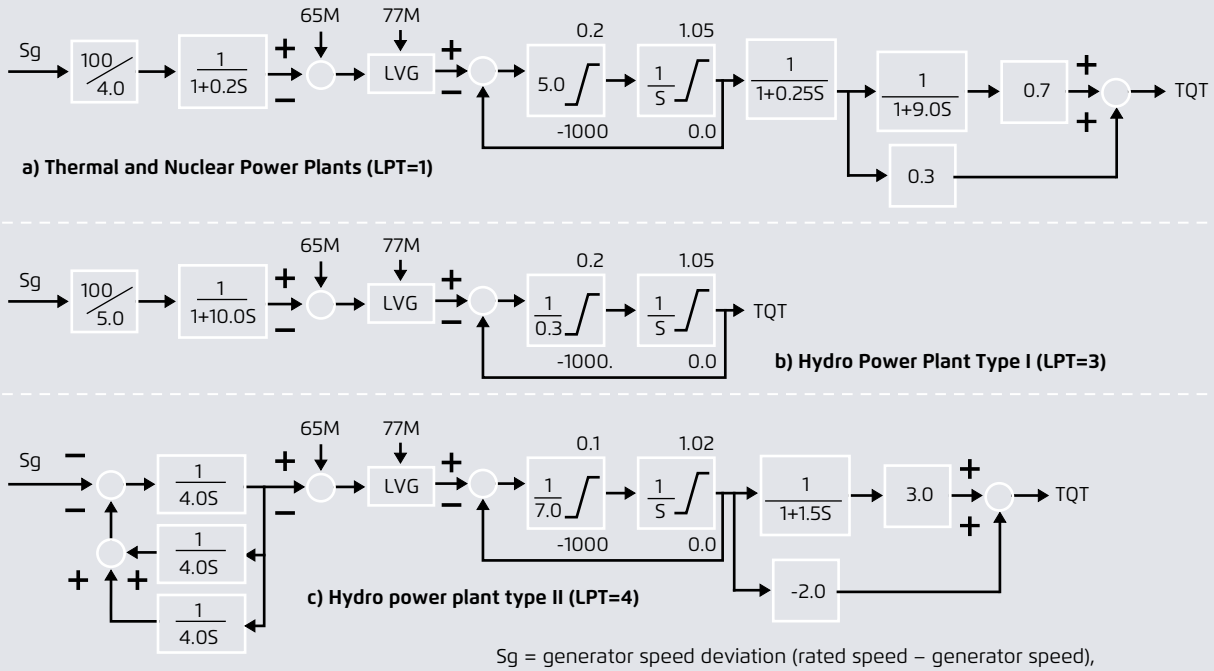

Sg = generator speed deviation (rated speed – generator speed),
TQT = turbine torque, 65M = turbine load reference, 77M = turbine load limiter

IEE Japan

normal operations when the governor is operating at 0.9 p.u., the generator is operating at its specified output. The next block in the graph - LVG (low valve gate) - sets the limit for governor. The limiting parameter is specified at 77M. This block will compare the input value with 77M and pass the lower value. This ensures that the governor does not operate beyond this limit. The limit may be set between 1.0 p.u. and 1.1 p.u., for example, depending on the simulation requirements.

According to the IEE model documentation, the spinning reserve within the simulation model is specified between 5% and 10% of the installed power. Taking the particular circumstances in Japan into account, nuclear power stations do not contribute to primary control reserve. This means that the governor control is deactivated for nuclear power plants.

For all of the scenarios and snapshots investigated, the available spinning reserve is adequate to limit the frequency drop after the event occurs in the proper way. Table 21 shows the activated primary control power values for the entire set of scenarios.

Overview of activated primary control reserves Table 21

	GovS		+RES	
	P_{PCR_EAST} [MW]	P_{PCR_WEST} [MW]	P_{PCR_EAST} [MW]	P_{PCR_WEST} [MW]
Low RES (S1)	1,471	1,473	1,670	1,518
Med RES (S2)	1,473	1,484	1,578	1,529
High RES, high Load (S2b)			1,491	1,516
High RES, low Load (S3)	1,446	1,466	1,492	1,489

GridLab (2019)

c. Inertia parameterisation

In order to perform frequency stability studies, it is important to account for the total system inertia. The total system inertia within the system at a specified time is dependent on the inertia constants of the online generators and the technology used. To clarify: renewables and power electronics-based generators have no inertia and therefore do not contribute – at least without special technical retrofitting – to the system's overall inertia. The typical inertia constants by generator type (as per information from Chown et al. 2017, Tielens et al. (2012), DNV Kema, 2013) are given in Table 22. It has to be considered that the exact inertia value within a certain generation type is still dependent on further technological dimensions and also on the power plant unit size.

Inertia constant values by generation type — Table 22

Generation type	Inertia constant H (MW*s/MVA)
CCGT	5
Nuclear	5
Hydro	4
Coal	4
GasCo	2
other	2

Chown et al. (2017), Tielens et al. (2012), DNV Kema (2013)

Some documentation also provides the inertia time constant Ta, which is equal to two times the inertia value (see equation 11-1).

$$T_a = 2 * H$$

With: T_a Inertia time constant [s]
H Inertia constant [MW*s/MVA]

Mapping the Japanese conventional power plants and load on to the IEE network models

In order to perform the 2030 simulations for the Japanese network, it was necessary to map the existing and future conventional power plants on to the IEE model. The basic reference for the mapping was the optimal power generation mix (OPGM) model developed by Mr. R. Komiyama from The University of Tokyo (Komiyama, 2016). The OPGM was further verified by REI in order to validate the conventional power plant mapping.

Once the geographical mapping of EPCOs and conventional power plants had been completed, the capacity allocated to the generators was entered into an excel sheet. Here the generators were categorised according to their Japanese prefecture name and number.[56]

The process was carried out for both the west and east models. After this mapping had been carried out, the total installed capacity within the IEE model generators was determined. This installed capacity was further divided into conventional generation in the form of hydro, pumped-hydro, coal, CCGT, cogeneration, and other. Later, the type of generation was decided on the basis of the highest installed generation technology within each generator.[57]

The principle that was subsequently used to geographically allocate the remaining thermal units for the grid stability analysis is summarised in the following:

→ Investigation of the power stations / units originally represented by each generator (G1-G30) for the eastern and western grids separately (using the IEE name list provided by REI, as well as (Komiyama, 2016) and our own inquiries)

56 The database for the allocation of the 2030 generation capacities to the respective generators (30-machine structure) and prefectures is available with this report.

57 The database for the list of new generators after adaption of conventional capacities for the 2030 time horizon is available together with this report.

→ Allocation of the prefecture information to the mapping procedure (also through the use of the list of existing plants and the IEE name list provided by REI).

→ Consideration of the generation capacity by fuel type overview for 2030 also provided with the prefecture information.

→ Assignment of the single generation capacity values to the generators (G1–G30) for the active power plants in 2030.

→ Establishment of the type of generator according to the dominant part of the (sometimes mixed) generation fleet, and implementing it in the model (especially in terms of the inertia constant used later).

Once the overall installed capacity had been calculated, the actual dispatch as per the snapshots was calculated. This was done using the switch model results for the different snapshot scenarios provided by REI. It was assumed that the distribution in the switch model corresponded to the distribution between the EPCO areas. The output of each generator unit was changed in proportion to the entire generation in each EPCO region'. The formula used to calculate this output is given below:

$$P_{(gen.new)} = P_{(gen.capacity)} * \frac{P_{(EPCO.snapshot)}}{P_{(EPCO.TotalCapacity)}}$$

Where,

$P_{(gen.new)}$ = Actual dispatch of active and reactive power of the respective individual generator as per the snapshot

$P_{(gen.capacity)}$ = Generation capacity (P&Q) of the respective generator as per the generation mapping by switch model

$P_{(EPCO.snapshot)}$ = Actual overall generation in the respective EPCO as per the snapshot dispatch

$P_{(EPCO.TotalCapacity)}$ = Total capacity installed in the respective EPCO as per the switch model data

Let us consider an example to understand more clearly how this procedure works. Consider generator G1 in the IEE East Japan model. Generation capacity of the G1 is 671 MW. Here G1 belongs to Tohoku EPCO. According to the switch model, the total installed capacity in Tohoku is 11964 MW. In the low RES snapshot in the +RE scenario, the actual dispatch within Tohoku is given as 6886 MW. Now when we substitute these values in the above formula,

$$P_{gen.new(G1)} = 671\ MW * \frac{6{,}886\ MW}{11{,}964\ MW} = 386\ MW$$

These calculations are performed for all the generators. The calculation was carried out in Excel.[58]

The new load distribution for the snapshot scenarios was carried out on the basis of the EPCO load distribution data provided by the REI. A formula similar to that used for the generators was used to perform the calculation in Excel.[59]

$$P_{load.new} = P_{basecase} * \frac{P_{EPCO\ new}}{P_{EPCO\ basecase}}$$

$$Q_{load.new} = P_{basecase} * \frac{Q_{basecase}}{P_{EPCO\ basecase}}$$

58 The database for the final dispatch for the three snapshots according to the SWITCH model output data is available with this report.

59 The database for the calculation of load values in the snapshots is available with this report.

Implementation of renewable energy sources within the IEE model

The switch model provides the data related to the installed RES capacity within the different prefectures for the various scenarios. This data is used to map the installed RES generation within the EPCOs and is considered as the base value. Each node within the IEE model is assumed to represent the prefectures within the respective EPCOs. At each such node, a wind farm and a PV system is connected. The dispatch power values of the generation units are calculated using the formulas below.

$$P_{(wind.prefecture)} = P_{(wind.prefecture.base)} * \frac{P_{wind.EPCO\ new}}{P_{wind*EPCO\ basecase}}$$

$$P_{(PV.prefecture)} = P_{(PV.prefecture.base)} * \frac{P_{PV.EPCO\ basecase}}{P_{PV.EPCO\ basecase}}$$

The above calculations were performed in excel for the East and West models.[60]

Validation of the IEE model

In order to validate the IEE static and dynamic model within PowerFactory, a static power flow and short circuit study was performed at the locations given in the IEE documentation. The PowerFactory results were compared with the standard IEE results provided. It needs to be noted that the FFR features and functionalities were not included in the original IEE model and are hence not part of the validation discussed in this section.

60 The database for the distribution of renewables and the calculation of particular infeed values for different snapshots is available with this report.

a. Validation of the IEE West model

In the West model, a three-phase short circuit was simulated. Figure 39, next page, compares the PowerFactory results and the IEE documentation. The location of Point D is selected to validate. As can be seen, the generator internal angles, generator active power and line active power flow are similar. We can confirm that the model used exhibits similar characteristics to that of the standard model.

Static power flow results:

Node 1340

	IEE Doc.	PowerFactory
Voltage p.u.	1.01	1.006
Angle	2.17	2.2
Power_In MW	1,780	1,776.7
Power_Out MW	1,780	1,776.4

b. Validation of the IEE East model

Similarly, in the East model, a three-phase short circuit was simulated. The figure below compares the the PowerFactory results and the IEE documentation.

The location of Point D is selected to validate. Figure 40, page 88, shows the results.

Static power flow results:

Node 2108

	IEE Doc.	PowerFactory
Voltage p.u.	1.096	1.096
Angle	16.1	16
Power_In MW	4,320	4,320.4
Power_Out MW	4,320	4,320.2

Results for a 1-circuit fault in the western grid at a specified disturbance point, with the fault clearing after 0.07 s

Figure 39

DIGSILENT PowerFactory **IEEJ Documentation**

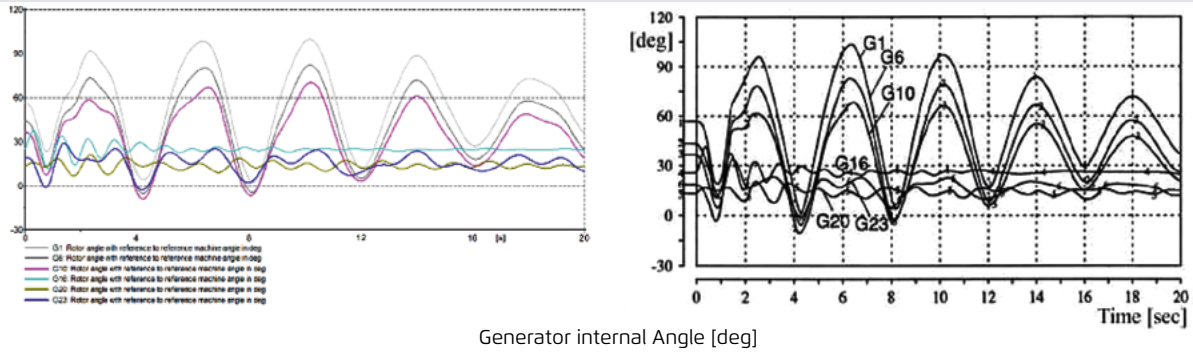

Generator internal Angle [deg]

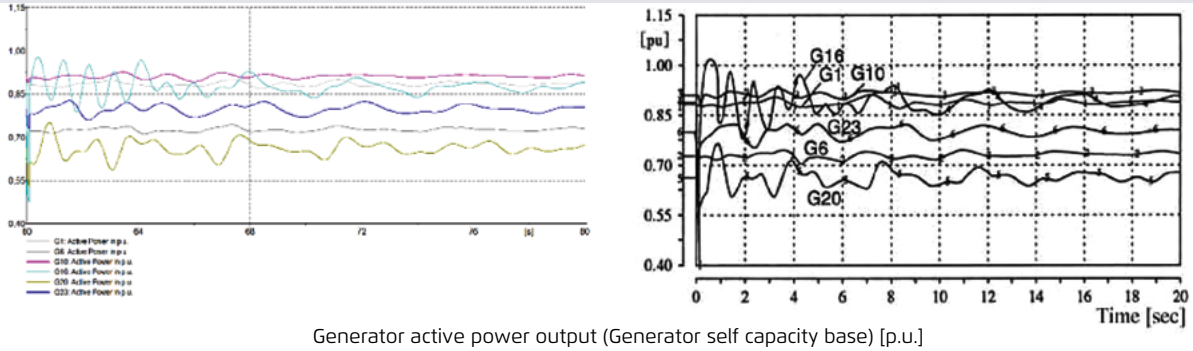

Generator active power output (Generator self capacity base) [p.u.]

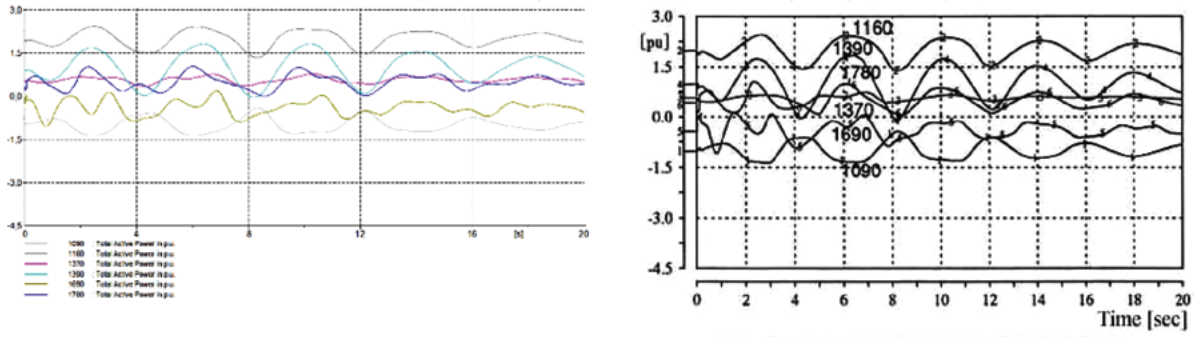

Line active power Flow [p.u.]

IEE Japan, GridLab

Results for a 1-circuit fault in the eastern grid at a specified disturbance point, with the fault clearing after 0.07 s

Figure 40

DIGSILENT PowerFactory | **IEEJ Documentation**

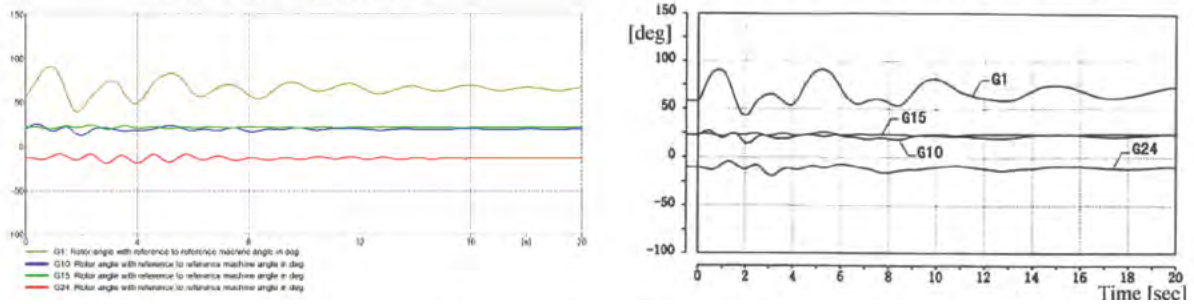

Generator internal Angle [deg]

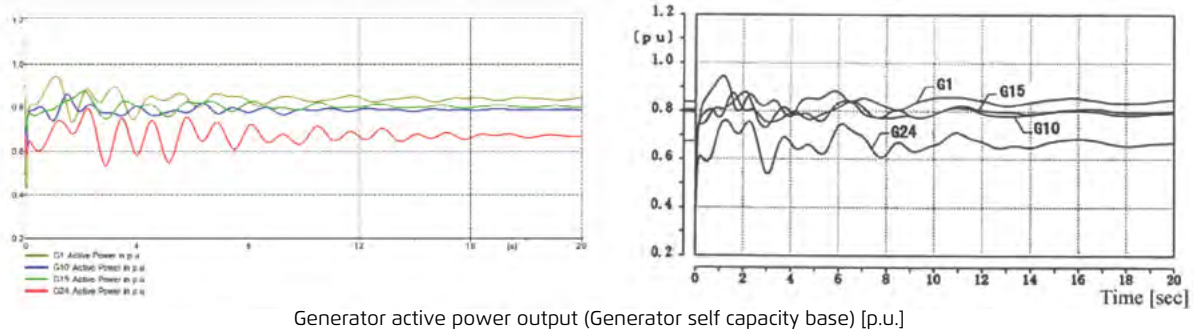

Generator active power output (Generator self capacity base) [p.u.]

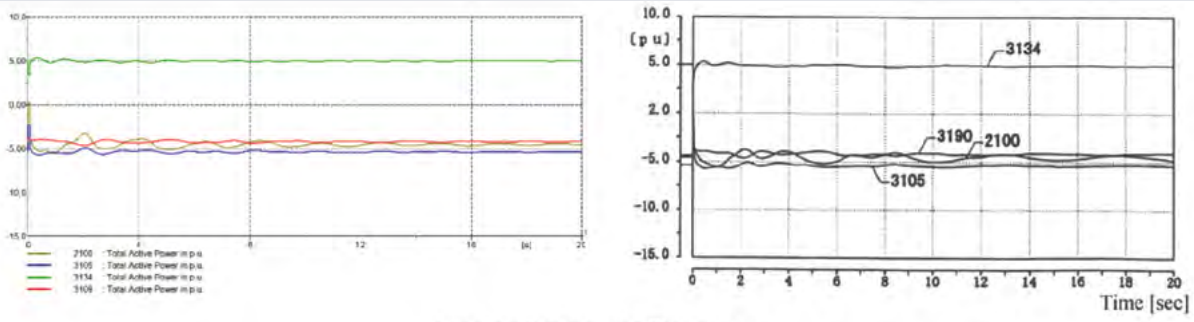

Line active power Flow [p.u.]

IEE Japan, GridLab

To conclude the model validation procedure, it can be seen that the extracted line active power flow results match the shape of the IEE model documentation perfectly. Furthermore, the dynamic modelling results show very good compliance with the curves given in the original IEE model. The transfer of the model into the new simulation environment is therefore successful and the model proves to be valid for further simulation and analysis.

Evaluation criteria for the dynamic analysis

The methodology for the grid stability analysis focusses on frequency stability issues and particularly on the inertial response in the period before the primary response comes into action (approx. 0–5 s) and which is an inherent property and autonomous reaction of synchronously rotating generators according to the following equation:

$$\frac{2H}{\omega_s} * \frac{d\omega}{dt} = P_m - P_e$$

With:
- H Inertia constant
- ω_s Synchronous speed
- $\frac{d\omega}{dt}$ (Mechanical) acceleration
- P_m Mechanical power
- P_e Electrical power

The frequency stability evaluation carried out consists of time domain simulations with respect to a normative or reference incident. The aim is in part to evaluate the minimum inertia and maximum RES penetration possible without compromising grid stability in the Japanese power system in 2030.

Different criteria were therefore proposed to evaluate the frequency response of the system at selected node locations in the Japanese network. These were:

- → **The frequency nadir**
- → **The derivative of the frequency (rate of change of frequency (RoCoF)**
- → **System inertia was defined as:**

$$H_{sys} = \sum_{i=1}^{N} S_{n\iota} H_{\iota}$$

Where:
- $S_{n\iota}$ is the rated apparent power of generator ι [MVA] and
- H_{ι} is the inertia constant of turbine generator ι [MW*s/MVA].

Frequency drop from nominal and RoCoF when load shedding starts for selected regions

Figure 41

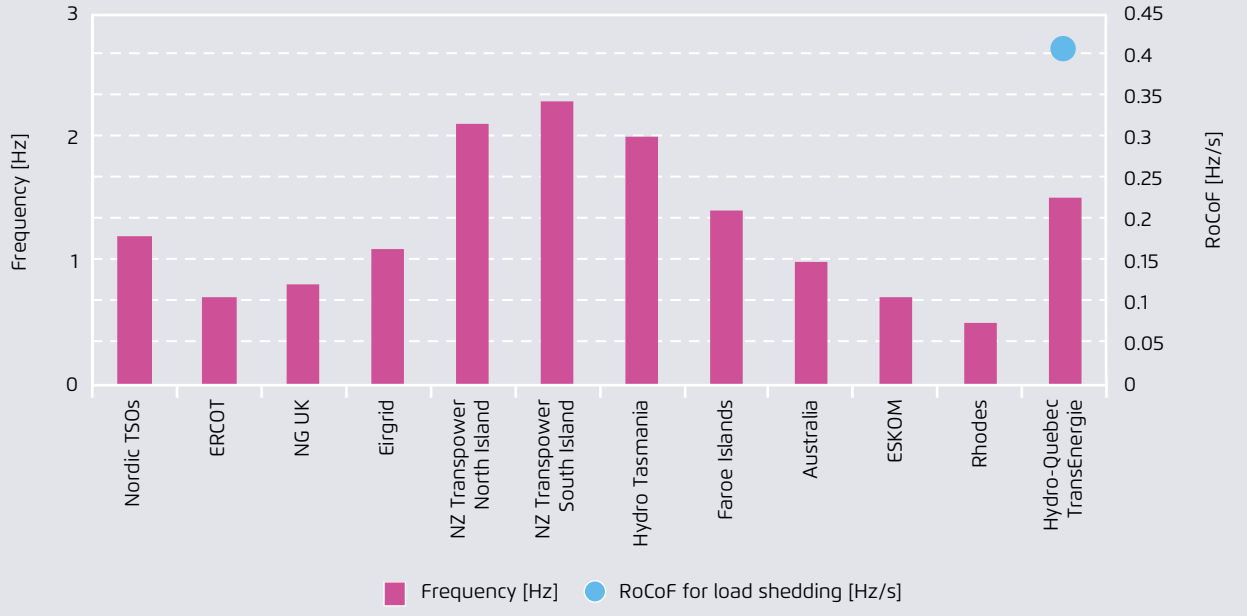

ENTSO-E (2018)

In the Japan transmission network, a RoCoF value of 0.2 Hz/s is considered a critical threshold for the later analysis.

It is important to understand the concrete influence of certain generator characteristics on the shape of the frequency response. As already mentioned, the *initial gradient of the frequency drop (RoCoF)* after the incident is directly linked to the *inertia in the system*. The level of inertia that arises within the first 5 seconds after the event also has *a significant impact on the frequency nadir value*. The activation of an appropriate amount of *primary control power* (which is enabled autonomously by the governor control mechanism) is *responsible for stopping the frequency drop and bringing the frequency back to a stable condition and value*. The new frequency level, however, is still below the nominal frequency, because of the applied proportional (P) controller scheme. Here a control deviation is always needed to ensure proper functioning due to the nature of this controller structure. The primary control power thus influences both the frequency nadir (in combination with the RoCoF) and the time span needed to restore stable frequency conditions. As can be seen in the results section in Chapter 4, the activation of the primary control reserve starts within 20 s after the event. More detailed information regarding the governor control is available in the above section of this annex.

In reality, the secondary control functionality would come into action at this point as an additional mechanism to restore the nominal frequency value. Secondary control power is not considered within the simulations in this project, therefore the frequency always remains lower than nominal frequency after the sudden loss of generation.

In this study, the largest contingency was defined as a sudden 1.5 GW loss of generation producing an under-frequency event. An example of a sudden loss of 1.5 GW thermal power plant generation in the Tohoku EPCO region is indicated in Figure 42.

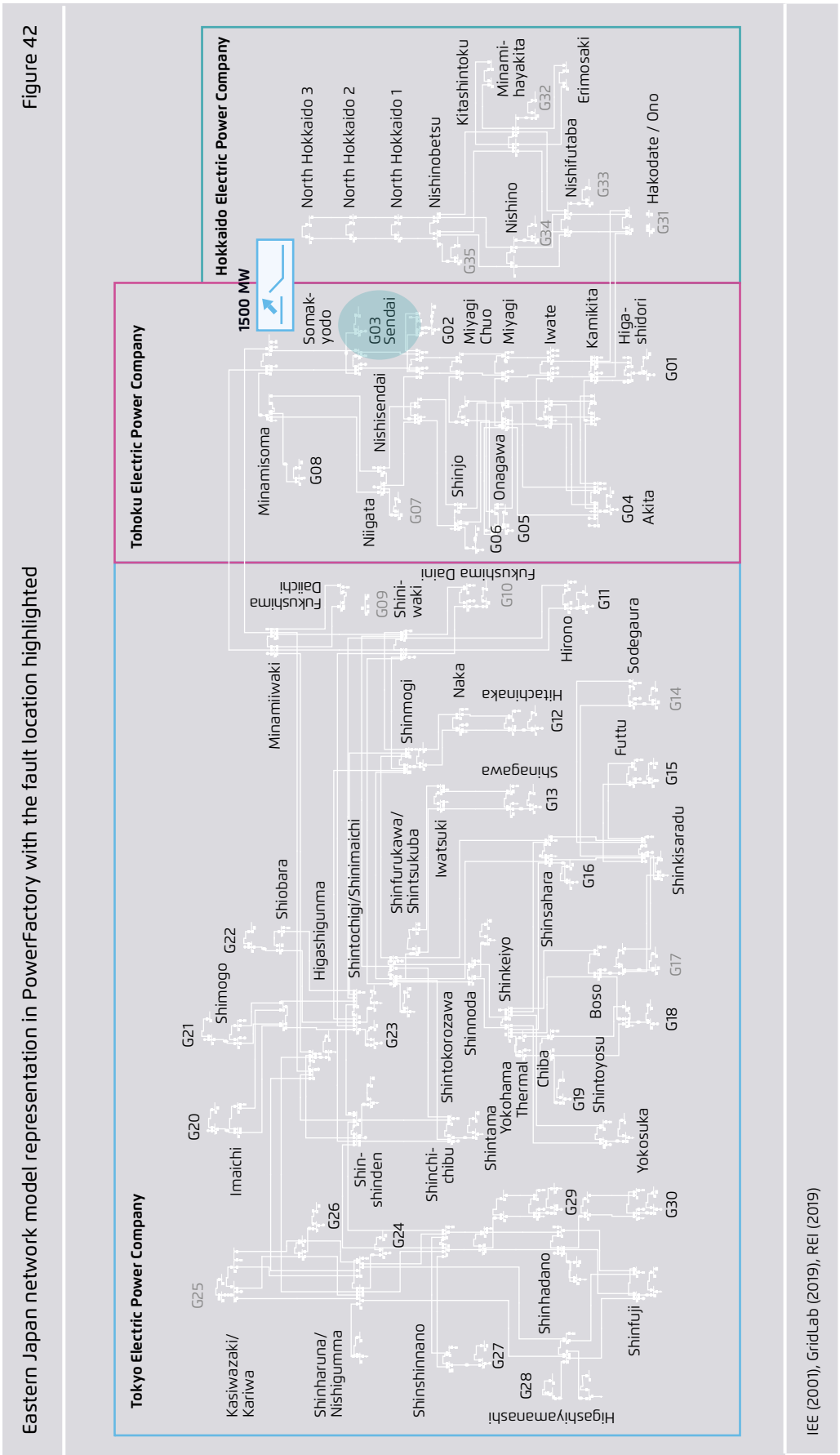

Figure 42

Eastern Japan network model representation in PowerFactory with the fault location highlighted

IEE (2001), GridLab (2019), REI (2019)

The frequency response results for this example (Figure 43) were taken as a base case scenario reflecting the original 2001 system conditions (i.e. without variable RES integration). The exact behaviour or shape of the frequency during the dynamic phase at a given point within the network depends on its distance from the fault location (see Figure 43). The specific RoCoF value for the system is a result of the method of computation. Here one may either follow an equational approach (see next page) or perform a graphical calculation (see Figure 45).

Frequency response for the base case scenario (2001 situation) Figure 43

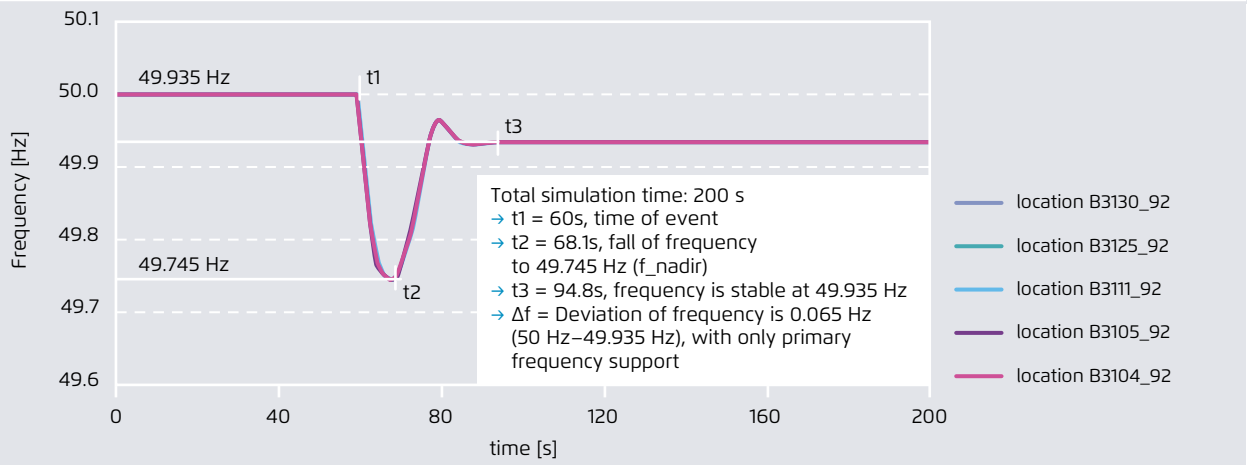

GridLab (2019)

Related RoCoF characteristics for different locations in the eastern Japan network Figure 44

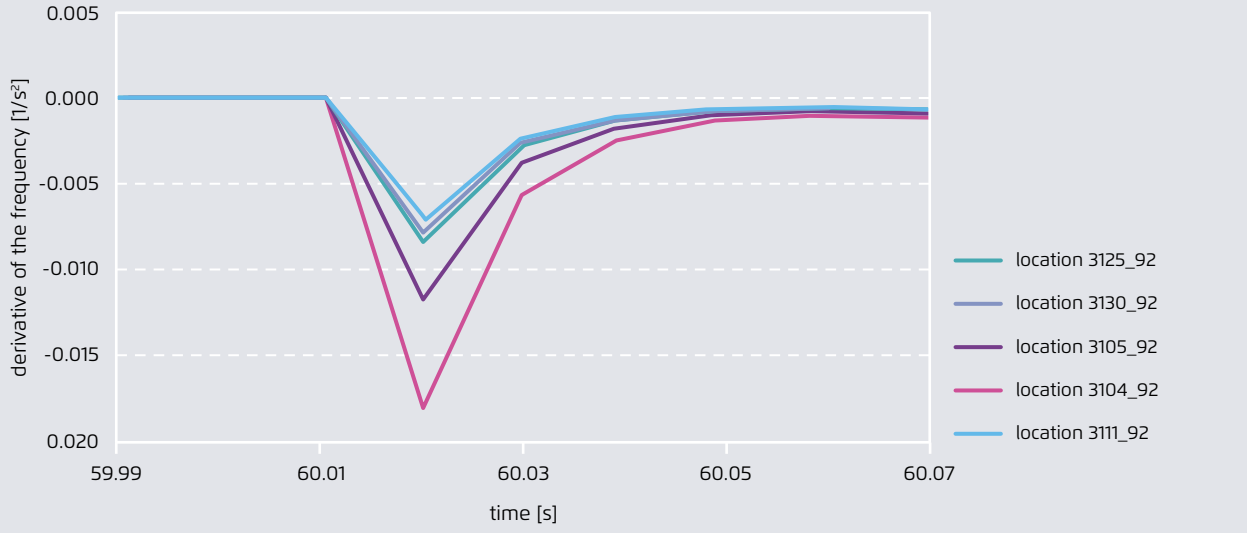

GridLab (2019)

$$\frac{df}{dt} * \frac{f_{sys}}{2} = \frac{\Delta P}{H_{sys\ Avail}}$$

With:

f_{sys}	System frequency
ΔP	Loss of generation
$H_{sys\ Avail}$	Available system inertia after loss of generation

Grid topology assumptions

Several assumptions were made concerning grid topology in this study, in order to assess how far RES integration is possible without changing the grid topology beyond a certain point. The original IEE 2001 model data remains unchanged, with no network enhancement measures applied to the grid model and no change in power line characteristics (line impedance, for example, was not altered).

Due to the fact that some DC transmission lines were not explicitly implemented in the original IEE grid model topology, the hourly snapshots at least considered the power flow exchange values as per the SWITCH model results. This affects the following corridors between EPCO regions in particular:

→ Hokkaido – Tohoku (eastern Japan grid),
→ Kansai – Shikoku (western Japan grid),
→ Kansai – Chugoku (western Japan grid),
→ Tokyo – Chubu (east – west interconnection line).

Furthermore, no change in load distribution was made. Only the hourly demand value was applied and distributed properly according to the selected snapshot.

The adaption of the generation mix (installed capacities) for the 2030 scenarios was carried out with respect to the local distribution of VRES for 2030 (selection of substations) according to a proposal by Komiyama (2016). The corresponding numeral distribution of wind and PV for each snapshot again resulted from a SWITCH model

Zoomed view of frequency response for the graphical RoCoF calculation — Figure 45

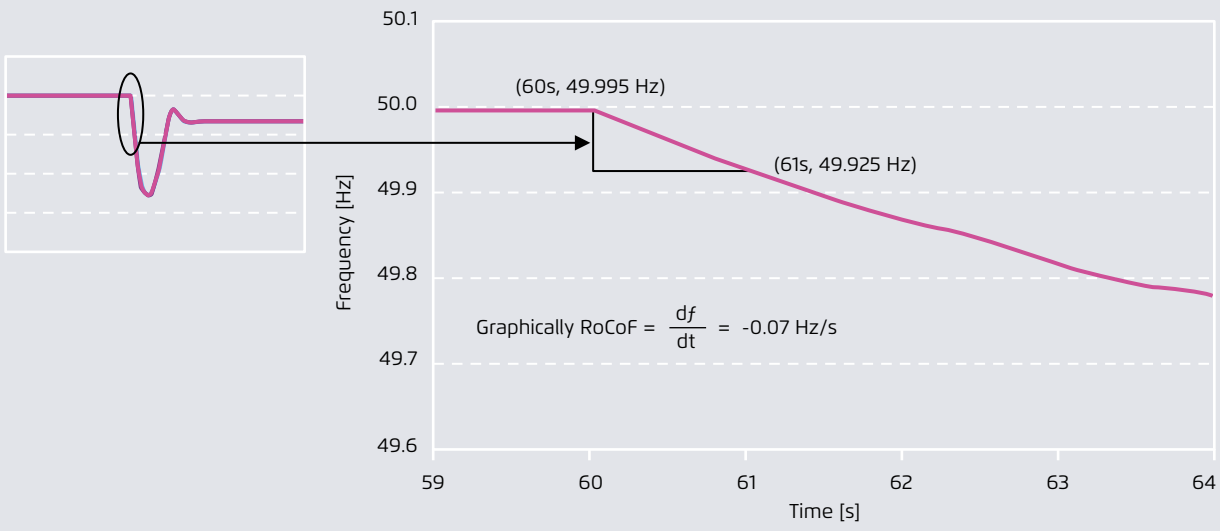

GridLab (2019)

calculation. On the basis of this input information, the conventional generation capacity was adapted according to 2030 conditions (at the prefectural level) and mapped back on to the 30-machine structure for the eastern and western grids. As a consequence of this procedure, the reactive power needs in the 2030 configuration changed significantly compared to the 2001 model. In order to enable proper grid operation, reasonable nodal voltage maintaining measures (reactive power compensation devices) had to be implemented in the grid model.

With regard to the stability assessment in this report, the term 'stable operation' must be understood in the sense of 'stable frequency characteristics can be reached after the incident occurs' in the context of the model used. It does not state whether the real and entire Japanese power system can be classified as 'stable' under these resulting operating conditions. Furthermore, the entire set of countermeasures that would be applied in real system operation could not be taken into account. Indeed, only inertia and primary control behaviour were implemented, in order to achieve pure frequency response results for further comparison and evaluation. In an additional sensitivity analysis, the impact of an ancillary controller provided by the DC link between East and West Japan was also investigated. In cases of a certain frequency deviation, an active power injection (from the eastern to the western grid or the other way around) occur automatically via the DC link. This frequency support is possible up to 600 MW.

Annex 5: Control strategies for frequency support from wind turbines and solar PV

Control strategies for frequency support from wind turbines

Wind turbines are connected to the network via power electronics converters. These converters monitor system parameters and ensure compliance with the grid connection requirements (grid codes) set by the system operators. Having a fully rated converter in place results in wind turbines being electrically decoupled from the network. Any change in the power system parameters (such as frequency or voltage) during a contingency is not inherently communicated to the wind turbines. These system parameters need to be sensed and made available to a controller, which can impose a reaction on the wind turbine based on a change in these parameters. In this study, the FFR response from the wind turbines was investigated.

Extensive research is currently being carried out to harness virtual inertia and fast frequency response (FFR) from wind turbines. These control strategies are briefly described in the next section.

a. Virtual inertia

Virtual inertia is essentially the emulation of the inertial response of the synchronous generators. Virtual inertia is defined as the controlled contribution of electrical torque from a unit that is proportional to the rate of change of frequency measured at the terminals of the unit (ENTSO-E, 2018). Figure 46 shows how the virtual inertial response can provide frequency support.

Virtual inertia response time frame — Figure 46

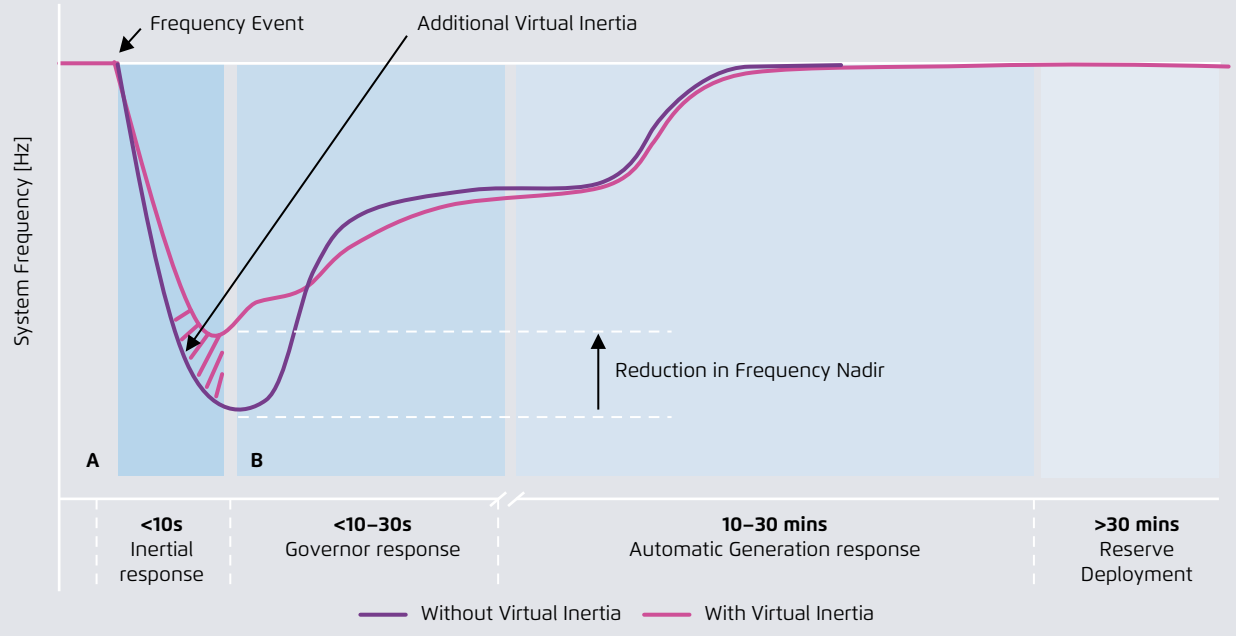

U. Tamrakar et al. (2016)

Within this control strategy, the rate of change of frequency (RoCoF) during the contingency is computed to provide the appropriate torque signal to the electrical machine, as shown in Figure 47 and Figure 48.

As the figures below show, modelling virtual inertia is a complex process. It requires accurate modelling of turbine dynamics, rotor dynamics, and speed controllers. The modelling of these systems is beyond the scope of this study, and virtual inertial response has therefore not been considered in this study as a source of frequency support.

Inertia coupling

Figure 47

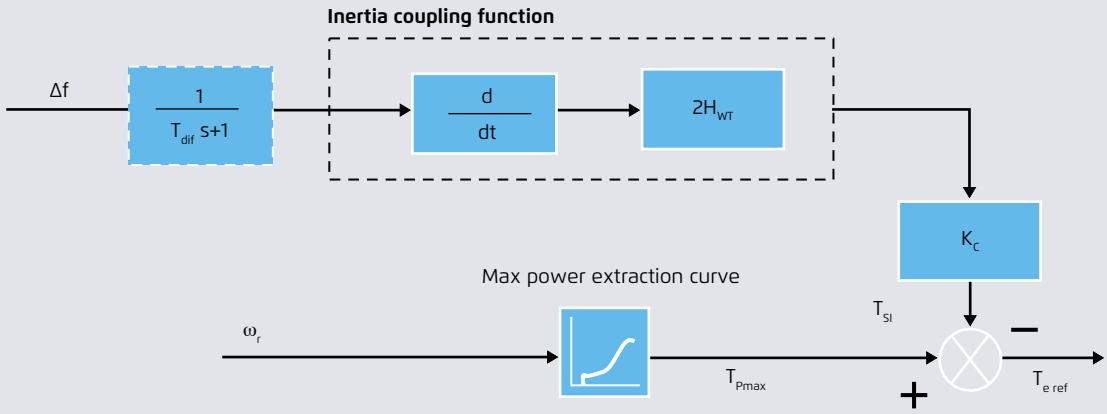

Chown et al. (2017)

Wind turbine virtual inertia response model

Figure 48

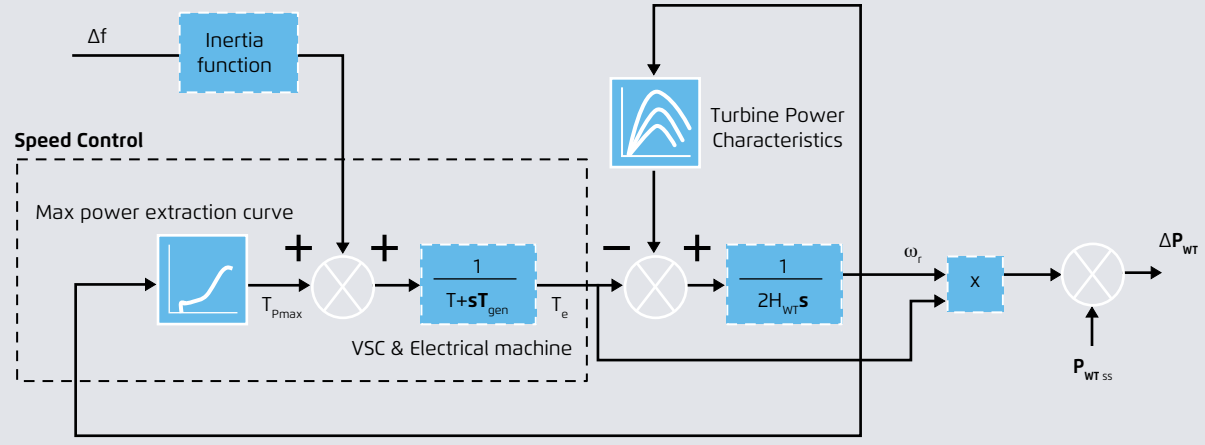

Chown et al. (2017)

b. Fast frequency reserve (FFR)

Fast frequency reserve (FFR) from wind turbines consists of a temporary boost in active power infeed. It is a system service that delivers a fast power change to mitigate the effect of reduced inertial response, so that frequency stability can be maintained (ENTSO-E, 2018). The fast frequency reserve approach is shown in Figure 49.

FFR characteristics of wind energy turbines — Figure 49

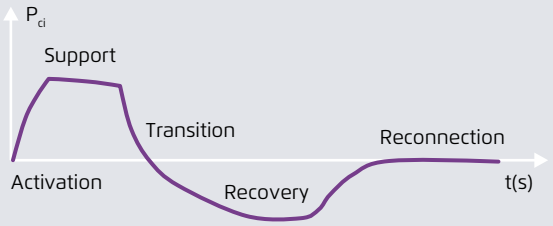

M. Persson (2017)

There are five phases in this process:

→ **The activation phase.** The controller constantly monitors the system frequency and when the system frequency is outside the given deadband (usually 20 mHz), it activates the support phase.

→ **The support phase.** When the controller is activated, it provides the new active power reference to the wind turbine. As the wind turbines are usually operated at their rated power for economic reasons, the additional active power is harnessed from the kinetic energy stored in the rotating masses of wind turbines.

→ **the transition phase.** As the power is drawn from the kinetic energy of the wind turbines, the speed of the turbines will drop. If the speed of the turbines drops below a certain limit, the turbine may stall, resulting in complete power loss. It is therefore necessary to restore the turbine to its rated speed. In this phase, then, the controller decides the appropriate time to switch from the support phase to the recovery phase.

→ **The recovery phase.** During this phase, the wind turbine returns to its original rotor speed. This is achieved by lowering the active power reference to a value lower than the rated power. This helps the turbine gain additional kinetic energy and restore the speed to the pre-disturbance value.

→ **The reconnection phase.** As soon as the nominal speed is achieved, the wind turbine is switched back to its rated power operational point.

Figure 50 shows the FFR scheme for wind turbines implemented in PowerFactory. In this scheme, an additional measurement delay has been implemented. This was done in order to compensate the fast frequency errors within the system during contingencies.

FFR modelling in DIgSILENT PowerFactory — Figure 50

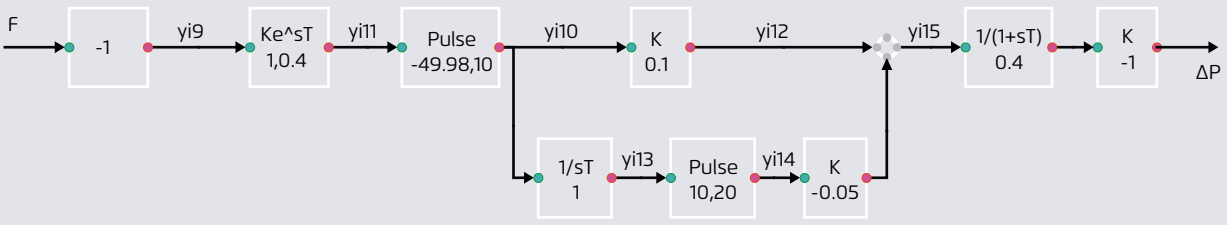

I. F. Moore (2012)

FFR controller response of a wind turbine Figure 51

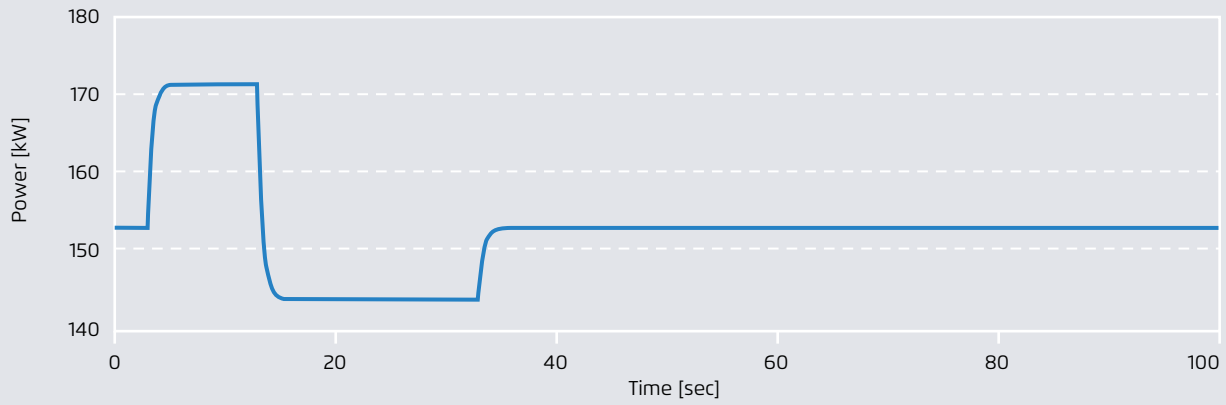

I. F. Moore (2012)

Within this controller, various parameters are set in order to achieve the required FFR from the WTs. The frequency deadband is set to 20 mHz. The increase in active power during the support phase is 10 % of the operating point for 10 s. Similarly, the reduction in active power during the recovery phase is 5 % of the operating point for 20 s. Figure 51 shows the response of the FFR modelled.

Control strategies for fast frequency support from PV systems

The inherent property of PV panels is to produce DC power. To connect the PV systems to an AC network, converters are used to convert DC power into AC. Together with the converters, these PV generators form a static system and therefore have no rotational mass as in conventional generation. A high level of PV penetration in the network can result in the lowering of the inertial reserves within the system. This could lead to critically low nadir frequency and higher RoCoF values during contingencies.

The control strategy for fast frequency response is similar to the behaviour of the conventional synchronous generator's speed governor. This principle is called the droop principle in the governors. The change in active power is proportional to the deviation of frequency outside the deadband (Rahmann, 2014). Due to the fast control capacities of the power electronics in the converters, the time frame of the change in active power is similar to the inertial response. During a loss of generation, the PV systems should increase their output power to control the frequency drop. To achieve this additional active power, the PV systems participating in FFR are operated under deloaded conditions. Instead of operating the PV system at its MPPT point, then, it is operated at the deloaded point, as shown in Figure 52.

Deloaded operation of PV systems Figure 52

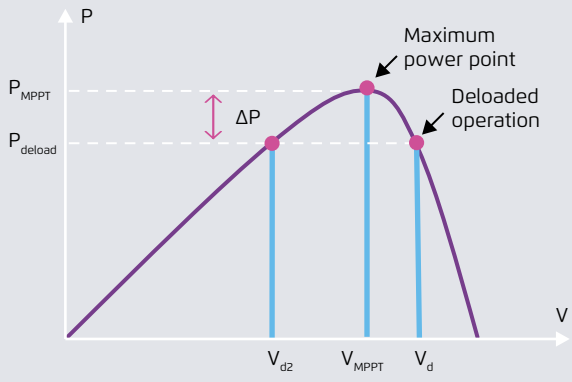

C. Rahmann, A. Castillo (2014)

For the purposes of simulation, we used the WECC model developed by the University of Kassel (G. Lammert et al., 2016). Physical processes inside the PV system were not considered here because they are irrelevant to the current research topic. The rated power of the PV systems in the simulation (PowerFactory) corresponds to the MPPT operation point that matches the PV system output in the respective RES scenario. To simulate FFR from PV, the active power operating points of the PV systems participating in FFR are reduced. To achieve the power balance, the output powers of these PV systems can be reduced by up to 20%. The additional power required is re-dispatched to the nearby thermal power stations. Figure 53 shows the frequency controller used for PV-FFR. Any deviation in frequency greater than the deadband generates a proportional active power reference.

The drop parameter (Dup) was set to 400 and the frequency deadband was set to ±0,0004 p.u.

Frequency controller in WECC model — Figure 53

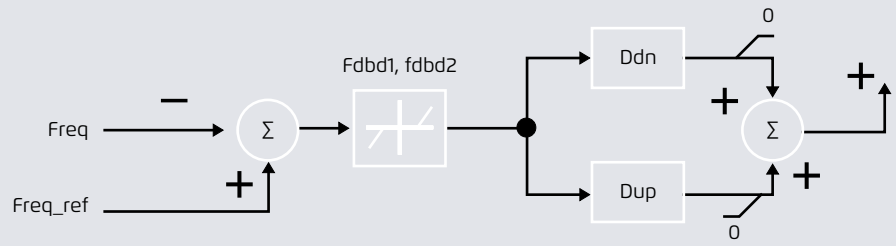

G. Lammert et al. (2016)

Annex 6: References

Chown GA., Wright J., van Heerden R. and Coker M. (2017). System inertia and Rate of Change of Frequency (RoCoF) with increasing nonsynchronous renewable energy penetration

DEA (2004). Wind turbines connected to grids with voltages, http://www.wt-certification.dk/Common/WindTurbinesConnectedtoGridswith Voltageabove100kV.pdf

DNV KEMA Energy & Sustainability (2013). RoCoF: An independent analysis on the ability of Generators to ride through Rate of Change of Frequency values up to 2Hz/s.

Eirgrid. WFPS Frequency Response Test Procedure

Elkraft/Eltra (2004). Wind turbines connected to grids with voltages above 100 kV, http://www.wt-certification.dk/Common/WindTurbinesConnectedtoGridswith Voltageabove100kV.pdf

ENTSO-E (2001). Definitions of Transfer Capacities in liberalised Electricity Markets, https://www.entsoe.eu/fileadmin/user_upload/_library/ntc/entsoe_transferCapacityDefinitions.pdf

ENTSO-E (2014). Incidents Classification Scale Methodology

ENTSO-E (2017). Guideline on Electricity Balancing. https://electricity.network-codes.eu/network_codes/eb/

ENTSO-E (2018). Future System Intertia 2, ENTSO-E Report https://docs.entsoe.eu/id/dataset/nordic-report-future-system-inertia/resource/6efce80b-2d87-48c0-b1fe-41b70f2e54e4

FEPC (2018). Electricity Statistics Information. Retrieved August 2018, from http://www5.fepc.or.jp/tok-bin-eng/kensaku.cgi

Fingrid (2018). FCR-N Prices Finland, https://www.fingrid.fi/en/electricity-market/reserves_and_balancing/reserve-market-information/frequency-controlled-disturbance-reserve/

German TSOs (2018). Frequenzstabilität – Notwendiges Zeitverhalten bei Über-und Unterfrequenz

Hydro-Québec. Technical Requirements for the connection of generation facilities to the Hydro-Quebec Transmission system

IEE Japan (2018). Japanese Power System Models. Retrieved March 2018, from http://www.iee.jp/pes/?page_id=141

IEE Japan (2018 b): Description of Bulk Power System Models. http://www.iee.jp/pes/?page_id=1052 , 2nd September 2018

ISEP (2018). The share of renewable energy in total power generation in Japan in 2017. Retrieved August 2018, from https://www.isep.or.jp/en/library/3362

Japan Meteorological Agency (2018). 各種データ・資料 (Data and Material). Retrieved April 2018, from http://www.jma.go.jp/jma/menu/menureport.html

Komiyama, Ryoich (2016). "Assessment of post-Fukushima renewable energy policy in Japan's nation-wide power grid

Komiyama, R., & Fujii, Y. (2018). National electric power grid model of Japan. IEW2018 (The 37th Edition of International Energy Workshop) 4G-Integration of VRE IV, Chalmers Conference Center.

G. Lammert, L. D. P. Ospina, P. Pourbeik, D. Fetzer, M. Braun (2016). "Implementation and Validation of WECC Generic Photovoltaic System Models in DIgSILENT PowerFactory",IEEE paper, DOI: 10.1109/PESGM.2016.7741608.

METI (2015). Long-term Energy Supply and Demand Outlook. http://www.meti.go.jp/english/press/2015/0716_01.html

METI (2017). 2030年エネルギーミックス実現のための対策 ～原子力　火力　化石燃料　熱～ http://www.enecho.meti.go.jp/committee/council/basic_policy_subcommittee/023/pdf/023_005.pdf

METI (2018). なっとく！再生可能エネルギー. Retrieved April 2018, from http://www.enecho.meti.go.jp/category/saving_and_new/saiene/statistics/index.html

METI (2018b). Strategic Energy Plan. Retrieved from http://www.meti.go.jp/english/press/2018/pdf/0703_002c.pdf

I. F. Moore (2012). "Inertial Response from Wind Turbines", Ph.D. thesis, Cardiff University, UK, 2012. Seitenumbruch vorletzte Seite nie löschen

NREL (2014). Western Wind and Solar Integration Study Phase 3 – Frequency Response and Transient Stability: Executive Summary

OCCTO. (2016). 周波数制御に対応したマージン及びその他のマージンについて.

M. Persson (2017). Frequency Response by Wind Farms in Power Systems with High Wind Power Penetration, Ph.D. thesis, Department of Electrical Engineering, Chalmers University of Technology, Sweden, 2017.

C. Rahmann, A. Castillo (2014). Fast Frequency Response Capability of Photovoltaic Power Plants: The Necessity of New Grid Requirements and Definitions, Journal, Energies 2014, 7, 6306-6322; doi:10.3390/en7106306.

REI (2015). 日本のエネルギー転換戦略の提案ー豊かで安全な日本へー https://www.renewable-ei.org/images/pdf/20150218/JREF_Energy_Transition.pdf

Shinichi Imai, T. Y. (2004). UFLS program to ensure stable island operation. IEEE PES Power Systems Conference and Exposition. New York.

Statista. (2018). Share of renewable energy in Japanese electricity production from fiscal year 2010 to 2016. Retrieved from https://www.statista.com/statistics/745908/japan-share-of-renewables-in-electricity-production/

Sugiyama, T., Komiyama, R., & Fujii, Y. (2016). Optimal Power Generation Mix Model considering Nationwide High-voltage Power Grid in Japan for the Analysis of Large-scale Integratin of PV and Wind Power Generation. IEEJ Transactions on Powr and Energy, 136(12), 864-875.

U. Tamrakar; D. Shrestha; M. Maharjan; B. Bhattarai; T. Hansen; R. Tonkoski (2017). Virtual Inertia: Current Trends and Future Directions, Paper, Applied Science, app7070654, June 2017

TEPCO (2018). Download past electricity demand data. Retrieved August 2018, from http://www.tepco.co.jp/en/forecast/html/download-e.html

Pieter Tielens, Dirk Van Hertem (2012). Grid Inertia and Frequency Control in Power Systems with High Penetration of Renewables

TSOs (2018). Germany Grid Development Plan Germany. https://www.netzentwicklungsplan.de/en/front

Tsujii, Y., Tsuji, T., Oyama, T., Nakachi, Y., & Chand Verma, S. (2016). A study on the frequency fluctuation in case of high penetration of renewable energy sources. IEEJ Transactions on Power and Energy, 136(1), 33–43.

Wakeyama, T. (2016). Impact of increasing share of reewables on the Japanese power system – model based analysis. 15th International Workshop on Large-scale Integration of Wind Power into Power Systems as well as on Transmission Networks for Offshore Wind Power Plants. Vienna: Energynautics.

Wakeyama, T. (2017). Evaluating the impacts of priority dispatch rule on RE curtailment in Japan. 16th International Wind Integration Workshop. Berlin.

Yuji Yamashita, R. S. (2018). Kyushu Electric mulls cutback on solar power. Asahi Shinbun

148/1-S-2019/EN

How do we accomplish the clean-energy transition?

Agora Energiewende develops scientifically based and politically feasible approaches for ensuring successful energy transition in Germany, Europe and worldwide. We see ourselves as a think-tank and policy laboratory, centered around dialogue with energy policy stakeholders. Together with participants from public policy, civil society, business and academia, we develop a common understanding of energy transitions, its challenges and courses of action.

Renewable Energy Institute was established in the aftermath of Fukushima Nuclear Accident, in August 2011, to establish renewable energy based society in Japan and other countries. REI conducts scientific studies on renewable energy policies, advocates the policy makers and introduces global knowledges of renewables to the public.

Agora Energiewende and Renewable Energy Institute initiated in 2016 a partnership with the goal to transfer expertise and deepen information exchanges about the ongoing energy transition in Germany and Japan.

This publication is available for download under this QR code.

Agora Energiewende
Anna-Louisa-Karsch-Straße 2
10178 Berlin | Germany
P +49 (0)30 700 14 35-000
F +49 (0)30 700 14 35-129
www.agora-energiewende.org
info@agora-energiewende.de

Renewable Energy Institute
8F, DLX Building, 1-13-1 Nishi-Shimbashi
Minato-ku, Tokyo 105-0003 | Japan
P + 81 (0)3-6866-1020
F + 81 (0)3-6866-1021
www.renewable-ei.org
info@renewable-ei.org

Agora Energiewende is a joint initiative of the Mercator Foundation and the European Climate Foundation.